

A REDUCED COMPLEXITY UNGERBOECK TYPE RECEIVER FOR
MULTI-CODE SIGNALING IN DISPERSIVE CHANNELS

A THESIS SUBMITTED TO
THE GRADUATE SCHOOL OF NATURAL AND APPLIED SCIENCES
OF
MIDDLE EAST TECHNICAL UNIVERSITY

BY

GÖKHAN MUZAFFER GÜVENSEN

IN PARTIAL FULFILLMENT OF THE REQUIREMENTS
FOR
THE DEGREE OF DOCTOR OF PHILOSOPHY
IN
ELECTRICAL AND ELECTRONICS ENGINEERING

JULY 2014

Approval of the thesis:

**A REDUCED COMPLEXITY UNGERBOECK TYPE RECEIVER
FOR MULTI-CODE SIGNALING IN DISPERSIVE CHANNELS**

submitted by **GÖKHAN MUZAFFER GÜVENSEN** in partial fulfillment of the requirements for the degree of **Doctor of Philosophy in Electrical and Electronics Engineering Department, Middle East Technical University** by,

Prof. Dr. Canan Özgen _____
Dean, Graduate School of **Natural and Applied Sciences**

Prof. Dr. Gönül Turhan Sayan _____
Head of Department, **Electrical and Electronics Engineering**

Prof. Dr. Yalçın Tanık _____
Supervisor, **Electrical and Electronics Eng. Dept., METU**

Assoc. Prof. Dr. Ali Özgür Yılmaz _____
Co-supervisor, **Electrical and Electronics Eng. Dept., METU**

Examining Committee Members:

Prof. Dr. Mete Severcan _____
Electrical and Electronics Eng. Dept., METU

Prof. Dr. Yalçın Tanık _____
Electrical and Electronics Eng. Dept., METU

Prof. Dr. Mehmet Şafak _____
Electrical and Electronics Eng. Dept., Hacettepe Univ.

Assoc. Prof. Dr. Melek Diker Yücel _____
Electrical and Electronics Eng. Dept., METU

Assoc. Prof. Dr. Çağatay Candan _____
Electrical and Electronics Eng. Dept., METU

Date: 17.07.2014

I hereby declare that all information in this document has been obtained and presented in accordance with academic rules and ethical conduct. I also declare that, as required by these rules and conduct, I have fully cited and referenced all material and results that are not original to this work.

Name, Last Name: GÖKHAN MUZAFFER GÜVENSEN

Signature :

ABSTRACT

A REDUCED COMPLEXITY UNGERBOECK TYPE RECEIVER FOR MULTI-CODE SIGNALING IN DISPERSIVE CHANNELS

Gökhan Muzaffer Güvensen,

Ph.D., Department of Electrical and Electronics Engineering

Supervisor : Prof. Dr. Yalçın Tanık

Co-Supervisor : Assoc. Prof. Dr. Ali Özgür Yılmaz

July 2014, 127 pages

The main aim in this thesis is to propose multiple signaling waveforms (multi-code) based yet spectrally efficient modulation schemes and competent receiver architectures realizing soft-input-soft-output (SISO) detection. We search for generic suboptimal receiver architectures for Multi-Code Signaling (MCS), which can be represented as selection of one out of M waveforms per signaling interval. The proposed receiver architectures exhibit almost optimal performance at significantly reduced complexity in highly dispersive channels.

First, an efficient reduced complexity implementation of the Ungerboeck type Maximum a Posteriori (MAP) receiver, directly operating on unwhitened channel matched filter and code matched filter outputs, is proposed for MCS by forming the factor graph (FG) and sum-product algorithm (SPA) framework. The proposed MAP receiver, generating the a posteriori probabilities by bidirectional reduced state sequence estimation (RSSE) recursions, is substantiated with symbol rate bidirectional decision feedback based on surviving paths in

order to eliminate the post- and pre-cursor inter-symbol interference (ISI) as well as multi-code interference due to the non-ideal properties of the signaling waveforms and multipath channel. Second, we extend the proposed Ungerboeck receiver to be exploited in multiple access channel by unifying the bidirectional RSSE applied to each user and the mitigation of multi-user interference fulfilled by the SPA based on the obtained Ungerboeck type FG, resulting in linear complexity in the number of interfering users. Finally, error probability analysis, which provides significant insight on the success of the proposed reduced state Ungerboeck receivers in case of uncoded MCS transmission, and the packet error rate analysis based on the random coding approach that determines the cutoff rate for coded transmission are provided. These analyses help the designer determine system parameters and open up new possibilities for a performance enhancement of reduced complexity Ungerboeck receivers via a proper selection of a modulation scheme for the general class of MCS especially in long ISI channels.

To sum up, the proposed receiver architectures here confirms, compares many previous works, and complements reduced complexity Ungerboeck structure by changing several system parameters generalized to MCS format with the help of the developed analytical tools.

Keywords: spectrally efficient communication, ISI channels, multidimensional signaling, Ungerboeck receiver, reduced complexity, bidirectional decision feedback, MAP, MLSE, RSSE, FG, SPA, MAC, error probability, bias, cutoff rate

ÖZ

DAĞITICI KANALLARDA ÇOK KODLU SİNYALLEŞME İÇİN DÜŞÜK KARMAŞIKLIKLI UNGERBOECK TİPİNDE ALICI YAPILARI

Gökhan Muzaffer Güvensen,
Doktora, Elektrik ve Elektronik Mühendisliği Bölümü
Tez Yöneticisi : Prof. Dr. Yalçın Tanık
Ortak Tez Yöneticisi : Assoc. Prof. Dr. Ali Özgür Yılmaz

Temmuz 2014, 127 sayfa

Bu tezdeki temel amaç, çok kodlu işaretleme kullanılarak görüngen verimliliğinin emsal sistemlere göre arttırıldığı kipleme yöntemleri ile, bu yöntemlere uygun etkili yumuşak-girdili-yumuşak-çıkıtlı (SISO) sezim işlemi gerçekleştirilen alıcı yapılarının ortaya konmasıdır. Genel olarak her bir işaretleme aralığında M adet dalga biçiminden birinin seçilip gönderildiği bir çok-kodlu işaretleme (MCS) için en iyi altı alıcı yapıları araştırılmaktadır. Önerilen alıcıların, oldukça dağıtıcı kanallarda bile en iyiye çok yakın bir başarıyı, çok düşük karmaşıklıkta sergiledikleri görülmektedir.

İlk olarak, çok-kodlu işaretleme için beyazlaştırıcı süzgece gerek duymayan, kanal uyumlu süzgeç ve kod uyumlu süzgeç çıkışları üzerinde doğrudan çalışan, Ungerboeck tipinde bir en büyük sonsal (MAP) alıcısı, faktör çizge (FG) ve toplam-çarpım algoritması (SPA) kullanılarak düşük karmaşıklıkta ve etkin bir biçimde gerçekleştirilmiştir. Sonsal olasılıkları ileri ve geri yönlü çalışan indirgen-

miş durumlu dizi kestirimiyle (RSSE) hesaplayan MAP alıcısı, kullanılan dalga biçimlerinin ideal olmayan özellikleri ve çok yollu kanal sebebiyle ortaya çıkan semboller arası girişim (ISI) ve çok kodlu girişim etkilerini ise, algoritmanın silinmeyip sona kalan izleri üzerinden çift yönlü karar geribeslemesi kullanarak ortadan kaldırmaktadır. İkinci olarak, önerilen Ungerboeck alıcı yapısı çoklu erişim kanalı için genişletilerek, her bir kullanıcı için çift yönlü RSSE ve çok kullanıcı girişim etkilerinin giderilmesinin, Ungerboeck tipinde FG modeli üzerinden SPA ile birleştirilmesiyle gerçekleşmiş ve kullanıcı sayısı ile doğrusal artan bir karmaşıklık elde edilmiştir. Son olarak, çok-kodlu işaretleşme için önerilen Ungerboeck tipli alıcı yapılarının başarımları hakkında önemli bir kavrayış sağlayan hata olasılığı analizleri gerçekleştirilmiştir. Ayrıca, rastgele kodlama yöntemine dayalı kesme hızını belirleyen paket hata olasılığına ait analitik ifadeler elde edilmiştir. Bu analizler, özellikle semboller arası girişimi uzun kanallarda genel MCS tabanlı iletim için, karmaşıklığı düşük ve etkin bir Ungerboeck MAP alıcısına ait sistem parametrelerinin belirlenmesi ve başarımlarını iyileştirilmesine dönük, tasarımcıya yardımcı önemli bir araç olarak ortaya çıkmaktadır.

Özetlemek gerekirse, geliştirilen analitik araçların kullanımı ile birlikte MCS formatına genelleştirilmiş sistem parametreleri değiştirilerek önerilen alıcı yapıları, literatürde yer alan birçok çalışmayı doğrulamakta, kıyaslamakta ve düşük karmaşıklıkta Ungerboeck alıcısının gerçekleşmesini tamamlamaktadırlar.

Anahtar Kelimeler: spectral verimli haberleşme, ISI kanalları, çok-kodlu işaretleşme, Ungerboeck alıcısı, indirgenmiş karmaşıklık, çift yönlü karar geri besleme, MAP, MLSE, RSSE, FG, SPA, MAC, hata olasılığı, yanlılık, kesme hızı

*to my beloved family,
to my dear friends,
and all those that supported me through time and believed in me*

ACKNOWLEDGMENTS

I would like to express my deepest gratitude to my advisor Prof. Dr. Yalçın Tanık for his guidance, patience, advice, encouragement, and insight throughout this thesis work. Without our frequent technical discussions and his supervision during my research, I would never have been able to complete the work presented in this thesis.

It is a great pleasure for me to thank my co-supervisor Assoc. Prof. Dr. Ali Özgür Yılmaz for his advice and motivation during my doctorate studies. The technical discussions with him will be invaluable experiences for me during my career.

I would like to thank Assoc. Prof. Dr. Çağatay Candan, Prof. Dr. Mehmet Şafak and Assoc. Prof. Dr. Defne Aktaş for their encouragement and advices during my studies as Thesis committee. I would also like to thank the other faculty members of the Telecommunication Research Team at METU for their contribution in establishing my background in the area. The technical discussions with Prof. Dr. Sencer Koç, Prof. Dr. Mete Severcan and Assoc. Prof. Dr. Çağatay Candan are gratefully acknowledged. I would like to appreciate the opportunity presented by ASELSAN Inc. and I gain a lot of experience as a member of the aforementioned research team.

I am grateful to The Scientific and Technological Research Council of Turkey (TÜBİTAK) and ASELSAN Inc. for their financial support during my doctorate studies.

I would also like to give big thanks to my friends Tuğcan Aktaş, Pınar Şen, Seçil Özdemir, Ali Bulut Üçüncü and Alptekin Yılmaz for their encouragement, suggestions and for their having such friendly environment at METU during my studies. Also, I believe that the friendship of my colleagues Ümit İrgin, Önder

Önsay, Baha Baran Öztan and Ahmet Şeker has to be honored.

Last but not the least; I am grateful to my dear parents for their endless support during my whole life. I truly owe all my success to them.

TABLE OF CONTENTS

ABSTRACT	v
ÖZ	vii
ACKNOWLEDGMENTS	x
TABLE OF CONTENTS	xii
LIST OF FIGURES	xvi
LIST OF ABBREVIATIONS	xx
CHAPTERS	
1 INTRODUCTION	1
1.1 Motivation	1
1.2 Outline and Contribution of the Thesis	4
2 A GENERIC REDUCED COMPLEXITY UNGERBOECK TYPE MAP RECEIVER FOR MULTI-CODE SIGNALING (MCS): SIN- GLE USER CASE	9
2.1 Introduction	9
2.2 System Model	12
2.3 MLSE Receiver for MCS based on Ungerboeck Observa- tion Model	14
2.3.1 Optimum Maximum Likelihood Detection	14
2.3.2 Discrete Time Equivalent Model for MCS	15

2.3.3	Comments on Forney and Ungerboeck Approaches	17
2.3.4	Symbol Rate Ungerboeck Type MLSE Receiver	18
2.3.5	Case Study: Ideal Spreading Codes	18
2.4	A Reduced Complexity MAP Receiver for MCS based on Ungerboeck type Factor Graph (FG) and Sum-Product Algorithm (SPA) Framework	20
2.4.1	Proposed Architecture based on Ungerboeck type Factorization	21
2.4.2	Bias Compensation in U-RSSE	23
2.4.3	Implementation Details and Computational Complexity	25
2.5	Error Probability Analysis for U-RSSE	28
2.5.1	Variance Analysis of the <i>Bias</i> Term in Ungerboeck Type RSSE	28
2.5.2	Approximate Bit Error Rate for U-RSSE with BDF	32
2.6	Simulation Results	33
2.6.1	BER Simulations	33
2.6.2	Extrinsic Information Transfer (EXIT) Chart Behaviour of the U-RSSE	44
2.6.2.1	The EXIT Chart	46
2.6.2.2	Simulation Results	46
2.7	Conclusions	50
3	CUTOFF RATE BASED ERROR PROBABILITY ANALYSIS OF CODED MCS SCHEME FOR FINITE BLOCK-LENGTH REGIME	51
3.1	Introduction	51
3.2	Cutoff Rate Analysis of Coded MCS Scheme	52

3.3	Performance Analysis based on MGF Generation of Cutoff Rate for Coded MCS	55
3.3.1	LBA Bound (Optimum Bound) based on Cutoff Rate	55
3.3.2	Analytical Calculation of the Moments	56
3.3.3	Moment Based Approximation of MGF	56
3.3.4	Packet Error Rate Calculation for Coded MCS Scheme	58
3.4	Ergodic Cutoff Rate Calculation for Coded MCS Scheme	59
3.5	Multidimensional Signaling Waveform Design Guidelines for MCS Scheme based on Cutoff Rate	59
3.6	Case Study: Ideal Signaling Waveforms	60
3.7	Performance Results	62
3.8	Conclusions	72
4	A GENERIC REDUCED COMPLEXITY UNGERBOECK TYPE MAP RECEIVER FOR MULTIPLE ACCESS CHANNEL (MAC)	75
4.1	Introduction	75
4.2	System Model	78
4.3	Ungerboeck type MLSE Receiver for MCS in MAC	79
4.3.1	Optimum ML Multi-User Detection for MCS	79
4.3.2	Discrete Time Equivalent MAC Model for MCS	80
4.4	Ungerboeck Type 2-D Factor Graph Construction for MCS in MAC	81
4.5	A Reduced Complexity Ungerboeck type Multi-User MAP Receiver for MCS	84
4.5.1	Message Schedule	86
4.5.2	Bias Compensation	88

4.5.3	Computational Complexity	89
4.6	Error Probability Analysis for Reduced Trellis Ungerboeck type MUD	89
4.6.1	Generalized Bias Analysis for MCS in MAC	89
4.6.2	Approximate Bit Error Probability for MU-RSSE with BDF	92
4.7	Simulation Results	93
4.8	Conclusions	96
5	CONCLUSION AND FUTURE WORKS	97
	REFERENCES	101
	APPENDICES	
A	ANALYSIS OF THE <i>BIAS</i> TERM IN UNGERBOECK TYPE RSSE	109
B	VARIANCE ANALYSIS OF THE BIAS TERM	113
C	APPROXIMATE BER ANALYSIS FOR U-RSSE-BDF	119
D	CUTOFF RATE ANALYSIS OF CODED MCS SCHEME	121
	CURRICULUM VITAE	125

LIST OF FIGURES

FIGURES

Figure 2.1 Block diagram of the optimum receiver for MCS: CMF followed by code MFs precedes MLSE type processing	15
Figure 2.2 CMF and code matched filter outputs sampled at $t = nT$, where $z_i(t) = r(t) * h^*(-t) * g_i^*(-t)$, $i = 1, \dots, M$	19
Figure 2.3 FG corresponding to the joint APP in (2.19) for MCS	23
Figure 2.4 A Reduced Complexity Receiver for MCS based on a correlator bank (CMF and code MFs) followed by Symbol Rate Ungerboeck Type RSSE with BDF	26
Figure 2.5 Variance of the normalized bias term in Ungerboeck RSSE after CMF and code MFs with respect to different number of independent Rayleigh channel taps, L_c , with exponentially decaying power delay profile for different S_{total} values (Spectral efficiency is $\frac{1}{2}$ in all curves).	31
Figure 2.6 $M = 8$, $P = 4$, $N_c = 16$, channel is composed of $L_c = 64$ independent Rayleigh taps with exponentially decaying power delay profile	35
Figure 2.7 $M = 8$, $P = 4$, $N_c = 16$, $SNR_c = \frac{E_c}{N_0} = 2$ dB, BER variation with respect to number of Rayleigh channel taps, L_c , with exponentially decaying power delay profile	37

Figure 2.8 Performance for $(M = 1, P = 4, N_c = 4)$, $(M = 4, P = 4, N_c = 8)$ and $(M = 16, P = 4, N_c = 12)$ schemes, channel is composed of $L_c = 128$ independent Rayleigh taps with exponentially decaying power delay profile	39
Figure 2.9 Performance variation of U-RSSE with BDF ($S_w = S_{ph} = 1$) and one forward and backward iteration in (2.23), analytical BER approximation in (2.29) and MFB with respect to different M, N_c values at $\nu = \frac{\log_2(MP)}{N_c} = \frac{1}{6}$, $P = 4$. Channel is composed of $L_c = 64$ independent Rayleigh taps with exponentially decaying power delay profile	40
Figure 2.10 Performance variation of U-RSSE with BDF ($S_w = S_{ph} = 1$) and one forward and backward iteration in (2.23), and analytical BER approximation in (2.29) with respect to different (M, P) values at $\nu = \frac{\log_2(MP)}{N_c} = \frac{6}{16}$, $N_c = 16$. Channel is composed of $L_c = 32$ independent Rayleigh taps with exponentially decaying power delay profile	41
Figure 2.11 Performance for the MCS scheme $(M = 4, P = 4, N_c = 8)$ with random codes transmitted through a static channel, RRC type low-pass filter with cut-off at $\frac{B}{2}$ and roll-off factor 0.3, $\frac{W}{B} = 4$ and 8.	43
Figure 2.12 Performance for the MCS schemes $(M = 4, P = 4, N_c = 8)$ and $(M = 16, P = 4, N_c = 12)$ with random codes transmitted through a static channel, RRC type low-pass filter with cut-off at $\frac{B}{2}$ and roll-off factor 0.3, $\frac{W}{B} = 6$	45
Figure 2.13 An EXIT chart at $\frac{E_b}{N_0} = 0$ dB, showing extrinsic vs. a priori information for block containing 200 MCS symbols. The channel is composed of $L_c = 128$ independent Rayleigh taps with exponentially decaying power delay profile. MCS waveforms for $(M = 4, P = 4, N_c = 8)$ and $(M = 16, P = 4, N_c = 12)$ are obtained by truncating Kasami Sequences.	47

Figure 2.14 An EXIT chart at $\frac{E_b}{N_0} = 5$ dB, showing extrinsic vs. a priori information for block containing 200 MCS symbols ($M = 4, P = 4, N_c = 8$). The channel is a static RRC low-pass filter with cut-off at $\frac{B}{2}$ and roll-off factor 0.3, and $\frac{W}{B}$ is set to 6. MCS waveforms for ($M = 4, P = 4, N_c = 8$) have chips randomly selected from the QPSK alphabet at each packet transmission.	48
Figure 2.15 Average mutual information at the detector output in the case of $I_A = 0$ for the MCS scheme ($M = 4, P = 4, N_c = 8$). The channel is composed of $L_c = 128$ independent Rayleigh taps with exponentially decaying power delay profile. MCS waveforms for ($M = 4, P = 4, N_c = 8$) are obtained by truncating Kasami Sequences.	49
Figure 3.1 Cutoff Rates for AWGN channel, Truncated Kasami Codes are used	63
Figure 3.2 AWGN, $N=100$, PER=0.01, $N_c = 64$, $\frac{\log_2(MP)}{N_c} = \frac{6}{64}$	64
Figure 3.3 Rayleigh Suburban Channel, $L_c = 8$, $N=100$, PER=0.01, $N_c = 64$, $\frac{\log_2(MP)}{N_c} = \frac{6}{64}$	65
Figure 3.4 AWGN, $N=100$, PER=0.01, $N_c = 8$, $\frac{\log_2(MP)}{N_c} = \frac{3}{4}$	66
Figure 3.5 Rayleigh Suburban Channel, $L_c = 8$, $N=100$, PER=0.01, $N_c = 8$, $\frac{\log_2(MP)}{N_c} = \frac{3}{4}$	67
Figure 3.6 Rayleigh Suburban Channel, $L_c = 8$, PER=0.01, Constant Packet Duration $N_{total} = N_c \times N = 6400$, $\frac{\log_2(MP)}{N_c} = \frac{1}{8}$	68
Figure 3.7 Rayleigh Suburban Channel, $L_c = 16$, PER=0.01, Constant Packet Duration $N_{total} = N_c \times N = 840$, $\frac{\log_2(MP)}{N_c} = \frac{1}{4}$	69
Figure 3.8 Rayleigh Suburban Channel, $L_c = 8$, PER=0.01, $N=100$, $\frac{\log_2(MP)}{N_c} \in \{0.25, 0.5, 0.75, 1\}$	70
Figure 3.9 Rayleigh Suburban Channel, PER=0.01, $N=100$, $N_c = 24$, $M = 16$ and $P = 4$, $\frac{\log_2(MP)}{N_c} = \frac{1}{4}$	71

Figure 3.10 Rayleigh Suburban Channel, $L_c = 16$, PER=0.01, $N_c = 32$, $M = 8$ and $P = 4$, $\frac{\log_2(MP)}{N_c} = \frac{5}{32}$	72
Figure 4.1 FG corresponding to the joint APP in (4.18) for MCS	85
Figure 4.2 $M = 4$, $P = 4$, $N_c = 16$, $L_c = 64$ Rayleigh distributed taps exponentially decaying power delay profile for MAC, $J_I^n = 0$ and $J_\theta^n = 0$, $SNR_c = \frac{E_c}{N_0} = 0$ dB	94
Figure 4.3 $M = 4$, $P = 4$, $N_c = 16$, $L_c = 64$ Rayleigh distributed taps exponentially decaying power delay profile for MAC, $J_I^n = 0$ and $J_\theta^n = 0$	95

LIST OF ABBREVIATIONS

APP	A Posteriori Probability
AWGN	Additive White Gaussian Noise
BCJR	Bahl Cocke Jelinek Raviv (algorithm)
BDF	Bidirectional Decision Feedback
BER	Bit Error Ratio
BFC	Block Fading Channel
CCK	Complementary Code Keying
CDMA	Code Division Multiple Access
CMF	Channel Matched Filter
CPM	Continuous Phase Modulation
DFE	Decision Feedback Equalization
DFT	Discrete Fourier Transform
DSSS	Direct Sequence Spread Spectrum
EXIT	Extrinsic Information Transfer
FDM	Frequency Division Multiplexing
FG	Factor Graph
FH	Frequency Hopping
FTN	Faster-Than-Nyquist
GSM	Global System for Mobile Communications
IC	Interference Cancellation
IDMA	Interleave Division Multiple Access
ISI	Inter Symbol Interference
LBA	Limit Before Average
LLR	Log-likelihood Ratio
MAC	Multiple Access Channel
MAP	Maximum A Posteriori
M-BOK	M-ary bi-orthogonal keying
MCI	Multi Code Interference
MCS	Multi-Code Signaling
MF	Matched Filter
MFB	Matched Filter Bound
MGF	Moment Generating Function

MIMO	Multiple Input Multiple Output
ML	Maximum Likelihood
MLSE	Maximum Likelihood Sequence Estimation
MMSE	Minimum Mean Squared Error
MU	Multi-User
MUD	Multi-User Detection
MUI	Multi-User Interference
MU-RSSE	Multi-User Ungerboeck type Reduced State Sequence Estimation
OFDM	Orthogonal Frequency Division Multiplexing
PA	Pade Approximation
PAM	Pulse Amplitude Modulation
PCR	Plain Correlator Receiver
pdf	Probability Density Function
PEP	Pairwise Error Probability
PER	Packet Error Rate
PMF	Probability Mass Function
PSK	Phase Shift Keying
RRC	Root Raised Cosine
RSSE	Reduced State Sequence Estimation
SISO	Soft-Input-Soft-Output
SNR	Signal-to-Noise Ratio
SPA	Sum Product Algorithm
SSK	Space Shift Keying
U-RSSE	Ungerboeck type Reduced State Sequence Estimation
UWA	Underwater Acoustic
UWB	Ultra-Wideband
WSSUS	Wide Sense Stationary Uncorrelated Scattering
ZMCSCG	Zero Mean Circularly Symmetric Complex Gaussian

CHAPTER 1

INTRODUCTION

1.1 Motivation

The wireless radio channel is a challenging medium for communication. This is not only due to its susceptibility to noise, interference, and other channel impediments but also due to the unpredictable variation of these impediments over time as a result of user movement and environment dynamics. In wireless channels, the received signal power varies over large distances due to path loss and shadowing. Also, it varies over short distances due to the constructive and destructive addition of signal components coming from different paths in a random manner [1]. This small-scale variation of the channel is called fading and it makes the wireless channel completely different from its wired counterpart where the channel impulse response is often constant and deterministic. There is also the effect of inter-symbol interference (ISI), that is a form of distortion of a signal in which one symbol interferes with other symbols. It stems from the resolvable multi-paths, which is the propagation phenomenon that results in radio signals reaching the receiving antenna by two or more paths [1], and has to be mitigated for a reliable communication.

The main aim in this thesis is to propose multiple signaling waveforms (multi-code) based yet spectrally efficient modulation schemes and efficient receiver structures for them. Basically, we search for generic suboptimal sequence detection algorithm for a general class of modulation schemes, which is proven to be robust against multi-path propagation and shows almost optimal performance at

significantly reduced complexity in severe ISI channels. Moreover, performance analysis tools, which are useful to assess and improve the performance of the proposed schemes, are developed.

A general modulation format is considered in this thesis for linear channels impaired by additive white Gaussian noise (AWGN). This modulation can be represented as selection of one out of M waveforms per signaling interval to which an additional phase modulation is applied. We call this general type of signaling scheme Multi-Code Signaling (MCS), which allows the use of non-orthogonal signaling waveforms to attain higher spectral efficiencies. Many modulation schemes such as M -ary orthogonal signaling for direct sequence spread spectrum (DSSS) radio in [2–6], direct sequence code division multiple access (DS-CDMA) [7,8], complementary code keying (CCK) [9], M -ary bi-orthogonal keying (M-BOK) for ultra-wideband (UWB) radio [10], [11], and underwater acoustic (UWA) communication [12], standard phase shift keying (PSK) [7]; and recently proposed space shift keying (SSK) [13] exploiting orthogonality in spatial domain can be put into this framework. This communication technique allows transmission with a low probability of interception, and simultaneous use of a common channel by multiple users. It is also preferred in military applications for combating jamming and self-interference [7].

Due to the extremely high signal bandwidth of practical MCS waveforms, the multi-paths of the channel can be finely resolved at the receiver, which usually utilizes a RAKE processor to capture as much multi-path power as possible [7]. However, the dense multi-path dispersion together with non-ideal correlation properties of the signaling waveforms may cause significant amount of ISI, which necessitates equalization [14].

Our focus is on the maximum likelihood sequence estimation (MLSE) based equalization for the MCS modulation in this thesis. MLSE-based receivers, which are optimal in the sense of lowest packet error rate, are based on one of the two classic approaches proposed by *Forney* [15] and *Ungerboeck* [16], which are known to be mathematically equivalent yet with rather different implementations [17]. Forney's algorithm requires a noise-whitening filter after matched

filtering (MF) that transforms the channel into its minimum phase equivalent, but has to adapt to channel variations. On the other hand, Ungerboeck MLSE is directly applied to unwhitened observations obtained from conventional channel matched filter (CMF) [16,18]. Due to the exponential complexity of Forney and Ungerboeck type MLSE, several low complexity suboptimal detection schemes have been developed. A promising reduced complexity alternative to MLSE is reduced state sequence estimation (RSSE) with decision feedback [19], [20], [18]. RSSE provides an excellent tradeoff between performance and complexity by reducing the memory order of the Viterbi algorithm and employing conditional decision feedback to cancel the effect of the ISI [18].

With the use of RSSE, the equivalence between Forney and Ungerboeck type structures begins to disappear [18]. RSSE based on Forney model is sensitive to channel phase, and the performance may not be good for non-minimum phase channels, whereas Ungerboeck model is insensitive to this issue, and it may show certain advantages for channels with large delay spread. Moreover, if the Forney structure is adopted, a very high number of states is necessary even with the use of an optimized whitening filter transforming the channel into its minimum phase equivalent suitable for RSSE since noise whitening results in scattering of multipath power among the taps [21]. Contrary to the Forney type, the strongest tap collects all the multipath power and it is always chosen as the main tap in Ungerboeck style RSSE. Moreover, whitening filter implementation brings a severe computational burden on receiver complexity for channels with large dispersion and time varying nature. Thus, we adopt Ungerboeck approach throughout the thesis work.

An Ungerboeck type RSSE algorithm for BPSK modulation was studied in [18]. Recently, other reduced complexity Ungerboeck type receivers based on factor graphs (FG) and channel shortening idea with a mismatched model were studied in [22–24]. However, there is still a performance gap between the studied equalizer structures and the optimal one when complexity is constrained to be low, especially for channels with long memory and non-sparse structure [25]. It is also known that Ungerboeck type RSSE suffers from significant pre-cursor ISI [18], and graph based detection algorithms result in many cycles in the FG of long

ISI channels [22]. These exacerbate the equalization problem for channels with long memory [18], [26], [27]. Thus, it is necessary to search for more efficient equalizer structures with near optimum performance to complement the receiver for MCS in long ISI channels. In this thesis work, we propose a symbol rate operating reduced complexity soft-input-soft-output (SISO) detection algorithm based on Ungerboeck model for the general MCS format and channels with large delay spread.

In the light of this motivation, we now elaborate on the contribution and the outline of the thesis in the next section.

1.2 Outline and Contribution of the Thesis

The main contribution of the thesis is three-fold:

- Derivation of a reduced state Ungerboeck type maximum a posteriori (MAP) receiver based on Reduced State Sequence Estimation (RSSE) with *bias* correction for MCS type modulation by forming the Factor Graph (FG) and using Sum-Product Algorithm (SPA) framework (Chapter 2).
- Extension to multi-user scenario by unifying the reduced state Ungerboeck type MAP equalization and FG based SISO detection used to mitigate multi-user interference (MUI) substantiated with bidirectional RSSE per user (Chapter 4).
- Error probability analysis, which provides significant insight on the success of the proposed reduced state MAP receiver (in Chapter 2 and 4) in case of uncoded MCS transmission, and the packet error rate (PER) analysis based on the random coding approach that determines the *cutoff rate* by using the moment generating function (MGF) of the cutoff rate for coded MCS transmission in multi-path fading channel (Chapter 3).

In Chapter 2, first, a generic reduced complexity Ungerboeck type MAP receiver, directly operating on unwhitened channel matched filter (CMF) and code matched filter (MF) outputs at symbol rate and providing the a posteriori

probabilities (APP) of the MCS symbols with the help of bidirectional RSSE recursions, is proposed by applying the SPA to the obtained FG based on the Ungerboeck (unwhitened) observation model. Ungerboeck RSSE operations are substantiated with symbol rate bidirectional decision feedback (BDF) based on surviving paths of each state in order to eliminate post-cursor and pre-cursor ISI as well as multi-code interference (MCI) due to the non-ideal properties of the signaling waveforms and multi-path channel. Furthermore, the bias, induced by the anticausal part of the Ungerboeck ISI channel in RSSE operations, is compensated by BDF. This proposed receiver can be seen as a highly efficient reduced complexity implementation of MAP detection based on the Ungerboeck channel model in [28] with the use of bidirectional RSSE substantiated by bias correction idea in [29] extended to the MCS format.

It is observed that the proposed MAP receiver achieves near-optimum performance even without channel coding in comparison to the matched filter bound (MFB) especially for channels with large dispersion. The main advantage of this Ungerboeck based architecture is that its complexity can be arranged flexibly depending on the signaling parameters and channel characteristics. Furthermore, as compared to other reduced complexity SISO detection techniques, the proposed receiver operates on unwhitened observations without the need of computationally expensive operations like whitening, pre-filtering or mismatched detection based on channel shortening [23] and resorting to Gaussian assumption of the input alphabet. These make the proposed structure a promising one especially for channels with long memory and time varying environments where the use of adaptive algorithms is necessary [29].

Second, an error probability analysis is also carried out in Chapter 2 in order to gain some insight on the success of the reduced state Ungerboeck receiver and the selection of system parameters in design. Also, the conducted analysis helps us identify a *bias* term, originating from the anticausal part of the ISI after CMF, and its statistical properties for a stochastic channel with Gaussian distributed taps in MCS transmission are determined. These analyses can be exploited to determine how to transport bits optimally in highly dispersive channels for MCS, and to improve the proposed receiver's performance by a proper choice of the

signaling parameters.

In Chapter 3, different than the case in Chapter 2 dealing with uncoded MCS transmission, PER performance is analyzed when an outer channel coding is utilized in order to relate the success of the selected MCS scheme to the modulation parameters and statistical properties of the multi-path fading channel. Instead of using a specific coding structure in MCS, we adopt a random coding approach utilizing *cutoff rate* as a performance measure [7], which is widely used to assess achievable rates of coded modulation schemes. In the recent literature, Monte Carlo Simulation based bounds for the information rate of the mismatched receivers [30] employing Forney or Ungerboeck metric are obtained in [25] and [24], respectively. However, their practical usage is limited especially for fading channels with long memory and non-sparse structure, since they are based on the channel shortening idea which requires the optimization of a mismatched front-end filter and simulation based calculation of the conditional probability density functions (pdf) by using the BCJR algorithm [31]. On the other hand, the upper PER bound of the proposed Ungerboeck MAP receiver with a given finite block length is obtained based on the cutoff rate measure analytically by using the error probability analysis in Chapter 2. The PER analysis is fulfilled by resorting to the limit-before-average (LBA) technique [32, 33] to tighten the bounds in quasi static fading, and approximating the MGF of the cutoff rate by employing a limited number of exactly specified moments with Pade approximation (PA) [34]. This cutoff rate based analysis of the coded MCS transmission leads also to a significant insight by demonstrating how the modulation related parameters such as bandwidth expansion ratio, number of signaling waveforms, outer channel coding rate are optimized to improve the performance of Ungerboeck type reception similar to the coding-spreading tradeoff idea in [35, 36].

In Chapter 4, the extension of the proposed reduced state Ungerboeck MAP receiver in Chapter 2 to multiple access channel (MAC) at symbol rate is realized by using an Ungerboeck type factorization of probability density functions. The resultant soft output iterative multi-user detector (MUD), which has linear complexity in the number of interfering users, is actually the unification of bidirectional Ungerboeck RSSE recursions in [37] (Chapter 2) applied to each

user separately for ISI and MCI compensation and the use of SPA framework to provide soft MUI mitigation similar to [22] based on the obtained Ungerboeck type FG for MAC. Similar to the bias correction technique in Chapter 2, the bias, induced by the the use of RSSE per user, is also compensated with the help of iterative BDF which is instrumental in eliminating the post- and pre-cursor ISI, MCI and MUI for MCS. The proposed MUD exhibits a close performance to the reference MFB even without outer channel coding at significantly lowered complexity in dense multi-path environments.

To sum up, in this thesis, a general MCS transmission model is developed and used to obtain an Ungerboeck FG, which is the basis for SPA to obtain the efficient implementation of the MAP receiver. The model provides a general description for many communication schemes in linear channels impaired by AWGN. Thus, the proposed receiver architectures here confirm, compare, and complement many previous work by changing several system parameters generalized to MCS format.

CHAPTER 2

A GENERIC REDUCED COMPLEXITY UNGERBOECK TYPE MAP RECEIVER FOR MULTI-CODE SIGNALING (MCS): SINGLE USER CASE

2.1 Introduction

A general modulation format is studied in this thesis for linear channels impaired by additive white Gaussian noise (AWGN). This modulation can be represented as selection of one out of M waveforms per signaling interval, to which an additional phase modulation is applied. As we mention in the introduction part, we call this general type of signaling scheme Multi Code Signaling (MCS), a more general form of the M -ary quasi orthogonal signaling, which allows use of non-orthogonal signaling waveforms to obtain higher spectral efficiencies. In this chapter, we propose a generic receiver for severe inter-symbol interference (ISI) channels based on maximum likelihood sequence estimation (MLSE) employing a generalized Ungerboeck metric with significantly reduced complexity for MCS. That is to say, it operates directly on the unwhitened matched filter (MF) outputs without using any pre-filtering or whitening type operations before sequence detection at symbol rate, and it generates soft output in a very efficient manner for MCS modulation. Before going into the details of the contribution in this chapter, it is better to mention previous works about the topic of interest in the literature.

The dense multi-path dispersion together with non-ideal correlation properties of the signaling waveforms may cause significant amount of ISI, which necessitates equalization [14]. In order to mitigate the effect of ISI, RAKE type correlators followed by *chip rate* unidirectional or bidirectional decision feedback (BDF) were investigated in [12, 38, 39] without any regard to noise correlations at the RAKE outputs. There are also studies based on minimum mean squared error (MMSE) equalization at *chip rate* for DS-CDMA systems such as [8]. Recently, conventional RAKE correlators [7] were replaced by channel matched filter (CMF) to capture all the available multipath diversity [11, 38, 39]. CMF followed by *symbol rate* decision feedback was proposed for M-BOK and CCK modulation in [11], [40].

As to the MLSE-based equalization techniques in the literature, Ungerboeck type chip rate MLSE, performed by the Viterbi algorithm, was proposed for DSSS systems in [41]. However, chip rate processing after MF requires excessive processing, especially if the delay spread of the channel is large. Alternatively, symbol rate MLSE with Ungerboeck formulation for classical DSSS radios was obtained in [42]. Among symbol rate operating receivers, Viterbi equalizers in [43], [44], the derivation of which are based on various simplifications, still need high complexity for channels with large dispersion.

The complexity reduction technique based on reduced state sequence estimation (RSSE) with decision feedback [19], [20] is among the most common variations of the MLSE. RAKE reception followed by symbol rate Viterbi equalization without any consideration to noise correlation was proposed for M-BOK DS-UWB systems in [10], where decision feedback was utilized to reduce complexity. A Forney type RSSE at symbol rate was studied for CCK modulation in [45] and [46]. Forney type reduced state algorithms are efficient and frequently employed with pre-filtering at reasonable complexity in practical applications such as Enhanced Data rates for Global System for Mobile Communications Evolution (GSM / EDGE) [47, 48] if the channel dispersion is limited with a moderate number of taps. Also, reduced state maximum a posteriori (MAP) sequence detection was proposed to produce soft outputs based on Forney model in [49–51].

The equivalence between Forney and Ungerboeck type structures begins to disappear in case of RSSE [18]. Ungerboeck model may show certain advantages for channels with large delay spread as explained in Chapter 1. Recently, Ungerboeck type receivers based on factor graphs (FG) and channel shortening with a mismatched model were studied in [22–24]. MAP equalization based on Ungerboeck type factorization is also used for the decoding of coded orthogonal frequency-division multiplexing (OFDM) schemes in [52]. However, there is still a performance gap between the studied receiver architectures and the optimal one when complexity is constrained to be low especially for channels with long memory and non-sparse structure [25].

The contribution of this chapter is two-fold. First, by forming the FG for the problem of interest and sum-product algorithm (SPA) framework based on the developed symbol rate vector-matrix signal model, a generic reduced complexity Ungerboeck type MAP receiver is proposed. It supplies the a posteriori probabilities (APP) with the help of symbol rate forward and backward Ungerboeck type RSSE recursions (similar to the Forney type reduced state BCJR algorithm in [50, 51]), where BDF is instrumental in eliminating the post- and pre-cursor ISI and multi code interference (MCI) for MCS. The proposed structure, showing almost optimal performance with reference to the matched filter bound (MFB) [53], performs the function of demodulation and symbol rate equalization jointly by taking the post- and pre-cursor ISI as well as MCI caused by non-ideal cross- and auto-correlations of the signaling waveforms and multipath channel into account after the CMF operation. This proposed soft output Ungerboeck RSSE with BDF can be regarded as the MCS extended reduced complexity implementation of the MAP receiver based on Ungerboeck model in [28] enhanced with the use of bias correction idea for RSSE in [18]. To the best of our knowledge, the main novelty lies in the introduction of a reduced state MAP receiver for the general MCS format, and its consequences regarding performance.

The proposed scheme here is the unification of Ungerboeck type reduced complexity MAP detection framework for MCS, and is closely related to many previous work by changing several system parameters related to modulation and complexity. Hence, it also confirms and complements many previous studies.

Although the results are depicted without outer channel coding, the proposed structure can be utilized as the equalization stage supplying APPs to a soft-input-soft-output (SISO) channel decoder, irrespective of whether the channel is minimum-phase, maximum-phase or mixed-phase. ¹

For performance evaluation; an error probability analysis is carried out that provides significant insight on the success of the reduced-state Ungerboeck type receiver structure and the selection of system parameters in design. The analysis indicates a *bias* term that originates from the anticausal part of the ISI and MCI left after CMF. The conducted analysis, resulting in an expression for the variance of the bias term of this scheme for a stochastic channel with Gaussian distributed taps, can be utilized to determine how to transport bits optimally in highly dispersive channels. Furthermore, we derive an analytical approximation for the bit error rate (BER) of the proposed Ungerboeck type RSSE with BDF in case of Rician faded channel taps. It is shown to be very accurate and reflects the dependence of performance on the system parameters and channel characteristics. To sum up, together with the simulation results, the high performance and competitiveness of the proposed approach for a proper choice of the signaling parameters for the MCS class are presented.

This chapter constitutes the basis for subsequent chapters, thus we mention and use the models and results obtained here frequently through the thesis. The journal version of this chapter can be found in our published work [37].

2.2 System Model

The studied modulation scheme is a general form of M -ary orthogonal keying where one of the M distinct signal waveforms is chosen for transmission at each signaling interval. Also, phase modulation with cardinality P is applied to each transmitted waveform. Then, the baseband equivalent of the transmitted signal

¹ Forney type reduced state equalizers are sensitive to this issue as reported in [20, 25, 51, 54].

$x(t)$ can be written as

$$x(t) = \sum_{n=0}^{N-1} g_{I_n}(t - nT)e^{j\theta_n} \text{ for } I_n \in \{1, \dots, M\} \quad (2.1)$$

where $g_i(t)$, $i = 1, \dots, M$ are signaling waveforms limited to a band $(-\frac{W}{2}, \frac{W}{2})$ with a bandwidth expansion ratio N_c .² The $\{I_n, \theta_n\}$ pair denotes the n^{th} transmitted symbol where I_n is the index of the transmitted waveform within $A_I = \{1, \dots, M\}$ and θ_n from $A_\theta = \{\frac{2\pi}{P}(i-1)\}_{i=1}^P$ is the phase information at the n^{th} signaling interval.³ The pair $\{I_n, \theta_n\}$ is determined according to the information bits sent. Transmitted waveforms $g_i(t)$ do not necessarily have to be orthogonal in our scheme. The duration to transmit each symbol ($\{I_n, \theta_n\}$) is T and bandwidth expansion ratio N_c is approximately taken as $N_c \approx WT$. One data block consists of N symbols, so it is possible to transmit $N \log_2(MP)$ bits over a block in the uncoded case. In this work, this modulation is called as Multi Code Signaling (MCS) in that it includes classical unspread PSK modulation ($M = 1, N_c = 1$), CCK, M-BOK, Direct Sequence UWB radio and SSK⁴ in spatial domain with proper choices of M, P, N_c values.

The signal in (2.1) is transmitted through a quasi-static channel having a baseband equivalent impulse response $h(t)$. The received waveform in the baseband can be written as

$$r(t) = h(t) * x(t) + n(t) = \sum_{n=0}^{N-1} s_{I_n}(t - nT)e^{j\theta_n} + n(t) \quad (2.2)$$

where $s_i(t) = g_i(t) * h(t)$, $i = 1, \dots, M$. The complex Gaussian baseband noise process $n(t)$ is assumed to have circular symmetry and a flat power spectral density $2N_0$ in the band of interest. The channel response $h(t)$ is assumed to be static over a duration T_0 which includes both the transmission time required for one block ($N \times T$) and the length of the channel impulse response (L_0), namely, $T_0 = NT + L_0$.

² $g_i(t)$ can be chosen to be composed of N_c chip pulses with duration $T_c \approx \frac{1}{W}$ as in DSSS communication.

³ PSK is chosen within MCS so that the constructed signal has small peak-to-average power ratio (PAPR). However, this restriction can be removed, and QAM constellations can be employed instead of using $e^{j\theta_n}$ in (2.1).

⁴ SSK can be put into the same equivalent model as MCS, where one can visualize each column of the $n_r \times n_t$ channel matrix in MIMO channel as the MCS signaling waveforms.

2.3 MLSE Receiver for MCS based on Ungerboeck Observation Model

In this section, we first derive the optimal detector based on symbol rate MLSE for MCS, directly applied to unwhitened matched filter (MF) outputs, which is known as the *Ungerboeck* type MLSE [16] in the literature. Then, a reduced complexity implementation for it is proposed in the subsequent section. To start with, the following definitions will be helpful in deriving the detector:

$$\mathbf{I}_N = \{I_0, I_1, \dots, I_{N-1}\} \text{ for } I_n \in A_I, \quad \Theta_N = \{\theta_0, \theta_1, \dots, \theta_{N-1}\} \text{ for } \theta_n \in A_\theta. \quad (2.3)$$

The sequences \mathbf{I}_N and Θ_N are to be detected by using the observation $r(t)$ described in (2.2).

2.3.1 Optimum Maximum Likelihood Detection

The optimal maximum likelihood (ML) detection rule [7] finds the candidate sequence $\{\hat{\mathbf{I}}_N, \hat{\Theta}_N\}$ of information symbols that maximizes the likelihood of the received signal during one block duration, namely, $r(t)$, $0 \leq t \leq T_0$. This is equivalent to maximizing the log-likelihood function, which can be reduced into the following form in terms of matched filter (MF) outputs and waveform correlations upon neglecting constant scaling factors and additive terms

$$\begin{aligned} \{\hat{\mathbf{I}}_N, \hat{\Theta}_N\} = \operatorname{argmax}_{\{\mathbf{I}_N, \Theta_N\}} & \left(2 \operatorname{Re} \left\{ \sum_n e^{-j\theta_n} r_n^{I_n} \right\} \right. \\ & \left. - \sum_{n_1} \sum_{n_2} R_{I_{n_1}, I_{n_2}}(n_2 - n_1) e^{j(\theta_{n_1} - \theta_{n_2})} \right) \end{aligned} \quad (2.4)$$

where

$$r_n^i \triangleq \int_{T_0} r(t) s_i^*(t - nT) dt = r(t) * h^*(-t) * g_i^*(-t) \Big|_{t=nT} \quad (2.5)$$

$$R_{i,j}(n) \triangleq \int_{T_0} s_i(u) s_j^*(u - nT) du = s_i(t) * s_j^*(-t) \Big|_{t=nT} \quad (2.6)$$

for $i, j = 1, \dots, M$ and $n = 0, \dots, N-1$. The receiver structure based on the detection rule in (2.4) is depicted in Fig. 2.1. The optimal detector is composed of a channel matched filter (CMF) followed by M code matched filters corresponding to different signaling waveforms $g_i(t)$ and MLSE type processing operating

at symbol rate. The first term in (2.4) corresponds to the MF operation and the second term in (2.4) is related to the cancellation of ISI and multi code interference (MCI), which is the cross interference among MF outputs caused by the channel and the non-ideal properties of the signaling waveforms. Equation

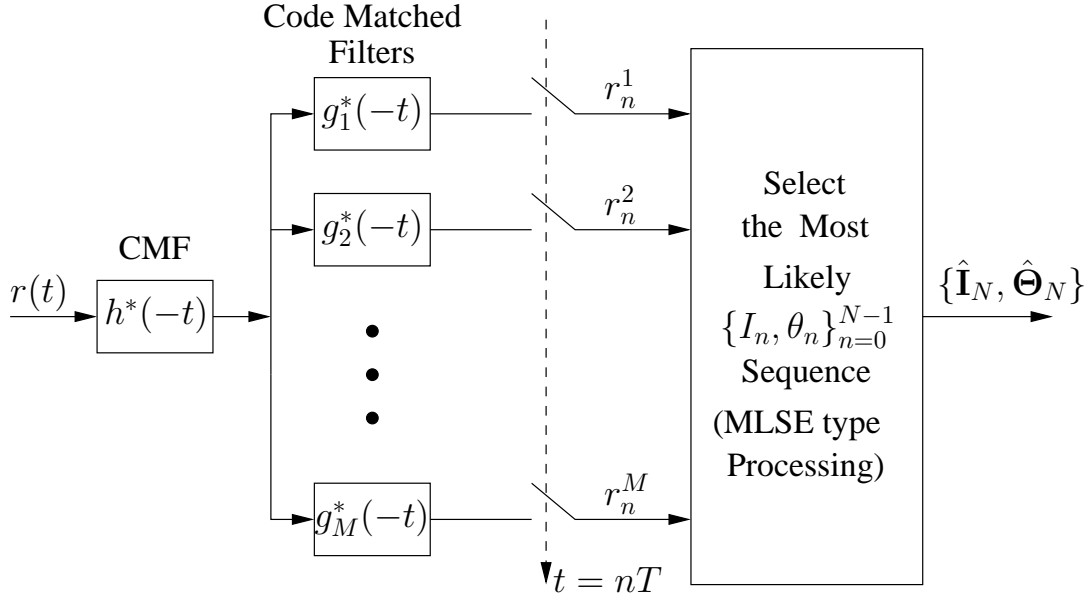


Figure 2.1: Block diagram of the optimum receiver for MCS: CMF followed by code MFs precedes MLSE type processing

(2.4) indicates that r_n^i 's become the sufficient statistics to detect sequences \mathbf{I}_N and Θ_N . At first glance, the computational complexity of the optimal detector can be thought as in the order of $O\{(MP)^N\}$. However, it is practically reasonable to assume that $R_{i,j}(n)$ is non-zero only for some finite n values due to the finite delay spread of the channel. This makes the recursive computation of (2.4) feasible when using the Viterbi algorithm as explained in Section 2.3.4.

2.3.2 Discrete Time Equivalent Model for MCS

In this part, the discrete time equivalent model for MCS is developed by using the MF outputs sampled at symbol rate. There is no loss of information if

observation $r(t)$ is sampled at the Nyquist rate W first ⁵, then CMF and code MF operations at the receiver side can be realized at rate W by utilizing the equivalent discrete time channel response $\{h_n\}_{n=0}^{L_c-1}$. ⁶ If the delay spread of the channel is T_d , then the number of equivalent channel taps and the equivalent channel vector can be expressed as $L_c = \lceil T_d W \rceil + 1$ and $\mathbf{h} = [h_0, \dots, h_{L_c-1}]^T$ respectively. Throughout the thesis, we assume that h_n 's are perfectly estimated at the receiver, ⁷ and the sampling rate W is approximately taken as $\frac{1}{T_c}$. ⁸ After symbol synchronization and CMF together with code MF operations at Nyquist rate, $R_{i,j}(n)$ in (2.6) can be calculated as

$$R_{i,j}(n) = \sum_{m_1=0}^{L_c-1} \sum_{m_2=0}^{L_c-1} h_{m_1} h_{m_2}^* r_g^{i,j}(nT - (m_1 - m_2)T_c) = \mathbf{h}^H \mathbf{R}_g^{i,j}(n) \mathbf{h} \quad (2.7)$$

where $\mathbf{R}_g^{i,j}(n)$ is an $L_c \times L_c$ Toeplitz matrix exhibiting the code correlations at different delays so that $(m, k)^{th}$ element of the Toeplitz matrix is $r_g^{i,j}(nT + (m - k)T_c)$. Here, $r_g^{i,j}(t)$ is the cross-correlation function between i^{th} and j^{th} signaling waveforms and is given by $r_g^{i,j}(t) = g_i(t) * g_j^*(-t)$.

MF outputs \mathbf{r}_n 's in (2.5), yielding the sufficient statistics, sampled at symbol period $T = N_c T_c$ can be modeled by using (2.2) and (2.6) as

$$\mathbf{r}_n = \sum_{l=-(L-1)}^{L-1} \mathbf{R}^T(l) \mathbf{c}_{n-l} e^{j\theta_{n-l}} + \mathbf{v}_n \quad (2.8)$$

for $n = 0, \dots, N - 1$, where

- $\mathbf{r}_n = [r_n^1, \dots, r_n^M]^T$ are the MF outputs at time $t = nT$,
- $\mathbf{R}(l)$ is the $M \times M$ sampled cross-correlation matrix of the signaling waveforms passing through the channel with $(i, j)^{th}$ element $R_{i,j}(l) = (s_i(t) * s_j^*(-t)) \Big|_{t=lT}$ given in (2.6),

⁵ $r(t)$ is first pre-filtered by a brick-wall filter of two-sided bandwidth W to sample it at the Nyquist rate, where $\frac{W}{2}$ is the bandwidth of the information carrying part of $r(t)$.

⁶ In general, $h(t)$ is time unlimited, so that there are an infinite number of nonzero $\frac{1}{W}$ spaced channel taps. However, $h(t)$ can be well approximated by a finite number of nonzero channel coefficients as $h(t) = \sum_{n=0}^{L_c-1} h_n \delta(t - \frac{n}{W})$ [55].

⁷ By using a training sequence in front of each block, it is possible to fulfill timing synchronization and estimation of these channel taps. Also, tracking of the channel taps is feasible in a decision directed mode for slowly time varying environment.

⁸ The channel can also be well approximated with chip-spaced taps if the signaling waveforms have small excess bandwidth or $T_d W \gg 1$.

- The variable L denotes the effective channel length in terms of symbol period,
- \mathbf{c}_k is the $M \times 1$ coordinate column vector whose i^{th} element is one if the i^{th} signaling waveform is transmitted at k^{th} epoch, and it can be seen as the equivalent codeword for MCS modulation. For example, if $M = 4$ and $I_k = 3$, then $\mathbf{c}_k = [0 \ 0 \ 1 \ 0]^T$.
- \mathbf{v}_n is the noise vector sequence after CMF and code MFs with correlation matrix $E\{\mathbf{v}_n \mathbf{v}_{n-l}^H\} = \mathbf{R}^T(l) N_0$.⁹

One can see that $\mathbf{R}(l) = \mathbf{R}^H(-l)$ since $r_g^{i,j}(\tau) = (r_g^{j,i}(-\tau))^*$. Also, $R_{i,j}(n) = 0$ in (2.7) $\forall i, j = 1, \dots, M$ for $|n| \geq L$ where

$$L = \begin{cases} \lfloor \frac{L_c-1}{N_c} \rfloor + 2 & \text{if } L_c > 1, \\ 1 & \text{if } L_c = 1 \end{cases} \quad (2.9)$$

since $\mathbf{R}_g^{i,j}(n)$ is all zero matrix if $n > \lfloor \frac{L_c-1}{N_c} \rfloor + 1$.

After matched filtering and sampling at symbol rate ($\frac{1}{T}$), the effective length of the channel L in (2.9) is significantly reduced due to spreading since it is expected to be fairly small compared to L_c . This model will be useful in deriving the reduced complexity receiver in the next section.

2.3.3 Comments on Forney and Ungerboeck Approaches

As can be seen from the equivalent model (2.8), both post- and pre-cursor ISI and MCI exist and the noise is colored. In the *Forney* approach [15], a filter is used to whiten the noise and remove the pre-cursor ISI component. On the other hand, we now derive a sequence detection for the general class of MCS, directly applied to unwhitened MF outputs, which is known as the *Ungerboeck* type MLSE [16] in the literature. It is known that *Forney* and *Ungerboeck* type approaches are mathematically equivalent for MLSE and maximum a posteriori (MAP) type receivers although their implementations are quite different [17], [28].

⁹ It is assumed that the baseband signaling waveforms have unit energy, then the term N_0 here is taken as $\frac{1}{\text{SNR}}$.

2.3.4 Symbol Rate Ungerboeck Type MLSE Receiver

An Ungerboeck decision metric based on (2.4), up to $(k+1)^{th}$ signaling interval, can be obtained after some mathematical manipulations and using the symmetry in the equivalent channel matrix given by $\mathbf{R}(l) = \mathbf{R}^H(-l)$ in (2.8) as

$$\begin{aligned} \Lambda_{k+1}(\mathbf{I}_{k+1}, \boldsymbol{\Theta}_{k+1}) &= 2 \operatorname{Re} \left\{ \sum_{n=0}^k r_n^{I_n} e^{-j\theta_n} \right\} - \sum_{n_1=0}^k \sum_{n_2=0}^k R_{I_{n_1}, I_{n_2}}(n_2 - n_1) e^{j(\theta_{n_1} - \theta_{n_2})} \\ &= \sum_{n=0}^k \mu_n(\cdot), \end{aligned} \quad (2.10)$$

where

$$\begin{aligned} \mu_n(\mathbf{r}_n, I_n, \theta_n, \{I_k, \theta_k\}_{k=n-(L-1)}^{n-1}) &= 2 \operatorname{Re}\{r_n^{I_n} e^{-j\theta_n}\} - R_{I_n, I_n}(0) \\ &\quad - 2 \operatorname{Re} \left\{ e^{-j\theta_n} \sum_{m=1}^{L-1} R_{I_{n-m}, I_n}(m) e^{j\theta_{n-m}} \right\}. \end{aligned} \quad (2.11)$$

Then, the optimal sequence detection is

$$\{\hat{\mathbf{I}}_N, \hat{\boldsymbol{\Theta}}_N\} = \operatorname{argmax}_{\{\mathbf{I}_N, \boldsymbol{\Theta}_N\}} \Lambda_N(\mathbf{I}_N, \boldsymbol{\Theta}_N). \quad (2.12)$$

In (2.11), it is practically reasonable to assume that $R_{i,j}(m)$ is non-zero only for some finite m values for $|m| < L$ due to the finite delay spread of the channel. The metric $\mu_n(\cdot)$ can be interpreted as the Ungerboeck type branch metric, depending on the unwhitened matched filter outputs, and it is required for the recursive computation of (2.10). Thus, there are totally $(MP)^{L-1}$ states comprising of the symbols $\{I_{k-1}, \dots, I_{k-(L-1)}\}$ and $\{\theta_{k-1}, \dots, \theta_{k-(L-1)}\}$ at the k^{th} instant to realize (2.12) via the Viterbi algorithm.

2.3.5 Case Study: Ideal Spreading Codes

It is generally beneficial to find signaling waveforms with good aperiodic cross- and auto-correlation properties to reduce ISI and MCI and improve performance. To obtain more insight into the operation, one may consider the ideal situation where the waveforms have ideal cross and auto correlation values

$$r_g^{i,j}(nT_c) = E_s^i \delta_{i-j} \delta_n, \quad (2.13)$$

where E_s^i is the total energy of $g_i(t)$ and δ_n is the Kronecker delta function. The occurrence of ISI depends on the length of the channel auto-correlation function $r_h(t) = h(t) * h^*(-t)$. The effective channel length L , where $R_{i,j}(n)$ is zero for $|n| \geq L$, can be written as $L = \lfloor \frac{L_c - 1}{N_c} \rfloor + 1$ for ideal waveforms $\{g_i(t)\}_{i=1}^M$.

The MCS under study can take advantage of reducing ISI and MCI substantially by expanding the symbol duration (T) as compared to unspread schemes. For low rate (high processing gain) military type spread spectrum applications, codes with good correlation properties can be found; in which case, ISI occurs only if the delay spread is greater than the symbol duration T with probability $\frac{1}{M}$ at each code MF output as shown in Fig. 2.2. Hypothetically, if the codes are ideal, it can be deduced from (2.7) and (2.13) that

$$R_{i,j}(n) = h_m * h_{(-m)}^* \Big|_{m=N_cn} E_s^i \delta_{i-j}. \quad (2.14)$$

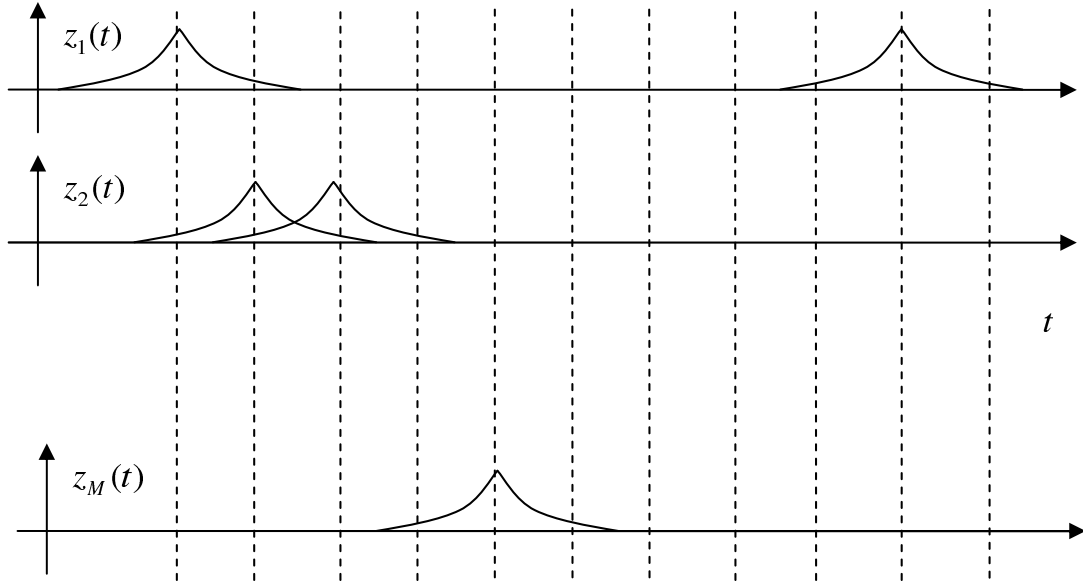


Figure 2.2: CMF and code matched filter outputs sampled at $t = nT$, where $z_i(t) = r(t) * h^*(-t) * g_i^*(-t)$, $i = 1, \dots, M$.

If the delay spread of the channel T_d is smaller than the symbol duration T , which implies $L_c < N_c$, $L = 1$. Thus, no ISI and MCI mitigation is needed. In

this case, we can write (2.14) as

$$R_{i,j}(n) = \left(\sum_{m=0}^{L_c-1} |h_m|^2 \right) E_s^i \delta_{i-j} \delta_n. \quad (2.15)$$

Then, the detection rule in (2.4) is reduced to

$$\{\hat{I}_k, \hat{\theta}_k\} = \operatorname{argmax}_{I_k, \theta_k} \left[2 \operatorname{Re} \left\{ e^{-j\theta_k} r_k^{I_k} \right\} - \left(\sum_{m=0}^{L_c-1} |h_m|^2 \right) E_s^{I_k} \right] \quad (2.16)$$

for $k = 0, \dots, N - 1$, which is similar to the classical symbol-by-symbol correlation detector for M -ary orthogonal signaling in AWGN channel [7]. This detector coherently combines all multipath components of the received signal via CMF. After code matched filtering, decision is made by selecting the largest output. This processing corresponds to the first two terms in the optimal branch metric calculation of the Ungerboeck type MLSE in (2.11). The third term in (2.11) is responsible for the ISI and MCI cancellation after RAKE correlator bank (composed of CMF and code MFs). With ideal signaling waveforms, the equivalent channel in (2.8) can be expressed as

$$r_n^i = E_s^i \left(\sum_{m=0}^{L_c-1} |h_m|^2 \right) \delta_{i-I_n} e^{j\theta_n} + v_n^i \quad (2.17)$$

for $i = 1, \dots, M$, which justifies that the total multipath diversity is attained.

2.4 A Reduced Complexity MAP Receiver for MCS based on Ungerboeck type Factor Graph (FG) and Sum-Product Algorithm (SPA) Framework

The complexity of the MLSE implementation in (2.10) can be reduced by confining the number of states to a value with the help of decision feedback. This approach is known as the Reduced State Sequence Estimation (RSSE) in the literature ([18], [19], [20]). The reduced state vector at time k can be defined as

$$S_k = \left[I_{k-1} \quad \dots \quad I_{k-J_I}, \theta_{k-1} \quad \dots \quad \theta_{k-J_\theta} \right]. \quad (2.18)$$

The total number of states used for waveform information ($I_k \in A_I$), and for the phase information ($\theta_k \in A_\theta$) are defined as $S_w = M^{J_I}$ and $S_{ph} = P^{J_\theta}$

respectively. Then, $S_{total} = S_w \times S_{ph} = M^{J_I} P^{J_\theta}$ states are required for the proposed RSSE.¹⁰ Since a reduced number of states cannot provide all the information needed to compute branch metrics in (2.11), RSSE utilizes the path, which possesses the best accumulated metric leading to each state, to extract the rest of the information. The case of $J_I = J_\theta = 0$ corresponds to the plain decision feedback equalization (DFE) after CMF and code MFs where no state memory is allocated.

The equivalence between the *Forney* and *Ungerboeck* approaches in MLSE begins to disappear in case of RSSE [18]. In the Ungerboeck approach, the strongest tap collects all the multipath power after CMF and it is always chosen as the main tap during RSSE; whereas noise whitening results in the scattering of multipath power, which diminishes the error event distances as the allocated state memory decreases in the Forney approach [18], [21].

2.4.1 Proposed Architecture based on Ungerboeck type Factorization

In this section, a reduced state MAP symbol detection algorithm based on RSSE, operating on forward and backward directions, is proposed for the general Ungerboeck observation model in (2.8). The focus of this part is to compute the a posteriori probability (APP) of each modulation symbol $\{I_k, \theta_k\}$ at each time epoch k given the MF outputs $\{\mathbf{r}_k\}_{k=0}^{N-1}$ and the a priori probabilities $P(\{I_k, \theta_k\})$ by assuming that the modulation symbols are independent of each other.

The joint APP of the transmitted symbols in terms of the reduced trellis states S_k and state dependent conditional symbol decisions in the survivor path of S_k

¹⁰ Set partitioning techniques can also be used to build S_k similar to ones in [45] for CCK modulation.

of RSSE can be expressed by using (2.10)

$$\begin{aligned}
& P\left(\{I_k, \theta_k, S_k\}_{k=0}^{N-1} \mid \{\mathbf{r}_k\}_{k=0}^{N-1}\right) \\
& \propto P\left(\{I_k, \theta_k\}_{k=0}^{N-1}\right) P\left(\{S_k\}_{k=0}^{N-1} \mid \{I_k, \theta_k\}_{k=0}^{N-1}\right) P\left(\{\mathbf{r}_k\}_{k=0}^{N-1} \mid \{I_k, \theta_k, S_k\}_{k=0}^{N-1}\right) \\
& \propto \exp\left\{\frac{\Lambda_N}{N_0}\right\} P(S_0) \prod_{k=0}^{N-1} P(\{I_k, \theta_k\}) p\left(S_{k+1} \mid S_k, I_k, \theta_k\right) \quad (2.19) \\
& = \prod_{k=0}^{N-1} P(S_0) \phi_k(\mathbf{r}_k, I_k, \theta_k) \psi_k(I_k, \theta_k, S_k) T_k(I_k, \theta_k, S_k, S_{k+1}) P(\{I_k, \theta_k\}),
\end{aligned}$$

where

$$\begin{aligned}
\phi_k(\mathbf{r}_k, I_k, \theta_k) & \triangleq \exp\left\{\frac{2 \operatorname{Re}\{r_k^{I_k} e^{-j\theta_k}\} - R_{I_k, I_k}(0)}{N_0}\right\} \\
\psi_k(I_k, \theta_k, S_k) & \triangleq \exp\left\{-\frac{2}{N_0} \operatorname{Re}\left\{e^{-j\theta_k} \left[\sum_{m=1}^{J_\theta} R_{I_k-m, I_k}(m) e^{j\theta_{k-m}} \right. \right. \right. \\
& \quad \left. \left. + \sum_{m=J_\theta+1}^{J_I} R_{I_k-m, I_k}(m) e^{j\hat{\theta}_{k-m}(S_k)} \right. \right. \\
& \quad \left. \left. + \sum_{m=J_I+1}^{L-1} R_{\hat{I}_{k-m}(S_k), I_k}(m) e^{j\hat{\theta}_{k-m}(S_k)} \right]\right\}\right\} \quad (2.20)
\end{aligned}$$

$$T_k(I_k, \theta_k, S_k, S_{k+1}) \triangleq p\left(S_{k+1} \mid S_k, I_k, \theta_k\right), \quad (2.21)$$

with the assumption that $0 \leq J_\theta \leq J_I \leq L-1$ ¹¹ for $k = 0, 1, \dots, N-1$, where $R_{i,j}(m) = \mathbf{h}^H \mathbf{R}_g^{i,j}(m) \mathbf{h}$, which can be calculated only once for each information block of length N by (2.7). In (2.20), $\{\hat{I}_m(S_k)\}_{m=0}^{k-(J_I+1)}$ and $\{\hat{\theta}_m(S_k)\}_{m=0}^{k-(J_\theta+1)}$ are the sequences of state dependent conditional symbol decisions in the surviving path of S_k in RSSE. The function $T_k(I_k, \theta_k, S_k, S_{k+1})$ is the trellis indicator function, equal to 1 if $\{I_k, \theta_k\}$, S_k , and S_{k+1} satisfy the trellis definition and to zero otherwise.

The reduced complexity algorithm is proposed based on the factor graph (FG) and the sum-product algorithm (SPA) [56] framework substantiated with RSSE. The Wiberg-type graph [56] corresponding to the joint APP in (2.19) is sketched in Fig. 2.3, where the hidden variables S_k have been explicitly represented. By applying the updating rules of the SPA, forward and backward Ungerboeck

¹¹ It is logical to take $0 \leq J_\theta \leq J_I \leq L-1$ since detected phase is meaningless if a wrong decision on I_k is made.

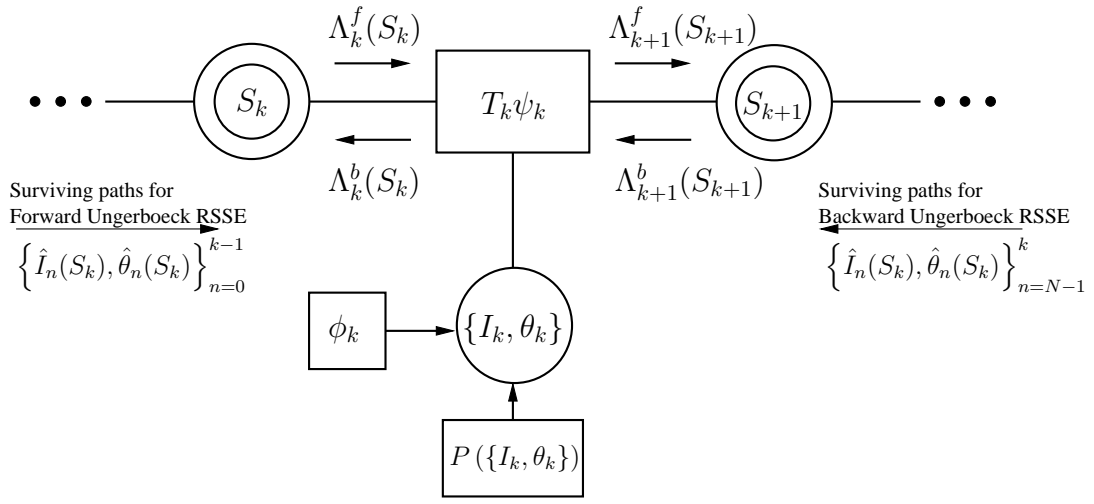


Figure 2.3: FG corresponding to the joint APP in (2.19) for MCS

messages, namely, $\Lambda_k^f(S_k)$ and $\Lambda_k^b(S_k)$ can be recursively computed similar to RSSE:

$$\begin{aligned}
 \Lambda_{k+1}^f(S_{k+1}) &= \sum_{\sim\{S_{k+1}\}} \Lambda_k^f(S_k) \phi_k(\cdot) \psi_k(\cdot) T_k(\cdot) P(\{I_k, \theta_k\}) \\
 \Lambda_k^b(S_k) &= \sum_{\sim\{S_k\}} \Lambda_{k+1}^b(S_{k+1}) \phi_k(\cdot) \psi_k(\cdot) T_k(\cdot) P(\{I_k, \theta_k\}), \quad (2.22)
 \end{aligned}$$

where we indicate by $\sum_{\sim\{x\}}$ the summary operator, i.e., a sum over all variables excluding x .

2.4.2 Bias Compensation in U-RSSE

The modification of the forward and backward Ungerboeck type RSSE recursions given in equation (2.22) is based on the concept of survivor paths from the classical Viterbi algorithm [50], [25] and a survivor map created during forward equalization is adopted for the backward recursion. However, it is known that the Ungerboeck type RSSE (U-RSSE) suffers from *correct path loss* even in the noiseless regime [18], [26], [27]. This phenomenon is caused by the untreated anti-causal interference, which aggravates the performance of reduced complexity equalization significantly for unspread conventional modulations. The pre-cursor ISI and MCI left after CMF and code MF operations are the sources of this anti-

causal interference. This interference leads to a *bias* that affects the tentative decisions in the survivor map, and the analytical expression for this *bias* term in Ungerboeck RSSE is obtained for general MCS scheme in Appendix A. This bias has to be compensated in forward surviving path construction by using (A.12) in Appendix A as

$$\left\{ \hat{I}_{k-J_I}(S_{k+1}), \hat{\theta}_{k-J_\theta}(S_{k+1}) \right\} = \arg \max_{\{I_{k-J_I}, \theta_{k-J_\theta}\}} \left[N_0 \ln \left(\Lambda_k^f(S_k) \phi_k(\cdot) \psi_k(\cdot) \right) - \beta_{k-J_\theta} \left(S_k, \{\tilde{I}_n, \tilde{\theta}_n\}_{n=0}^{N-1} \right) \right] \quad (2.23)$$

where

$$\begin{aligned} \beta_{k-J_\theta} \left(S_k, \{\tilde{I}_n, \tilde{\theta}_n\}_{n=0}^{N-1} \right) &= 2 \operatorname{Re} \left\{ \sum_{m=k-L+2}^{k-J_I} \sum_{l=k-m+1}^{L-1} R_{\hat{I}_m(S_k), \tilde{I}_{m+l}}(l) e^{j(\hat{\theta}_m(S_k) - \tilde{\theta}_{m+l})} \right. \\ &\quad \left. + \sum_{m=k-J_I+1}^{k-J_\theta} \sum_{l=k-m+1}^{L-1} R_{I_m(S_k), \tilde{I}_{m+l}}(l) e^{j(\hat{\theta}_m(S_k) - \tilde{\theta}_{m+l})} \right\} \\ &= 2 \operatorname{Re} \left\{ \mathbf{h}^H \left[\sum_{m=k-L+2}^{k-J_I} \sum_{l=k-m+1}^{L-1} \mathbf{R}_g^{\hat{I}_m(S_k), \tilde{I}_{m+l}}(l) e^{j(\hat{\theta}_m(S_k) - \tilde{\theta}_{m+l})} \right. \right. \\ &\quad \left. \left. + \sum_{m=k-J_I+1}^{k-J_\theta} \sum_{l=k-m+1}^{L-1} \mathbf{R}_g^{I_m(S_k), \tilde{I}_{m+l}}(l) e^{j(\hat{\theta}_m(S_k) - \tilde{\theta}_{m+l})} \right] \mathbf{h} \right\} \quad (2.24) \end{aligned}$$

for $k = 0, \dots, N-1$. In (2.23), $\beta_k(\cdot)$ is a state dependent bias correction term based on tentative decisions for future symbols $\{\tilde{I}_n, \tilde{\theta}_n\}_{n=0}^{N-1}$. The forward and backward RSSE stages in (2.22) are substantiated with bidirectional decision feedback (BDF), where the Viterbi like surviving path construction in (2.23) subtracts the effect of bias term $\beta_k(\cdot)$ by inserting the tentative decisions of post-cursor interference obtained from the surviving paths for each state $\left(\left\{ \hat{I}_m(S_k) \right\}_{m=0}^{k-(J_I+1)} \right.$ and $\left. \left\{ \hat{\theta}_m(S_k) \right\}_{m=0}^{k-(J_\theta+1)} \right)$ and the tentative decisions of pre-cursor ISI for future symbols $\left(\{\tilde{I}_n, \tilde{\theta}_n\}_{n=0}^{N-1} \right)$ in an iterative fashion. The detector eliminates the bias more accurately as the hard tentative decisions on MCS symbols obtained from the previous iteration become more reliable.

To simplify the calculation of $\beta_{k-J_\theta} \left(S_k, \{\tilde{I}_n, \tilde{\theta}_n\}_{n=0}^{N-1} \right)$, only the leading terms for $m = k - J_I$ and $m = k - J_\theta$ that correspond to *weight one* error events can be used in (2.24). The tentative decisions for future symbols $\left(\{\tilde{I}_n, \tilde{\theta}_n\}_{n=0}^{N-1} \right)$ are

exchanged between forward and backward RSSE stages such that the surviving path of backward stage is utilized as the tentative decisions for future symbols to construct the forward survivor map in (2.23) and vice versa. The survivor map for backward RSSE is constructed similar to forward map construction in (2.23) by reversing the input sequence, the equivalent channel and the corresponding MF outputs, and obtaining forward Ungerboeck metric in the reversed direction. In this case, the reversed sequence to be detected by the backward RSSE is $\{I'_n, \theta'_n\}_{n=0}^{N-1}$ where $I'_n = I_{N-1-n}$, $\theta'_n = \theta_{N-1-n}$, the corresponding channel and MF outputs are $\mathbf{R}'(l) = \mathbf{R}(-l)$ and $\mathbf{r}'_n = \mathbf{r}_{N-1-n}$ respectively. This approach is utilized only for the survivor map construction (2.23), required for forward and backward Ungerboeck path metric computation in (2.22). Finally, the marginal symbol APPs can be calculated by means of the following completion based on FG in Fig. 2.3 and by using the bias correction term $\beta_k(\cdot)$ in (A.12)

$$P\left(\{I_k, \theta_k\} \mid \{\mathbf{r}_n\}_{n=0}^{N-1}\right) = P(\{I_k, \theta_k\}) \sum_{\sim\{I_k, \theta_k\}} \left[\Lambda_k^f(S_k) \Lambda_{k+1}^b(S_{k+1}) \phi_k(\cdot) \psi_k(\cdot) T_k(\cdot) \exp\left\{-\frac{1}{N_0} \beta_k\left(S_k, \{\tilde{I}_n, \tilde{\theta}_n\}_{n=0}^{N-1}\right)\right\} \right] \quad (2.25)$$

and the corresponding MAP symbol detection rule is

$$\{\hat{I}_k, \hat{\theta}_k\} = \arg \max_{\{I_k, \theta_k\}} P\left(\{I_k, \theta_k\} \mid \{\mathbf{r}_n\}_{n=0}^{N-1}\right) \quad (2.26)$$

where $\phi_k(\cdot)$ is responsible for CMF and code MF operations, $\psi_k(\cdot)$ and the bias correction $\beta_k(\cdot)$ cancel post-cursor and pre-cursor ISI and MCI terms that are not included in state S_k respectively.

2.4.3 Implementation Details and Computational Complexity

We call the receiver in (2.26) soft output symbol rate U-RSSE with BDF which realizes the operation of demodulation and equalization in a bidirectional fashion. The proposed receiver shown in Fig. 2.4 is composed of CMF and code MFs followed by bidirectional soft output U-RSSE at symbol rate. In Fig. 2.4, $\mathbf{h}^H \mathbf{R}_g^{i,j}(l) \mathbf{h}$, $i, j = 1, \dots, M$, $l = 0, \dots, L-1$ can be calculated only once for a certain estimated channel, and the RSSE stages decide on which $\{i, j, l\}$ values have to be used in BDF according to tentative conditional decisions obtained

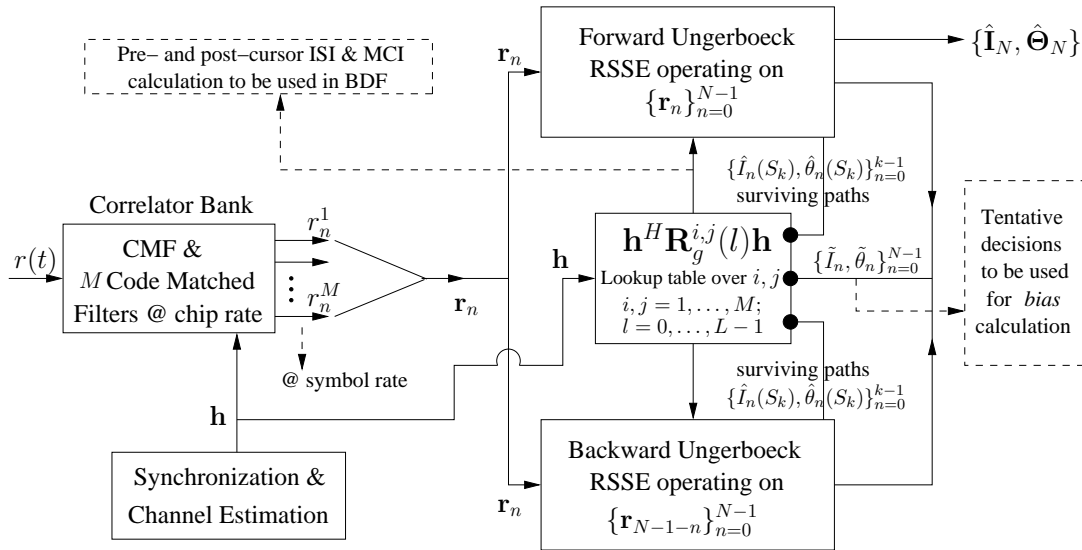


Figure 2.4: A Reduced Complexity Receiver for MCS based on a correlator bank (CMF and code MFs) followed by Symbol Rate Ungerboeck Type RSSE with BDF

from the survivor map. For additional performance gain, the forward and backward stages can be run in an iterative fashion. Forward and backward U-RSSE blocks exchange the information about post- and pre-cursor ISI and MCI, obtained from the survivor map, in order to calculate the bias in (2.24). In the first iteration of the algorithm, there are no tentative decisions for future symbols. Thus, forward and backward recursions are performed as if there were no bias. Then, the next forward or backward recursion utilizes the result of the previous recursion to compensate the bias with BDF. It has been observed in simulations that one forward and one backward iteration is sufficient to achieve near-optimum performance for the parameter set we choose. Throughout our study, hard tentative decisions about future symbols, namely, $\left(\{\tilde{I}_n, \tilde{\theta}_n\}_{n=0}^{N-1}\right)$ are exchanged between forward and backward stages in order to cancel the effect of bias in BDF operation in (2.23). Alternatively, one can utilize the soft decisions of the MCS symbols to cancel the effect of bias in (2.24) since the proposed detector supplies APPs of them iteratively.¹²

¹² The proposed MAP receiver can be seen as the inner channel decoder supplying symbol APPs to a SISO outer decoder in a turbo fashion. A priori information of the coded bits, provided by the SISO decoder, can also be exploited to construct soft estimates of the transmitted MCS symbols similar to [57]. These estimates are used for bias correction in the subsequent iterations.

The main advantage of the receiver given in Fig. 2.4 is that the main tap, containing all the paths' power, does not change in the forward or backward direction of U-RSSE. Thus, the performance does not depend on the direction of equalization from which the surviving path is constructed, and it is not sensitive to whether the channel is minimum, maximum or mixed phase. On the other hand, the performance highly depends on the direction of initial recursion from which the tentative decisions are obtained in Forney type RSSE [20, 25, 51, 54].

The proposed U-RSSE with BDF, providing soft outputs by operating bidirectionally, can be seen as the reduced complexity implementation of the MAP decoding based on Ungerboeck model in [28] with the use of bias correction idea in RSSE in [18]. It is the unification of Ungerboeck type sequence detection framework for the MCS format. Some of the receiver architectures in the literature are the special cases of the proposed U-RSSE based receiver. For example, the proposed U-RSSE with BDF for MCS reduces to the bidirectional iterative detection with soft decision feedback [21] for $J_\theta = J_I = 0$ with $M = 1, P = 2, N_c = 1$, to hard output BDF equalization of M-BOK after RAKE correlator bank in [11] for $J_\theta = J_I = 0$, and to hard output U-RSSE structure with bias correction for $M = 1$ in [18].

As to the complexity issue of the proposed U-RSSE with BDF for MCS, the bias correction does not contribute significantly to the computational load and storage requirement of the algorithm, which are mainly due to the forward and backward RSSE recursions in (2.22). Although, the use of code selection, i.e., increasing M requires more correlation operations at the receiver, it also does not have a remarkable effect on complexity. Throughout the work, we compare the systems at the same bandwidth and spectral efficiency by varying symbol duration T , thus we can calculate the complexity per packet duration T_0 . Since the computational complexity per state is $O(MP)$ from (2.22), and there are total $M^{J_I}P^{J_\theta}$ states, the computational load and storage requirement per packet can be expressed as in the order of $O(\frac{T_0}{T}M^{J_I+1}P^{J_\theta+1})$. Here, $\frac{T_0}{T} = N$, and there are total NN_c chips per packet implies that $O(\frac{1}{N_c}M^{J_I+1}P^{J_\theta+1})$ can be regarded as the complexity per chip while talking about complexity of the proposed algorithm U-RSSE with BDF. Since the proposed structure can be

seen as the MCS extended soft output Ungerboeck type reduced trellis MLSE with bias correction, it is possible to see that the complexity will become similar to that of the hard output U-RSSE structure for $M = 1$ in [18], and to many other previous works by properly choosing the modulation related parameters.

2.5 Error Probability Analysis for U-RSSE

2.5.1 Variance Analysis of the *Bias* Term in Ungerboeck Type RSSE

In this part, we inspect the *bias* term [18], [26], [27] originating from the anticausal part of the Ungerboeck ISI channel and affecting the performance of Ungerboeck type RSSE receivers for MCS by using an error probability analysis based on the equivalent signal model in (2.8). The *bias* term is analyzed for the general modulation format in Appendix A. The bias term is a random variable depending on error events, future inputs leading to anti-causal interference after CMF and multi-path channel. At this point, we evaluate the variance of this bias term in order to gain some insight on how it is affected by system parameters and channel characteristics. The variance of the bias term given the multi-path channel tap realization \mathbf{h} is obtained analytically in Appendix B by taking the expectation over all possible *weight one* error event distances and future inputs as

$$E_{\mathbf{e}, \mathbf{b}'_1 | \mathbf{h}} \{ |\gamma|^2 \} = \frac{2}{M^2 [MP - 1 + \mathbf{1} \{J_I > J_\theta\} (P - 1)]} \left[\sum_{l=J_I+1}^{L-1} \sum_{m_1=1}^M \sum_{m_2=1, m_2 \neq m_1}^M \sum_{p=0}^{P-1} \sum_{n=1}^M \left| \mathbf{h}^H \mathbf{A}_l^{(m_1, m_2, p, n)} \mathbf{h} \right|^2 + \sum_{l=J_\theta+1}^{L-1} \sum_{m_1=1}^M \sum_{p=1}^{P-1} \sum_{n=1}^M (1 + \mathbf{1} \{J_I > J_\theta\} \mathbf{1} \{l > J_I\}) \left| \mathbf{h}^H \mathbf{B}_l^{(m_1, p, n)} \mathbf{h} \right|^2 \right], \quad (2.27)$$

where

$$\mathbf{A}_l^{(m_1, m_2, p, n)} = \mathbf{R}_g^{m_1, n}(l) - e^{-j \frac{2\pi}{P} p} \mathbf{R}_g^{m_2, n}(l), \quad \mathbf{B}_l^{(m_1, p, n)} = 2 \sqrt{\sin^2 \left(\frac{\pi}{P} p \right)} \mathbf{R}_g^{m_1, n}(l), \quad (2.28)$$

and $\mathbf{R}_g^{m_1, m_2}(l)$ is an $L_c \times L_c$ Toeplitz matrix comprised of the waveform correlations at different delays as given in (2.7).

The channel is quasi-static over each information block by assumption, but it changes independently from packet to packet with duration T_0 . Thus, the variance is evaluated in an average sense by taking the expectation over the fading multi-path channel. The distribution of the equivalent channel vector \mathbf{h} in (2.7) is taken as jointly complex Gaussian with an $L_c \times 1$ complex valued mean vector $\boldsymbol{\mu}_h$ and $L_c \times L_c$ covariance matrix \mathbf{P}_h , namely, $CN(\boldsymbol{\mu}_h, \mathbf{P}_h)$. We take the possible correlation between multi-path components into account in our analysis. The correlation between equivalent channel taps (h_n 's) decreases as the delay spread of the channel becomes large compared to T_c for wide sense stationary uncorrelated scattering (WSSUS) channels [55]. The channel correlation matrix \mathbf{P}_h is assumed to be full rank, i.e., $\text{rank}\{\mathbf{P}_h\} = L_c$. It is possible to obtain the expectation of (2.27) over \mathbf{h} analytically. The averages $E_{\mathbf{h}} \left\{ \left| \mathbf{h}^H \mathbf{A}_l^{(m_1, m_2, p, n)} \mathbf{h} \right|^2 \right\}$ and $E_{\mathbf{h}} \left\{ \left| \mathbf{h}^H \mathbf{B}_l^{(m_1, p, n)} \mathbf{h} \right|^2 \right\}$, depending on waveform correlations and channel parameters, can be calculated analytically by using the moment generating function (MGF) based approach described in Appendix B.

In Fig. 2.5, the variance of the bias term in (2.27), which is normalized by symbol energy (E_s), is plotted for different MCS schemes by changing several system parameters such as M, P, N_c, J_I, J_θ at the same spectral efficiency. Three different MCS schemes, namely, $(M = 1, P = 4, N_c = 4)$, $(M = 4, P = 4, N_c = 8)$ and $(M = 16, P = 4, N_c = 12)$ are compared in terms of their corresponding bias values in case of U-RSSE for the same level of channel dispersion, data rate ($\nu = \frac{\log_2(MP)}{N_c} = \frac{1}{2}$ bits per channel use), and bandwidth by varying the spreading factor N_c . Each waveform is composed of N_c chips, and they are obtained by truncating length-255 *Kasami* codes [1]. Among the 16 *Kasami* length-255 sequences, M sequences are chosen and their lengths are reduced by simply choosing the first N_c chips. While constructing these M sequences with length N_c , the sequences with better correlation properties are chosen in order to get better bias reduction.¹³ By assuming a small excess bandwidth in the

¹³ In fact, multi-path channel may degrade the correlation and distance properties of the signaling waveforms substantially, thus it will be better to optimize sequences according to the given channel

chip pulse shape, we utilize a chip-spaced channel representation and generate chip-spaced sampled observations in simulations.

The plots (Fig. 2.5) for each MCS scheme are obtained at different complexity levels (different J_I and J_θ values) by varying the channel length (L_c) for exponentially decaying power delay profile [7]. It turns out that by a proper choice of the signaling parameters, e.g., using a sufficient number M of different waveforms for the encoding of information in order to be able to select a large modulation interval (T) for a given spectral efficiency, the performance can be optimized. As can be observed, it is not possible to get impressive improvement on the bias reduction for plain PSK modulation ($M = 1, P = 4, N_c = 4$) by increasing the number of states S_{total} for channels with large delay spread. On the other hand, the bias can be kept small enough for MCS with sufficiently large M for the same spectral efficiency and receiver complexities. For a proper operation, $E\{|\gamma|^2\}$ should be held much smaller than $E\{2N_0d^2(\mathbf{e})\}$ for a given error event \mathbf{e} based on (A.9). It is noted that this criterion is easily satisfied for MCS ($M = 16, P = 4, N_c = 12$) at operational SNR levels. This roughly corresponds to keeping the normalized variance of the bias below 0.1 for the successful operation of U-RSSE stages in case of no a-priori knowledge of the MCS symbols at first iteration. Otherwise, the effect of the anti-causal part of the Ungerboeck ISI will be more effective, and the residual bias cannot be reduced or removed with the help of iterative processing. Outer channel codes may also help MAP equalizer to cope with larger initial bias.

The key to the success of the proposed U-RSSE receiver lies in its usage of MCS with proper choices of M, P, N_c and symbol rate processing especially for channels with extremely long memory. CMF alleviates the post- and pre-cursor ISI and MCI significantly such that the bias correction term $\beta_k(\cdot)$ and $\psi_k(\cdot)$ become smaller compared to $\phi_k(\cdot)$ in (2.25). $\phi_k(\cdot)$, the only dominating term after CMF, collects all multi-path diversity on the main tap before RSSE operation. Moreover, the correlation between multi-path channel taps, leading to larger

characteristic, which brings performance enhancement due to the smaller bias and increased distances between codes. The bias analysis can be useful to make such optimization. Therefore, there are more efficient approaches (other than the truncation of *Kasami* codes) yielding waveforms with better cross- and auto-correlation properties, but this is beyond the scope of this study.

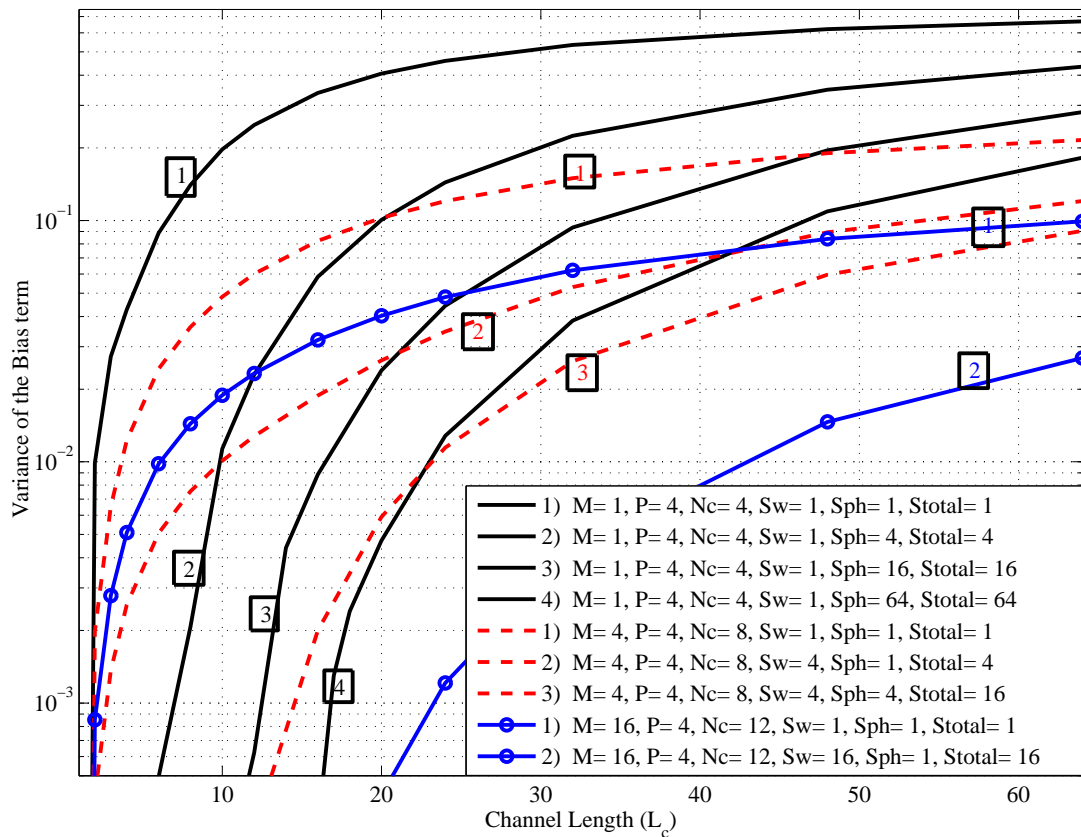


Figure 2.5: Variance of the normalized bias term in Ungerboeck RSSE after CMF and code MFs with respect to different number of independent Rayleigh channel taps, L_c , with exponentially decaying power delay profile for different S_{total} values (Spectral efficiency is $\frac{1}{2}$ in all curves).

bias values, aggravates the performance of the reduced trellis based Ungerboeck receiver. However, the correlation is known to become negligible as the channel length increases for WSSUS channels [55]. This makes the compensation of the bias feasible by an iterative bidirectional equalization proposed in Section 2.4.1.

The bias analysis in (2.27) appears as a useful design tool which provides interesting insights about how to determine the related system parameters of the general MCS scheme and the required complexity level (J_I and J_θ) to attain near optimum performance in highly dispersive channels. Moreover, one can optimize MCS waveforms, yielding average normalized bias below a threshold, to sustain proper U-RSSE operations for a given channel properties, complexity, and spectral efficiency.

2.5.2 Approximate Bit Error Rate for U-RSSE with BDF

In this part, we obtain an approximation for the BER performance of the proposed U-RSSE with BDF for MCS. The error events with *weight one* dominates the BER at operational SNR levels. In other words, the states in a reduced trellis pattern diverge from the correct sequence of states either at time $n = k - J_I$ or $n = k - J_\theta$ and remerge with it at a later time $n = k + 1$. Also, the bias term is assumed to be eliminated with the proposed symbol rate BDF operation reliably in the absence of error propagation from any previous error event during U-RSSE. The following approximation for BER is obtained in Appendix C

$$\begin{aligned}
P_b \approx & \frac{1}{2KM} \sum_{i=1}^K \left[\sum_{\Omega_1} w_b(I_1, I_2, p) \frac{\exp\left(-\boldsymbol{\mu}_h^H \mathbf{T}_3^{(I_1, I_2, p, i)} \boldsymbol{\mu}_h\right)}{\left| \mathbf{I}_{L_c} + \frac{E_c/N_0}{4 \sin^2\left(\frac{\pi}{2K}i\right)} \mathbf{T}_1^{(I_1, I_2, p)} \mathbf{P}_h \right|} \right. \\
& \left. + \sum_{\Omega_2} w_b(I_1, I_1, p) \frac{\exp\left(-\boldsymbol{\mu}_h^H \mathbf{T}_4^{(I_1, p, i)} \boldsymbol{\mu}_h\right)}{\left| \mathbf{I}_{L_c} + \frac{E_c/N_0}{4 \sin^2\left(\frac{\pi}{2K}i\right)} \mathbf{T}_2^{(I_1, p)} \mathbf{P}_h \right|} \right], \quad (2.29)
\end{aligned}$$

where the sets Ω_1 and Ω_2 are defined as

$$\begin{aligned}
\Omega_1 &= \{I_1, I_2, p \mid I_1, I_2 = 1, \dots, M, I_1 \neq I_2, p = 0, \dots, P-1\}, \\
\Omega_2 &= \{I_1, p \mid I_1 = 1, \dots, M, p = 1, \dots, P-1\}, \quad (2.30)
\end{aligned}$$

and

$$\begin{aligned}
w_b(I_1, I_2, p) &= \frac{1}{\log_2(MP)} \left[\frac{1}{P} \sum_{q=0}^{P-1} w_b^{\text{phase}}(q, \text{mod}\{q+p, P\}) + w_b^{\text{amplitude}}(I_1, I_2) \right], \\
\mathbf{T}_1^{(I_1, I_2, p)} &= \mathbf{R}_g^{I_1, I_1}(0) + \mathbf{R}_g^{I_2, I_2}(0) - \left\{ e^{j\frac{2\pi}{P}p} \mathbf{R}_g^{I_1, I_2}(0) + e^{-j\frac{2\pi}{P}p} (\mathbf{R}_g^{I_1, I_2}(0))^H \right\} \\
\mathbf{T}_2^{(I_1, p)} &= 4 \sin^2 \left(\frac{\pi}{P} p \right) \mathbf{R}_g^{I_1, I_1}(0) \tag{2.31}
\end{aligned}$$

$$\begin{aligned}
\mathbf{T}_3^{(I_1, I_2, p, i)} &= \mathbf{P}_h^{-1} - \mathbf{P}_h^{-1} \left(\frac{E_c/N_0}{4 \sin^2(\frac{\pi}{2K}i)} \mathbf{T}_1^{(I_1, I_2, p)} + \mathbf{P}_h^{-1} \right)^{-1} \mathbf{P}_h^{-1} \\
\mathbf{T}_4^{(I_1, p, i)} &= \mathbf{P}_h^{-1} - \mathbf{P}_h^{-1} \left(\frac{E_c/N_0}{4 \sin^2(\frac{\pi}{2K}i)} \mathbf{T}_2^{(I_1, p)} + \mathbf{P}_h^{-1} \right)^{-1} \mathbf{P}_h^{-1}. \tag{2.32}
\end{aligned}$$

In (2.31), $w_b^{\text{phase}}(p, q)$ and $w_b^{\text{amplitude}}(m, n)$ denote the number of bit errors if $\theta_k = \frac{2\pi}{P}p$, $I_k = m$ are transmitted, but $\theta_k = \frac{2\pi}{P}q$, $I_k = n$ are detected for $m \neq n$ and/or $p \neq q$, respectively. In (2.31)-(2.32), $\mathbf{R}_g^{i,j}(0)$ is an $L_c \times L_c$ correlation matrix between the i^{th} and j^{th} signaling waveforms as explained for (2.7). The chip pulses are assumed to have unit energy ($E_c = 1$), and the chip signal-to-noise ratio (SNR_c) is taken as $SNR_c = \frac{E_c}{N_0}$. In this analysis, the union bounding technique is used in a similar fashion to the analysis conducted for space-time block codes in [58]. Other bounding techniques such as given in [59] can be used to construct much tighter bounds, but the above approximation is accurate enough for $\text{BER} < 10^{-2}$, as can be seen in the simulation results section. Moreover, a careful inspection of (2.29) reveals that a full multipath diversity of order L_c is achieved if the signaling waveforms, $g_i(t)$'s, $i = 1, \dots, M$ are selected such that

$$\min_{I_1, I_2, p \in \Omega_1, \Omega_2} \left\{ \text{rank}\{\mathbf{T}_1^{(I_1, I_2, p)}\}, \text{rank}\{\mathbf{T}_2^{(I_1, p)}\} \right\} = L_c. \tag{2.33}$$

2.6 Simulation Results

2.6.1 BER Simulations

In this part, we investigate the performance of the proposed Ungerboeck RSSE (U-RSSE) for MCS. In our scheme, it is not necessary to exploit information from channel decoding and therefore, merely the U-RSSE is employed for attaining the multipath diversity without using any outer channel code. Error

rates at different receiver complexities are compared with that of the matched filter bound (MFB) [53]. MFB corresponds to the perfect ISI and MCI removal after CMF and code MF operations which yields the equivalent model $\mathbf{r}_n = \mathbf{R}^T(0)\mathbf{c}_n e^{j\theta_n} + \mathbf{v}_n$, $n = 0, \dots, N - 1$ from (2.8).

Fig. 2.6 shows the performance of U-RSSE for MCS where 8 signaling waveforms with QPSK modulation are transmitted, i.e., $M = 8, P = 4$. Each waveform is composed of 16 chips ($N_c = 16$), and they are obtained by truncating length-255 *Kasami* codes by simply choosing the first N_c chips of 16 Kasami sequences as explained in Fig. 2.5. There are more efficient approaches yielding waveforms with better cross- and auto-correlation properties, but we have shown that the proposed receiver performs well even without such optimizations. The MFB is obtained by using the $\mathbf{R}(0)$ matrix for these specific codes. Gray bit mapping is utilized for phase symbols. The channel is composed of 64 Rayleigh fading taps ($L_c = 64$) chosen from an exponentially decaying power delay profile where there is a 30 dB difference between the first and the last channel tap powers. The channel taps are assumed to be independent and a block fading model [1] is assumed with a block of length 100 M -ary symbols ($N = 100$). In this case, the spectral efficiency is $\nu = \frac{\log_2(MP)}{N_c} = \frac{5}{16}$ bits per channel use, and the effective channel length after MF and symbol rate sampling is 5 ($L = 5$). For full state MLSE, a total of $(MP)^{L-1} = 2^{20}$ states are required. Therefore, RSSE is used in order to attain an affordable, practical realization. It is important to note that different classes of bits impacting phase modulation or selecting waveforms have different BER, but here we plot the average of them.

The required complexity per signaling interval is $O(M^{J_I+1}P^{J_\theta+1})$. As can be seen from Fig. 2.6, if the ISI and MCI are not taken into account at MF outputs, which corresponds to the plain correlator receiver (PCR) [7], the performance is far apart from MFB. On the other hand, U-RSSE with one forward iteration, even for $J_I = 1$ and $J_\theta = 0$ ($S_w = 8, S_{ph} = 1, S_{total} = 8$), achieves roughly the full multipath diversity and there is only a remarkable 0.3 dB difference between its performance and the hypothetical MFB at uncoded BER = 10^{-4} . With the use of symbol rate BDF in U-RSSE operation proposed in (2.23) and shown in Fig. 2.4, the receiver perfectly removes post- and pre-cursor ISI and MCI components

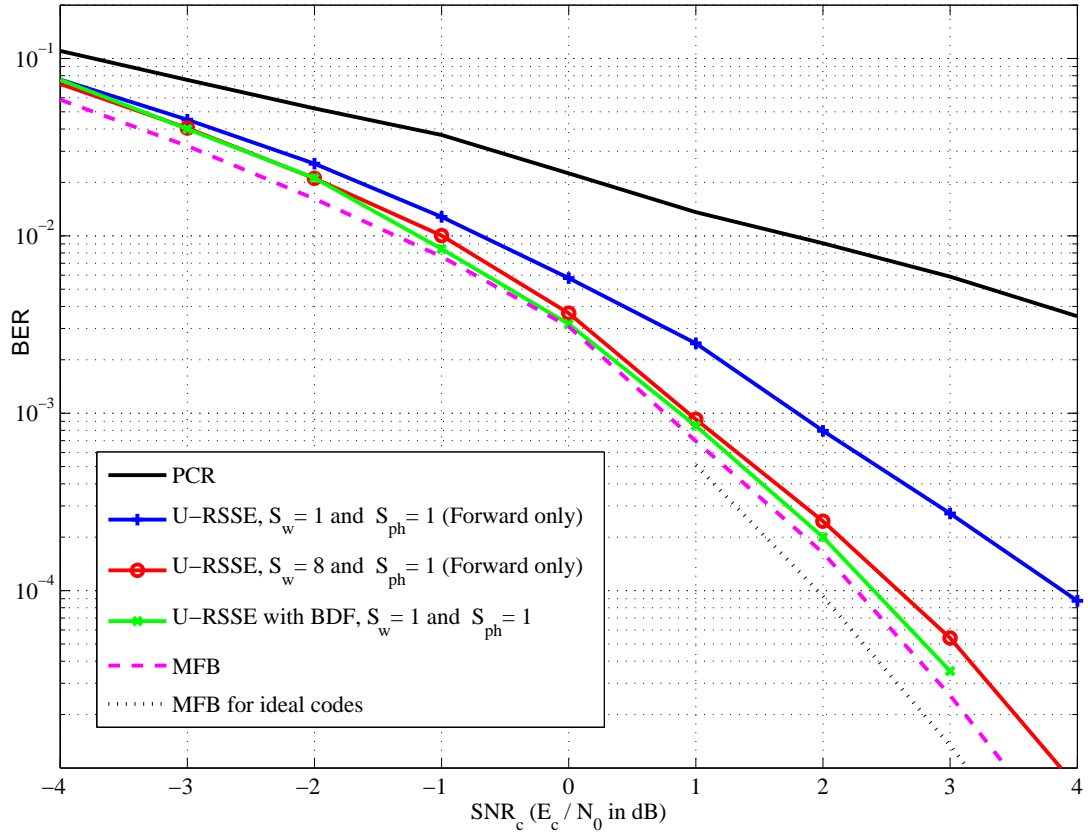


Figure 2.6: $M = 8$, $P = 4$, $N_c = 16$, channel is composed of $L_c = 64$ independent Rayleigh taps with exponentially decaying power delay profile

at the output of the CMF even for *one forward and backward iteration*, thus a performance approaching 0.1 dB to the MFB is attained even for $J_I = J_\theta = 0$ ($S_{total} = 1$). Note that this mode of operation corresponds to the plain decision feedback mode without allocating any state memory. Forward stage of U-RSSE with BDF for $J_I = J_\theta = 0$ is similar to the structure proposed in [11] for M-BOK. Moreover, the MFB obtained for the selected signaling waveforms is just 0.2 dB away from the MFB of ideal codes. Thus, we can say that the optimization on waveforms may not be so critical with the use of U-RSSE with BDF for this scenario.

In Fig. 2.7, the performance variation of various U-RSSEs (at different complexity levels) with respect to channel length (L_c) is shown at $SNR_c = 2$ dB. In this figure, the delay spread of the channel is held constant and the transmission rate (and bandwidth) is changed by varying T_c . In U-RSSE, the performance improves as the transmission bandwidth increases up to some point due to multipath diversity, then the performance begins to degrade gradually due to the aggravated effect of the *bias* term after MF operations. With a reasonable complexity, U-RSSE performance ($J_I = J_\theta = 1$, $S_{total} = M^{J_I} P^{J_\theta} = 32$) can be kept close to the MFB up to $L_c = 96$, which is 6 times larger than the symbol duration. Also, the performance degrades gracefully as the channel length increases. On the other hand, with the use of BDF in U-RSSE operation (explained in Fig. 2.4) to mitigate the effect of *bias* term, the receiver shows almost optimal performance up to $L_c = 256$, which is 16 times larger than the symbol duration. This remarkable performance is achieved at fully reduced complexity ($J_I = J_\theta = 0$, $S_{total} = 1$) and even with *one forward and backward* U-RSSE operation. These results show the robustness of the proposed scheme against multipath fading and justify the use of MCS as an effective modulation technique especially for extremely dispersive channels at low transmit power.

In Fig. 2.8, the performances of U-RSSE with with BDF for different MCS schemes are shown. Three different MCS schemes, namely, ($M = 1, P = 4, N_c = 4$), ($M = 4, P = 4, N_c = 8$) and ($M = 16, P = 4, N_c = 12$) are compared for the same spectral efficiency as done in Fig. 2.5. Here, the performance is shown as a function of bit SNR (E_b/N_0) for the same level of dispersion and same data rate

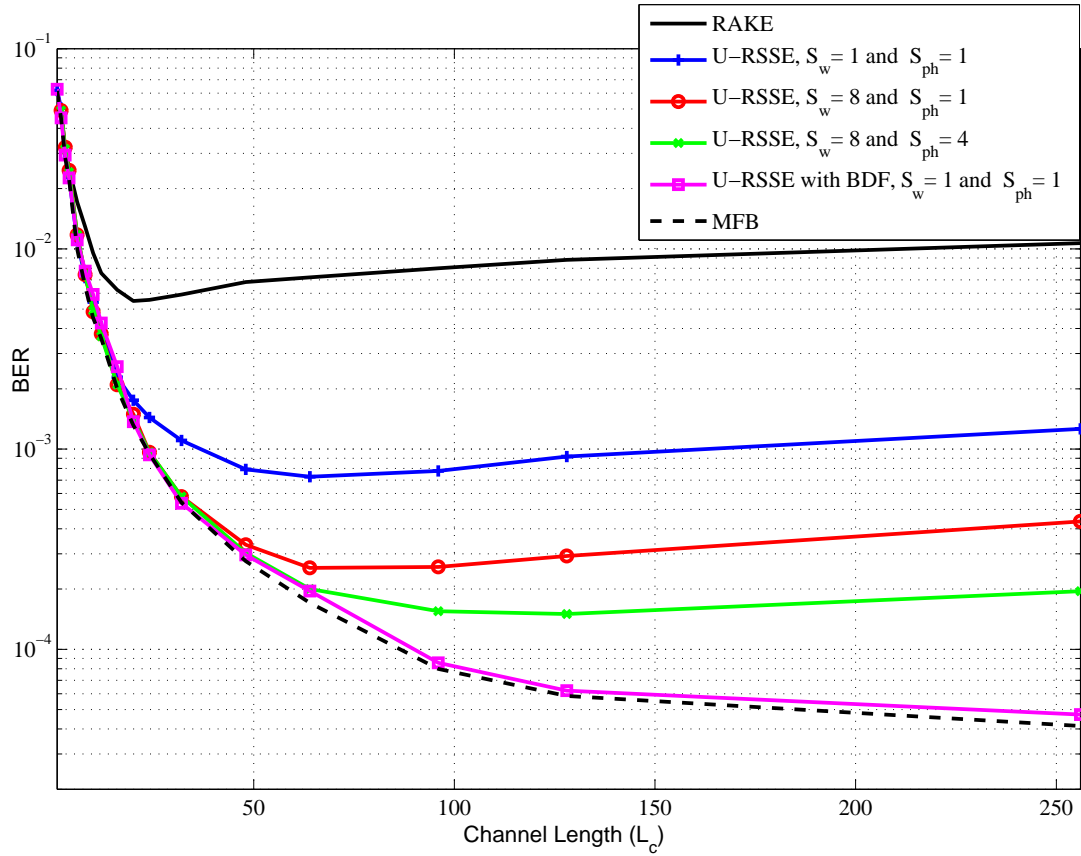


Figure 2.7: $M = 8$, $P = 4$, $N_c = 16$, $SNR_c = \frac{E_c}{N_0} = 2$ dB, BER variation with respect to number of Rayleigh channel taps, L_c , with exponentially decaying power delay profile

by varying spreading factor N_c . This is a reasonable comparison of the schemes with the same bandwidth, same data rates, and same energy per bit. MFB and ML performance in Additive White Gaussian Noise (AWGN) channel are also drawn for comparison. It is seen that by using sufficiently higher number M in order to be able to select larger modulation interval (T) for the given spectral efficiency, the performance can be improved. First, utilizing higher M results in larger error event distances, thus an enhancement in error performance. Second, U-RSSE with BDF shows closer performance to its MFB when M is kept high enough even for lower number of states ($S_{total} = S_w S_{ph}$). In this case, the bias value is small enough to be compensated at the forward stage of U-RSSE with BDF in one iteration. For the case of smaller modulation interval, the bias is expected to be larger as seen in Fig. 2.5, which is the reason of performance loss for ($M = 1, P = 4, N_c = 4$) case in Fig. 2.8. Thus, it is necessary to increase the complexity (number of states in RSSE) or the number of forward and backward U-RSSE iterations to further diminish the effect of bias.

In Fig. 2.9, several MCS schemes with different parameters are compared for the same spectral efficiency, and the advantages of MCS compared to classical DSSS and the tightness of the approximate BER for U-RSSE with BDF obtained in (2.29) are depicted. The channel length L_c is taken as 64, and M is increased while the spectral efficiency is kept constant at $\nu = \frac{\log_2(MP)}{N_c} = \frac{1}{6}$ bits per channel use by arranging N_c . It is seen that there is a 3.5 dB gain of the U-RSSE with $M = 64, P = 4, N_c = 48$ over U-RSSE with $M = 1, P = 4, N_c = 12$ (Classical DSSS). Therefore, it is seen that it is more beneficial to increase M to attain more spreading gain at a given spectral efficiency (or processing gain). The explanation is that the effective ISI length is reduced if one utilizes larger values of M , which reduces the effect of pre-cursor ISI and MCI leading to a reduction in bias for U-RSSE. Moreover, it is observed that MFB is achieved by using only one state for all M values ($S_w = S_{ph} = 1$), and the analytical BER approximation for $K = 8$ in (2.29) is tight enough below 10^{-2} and can be used to determine system parameters (N_c, M, P) depending on channel statistics (L_c , power delay profile) for a given target BER. Thus, this provides an interesting insight into how to transport bits optimally in highly dispersive channels for

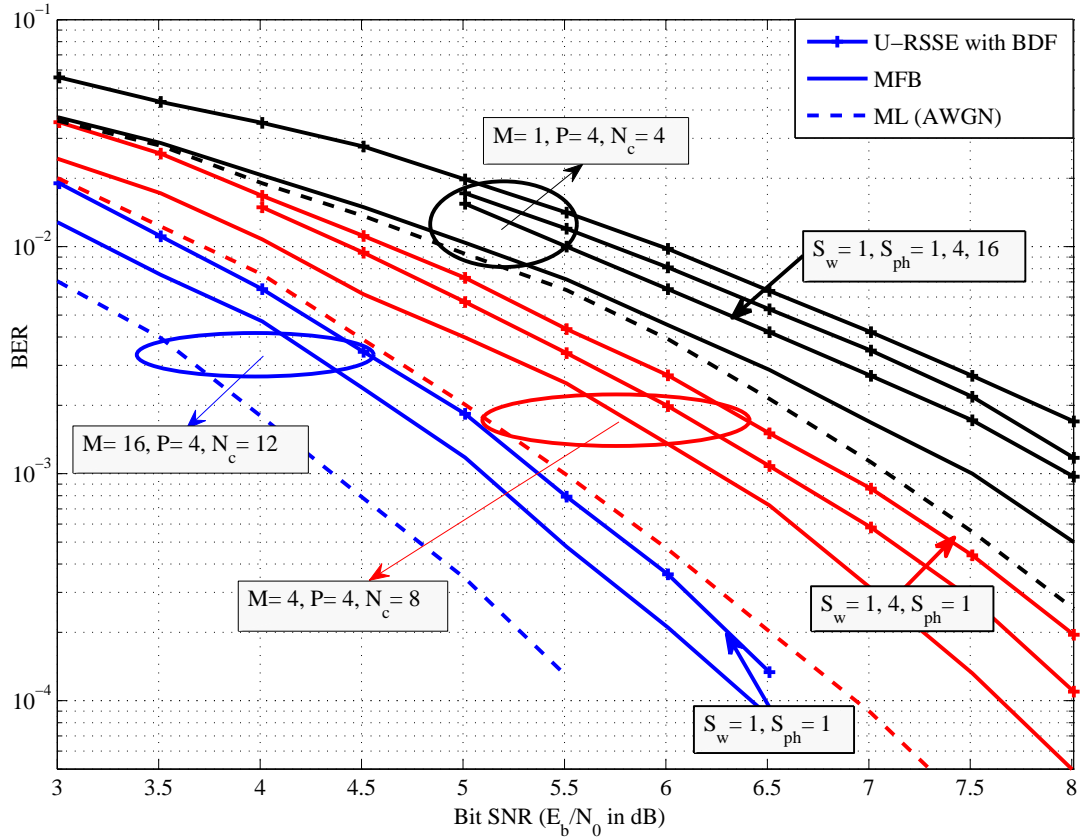


Figure 2.8: Performance for $(M = 1, P = 4, N_c = 4)$, $(M = 4, P = 4, N_c = 8)$ and $(M = 16, P = 4, N_c = 12)$ schemes, channel is composed of $L_c = 128$ independent Rayleigh taps with exponentially decaying power delay profile

a given spectral efficiency. The performance approximation becomes slightly worse for higher M due to the use of union bounding technique in (2.29).

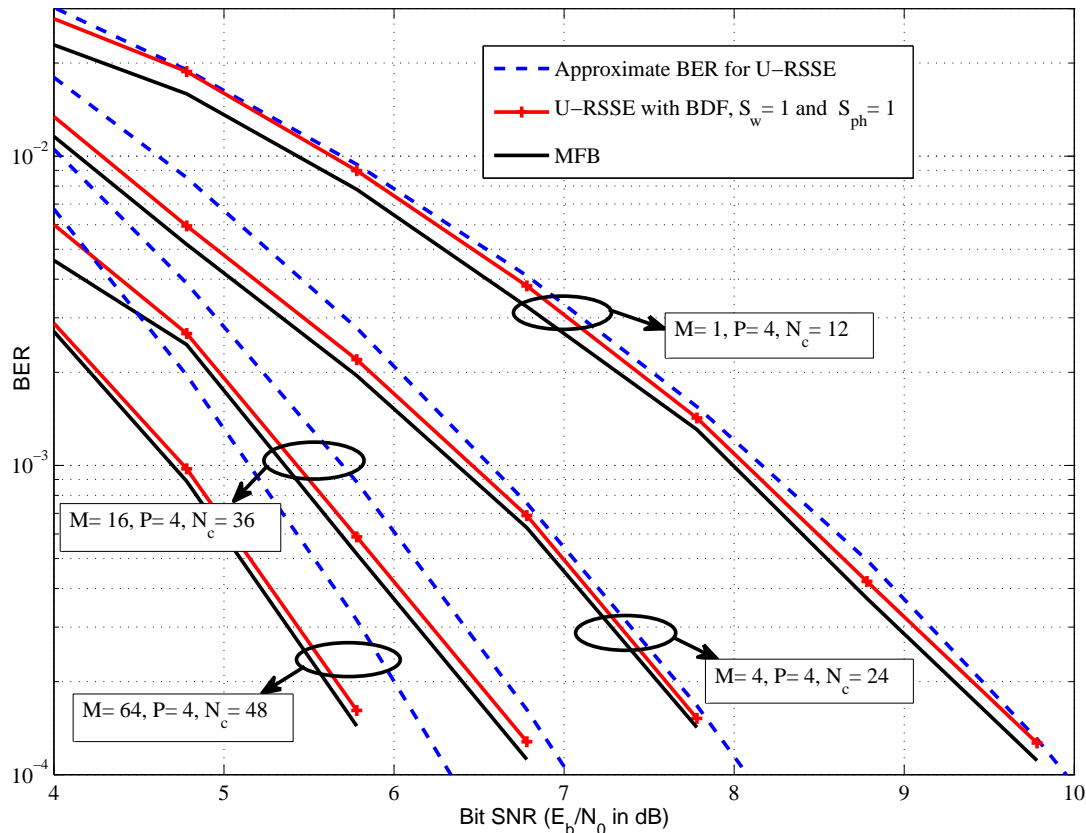


Figure 2.9: Performance variation of U-RSSE with BDF ($S_w = S_{ph} = 1$) and one forward and backward iteration in (2.23), analytical BER approximation in (2.29) and MFB with respect to different M, N_c values at $\nu = \frac{\log_2(MP)}{N_c} = \frac{1}{6}$, $P = 4$. Channel is composed of $L_c = 64$ independent Rayleigh taps with exponentially decaying power delay profile

In Fig. 2.10, the performance of the proposed bidirectional U-RSSE with BDF and its analytical BER approximation for $K = 8$ in (2.29) are shown for different (M, P) pairs at fixed spreading factor $N_c = 16$ and spectral efficiency $\nu = \frac{\log_2(MP)}{N_c} = \frac{6}{16}$. The comparison between different MCS schemes are made for the same bandwidth and data rates by keeping the complexity levels constant for all values at $S_w = S_{ph} = 1$, and the channel length (L_c) is taken as 32. It is seen that $(M, P) = (16, 4)$ yields the best performance among the other alternative values

in this scenario, and the BER approximation using (2.29) is accurate enough to make a system design based on it. The main concern is how to optimize the receiver performance by properly choosing the signaling parameters for highly dispersive channels. In the beginning, it is better to augment M value up to some point to observe larger error event distances, then the performance begins to degrade due to the increased effect of cross-correlations between signaling waveforms resulting in smaller error event distances.

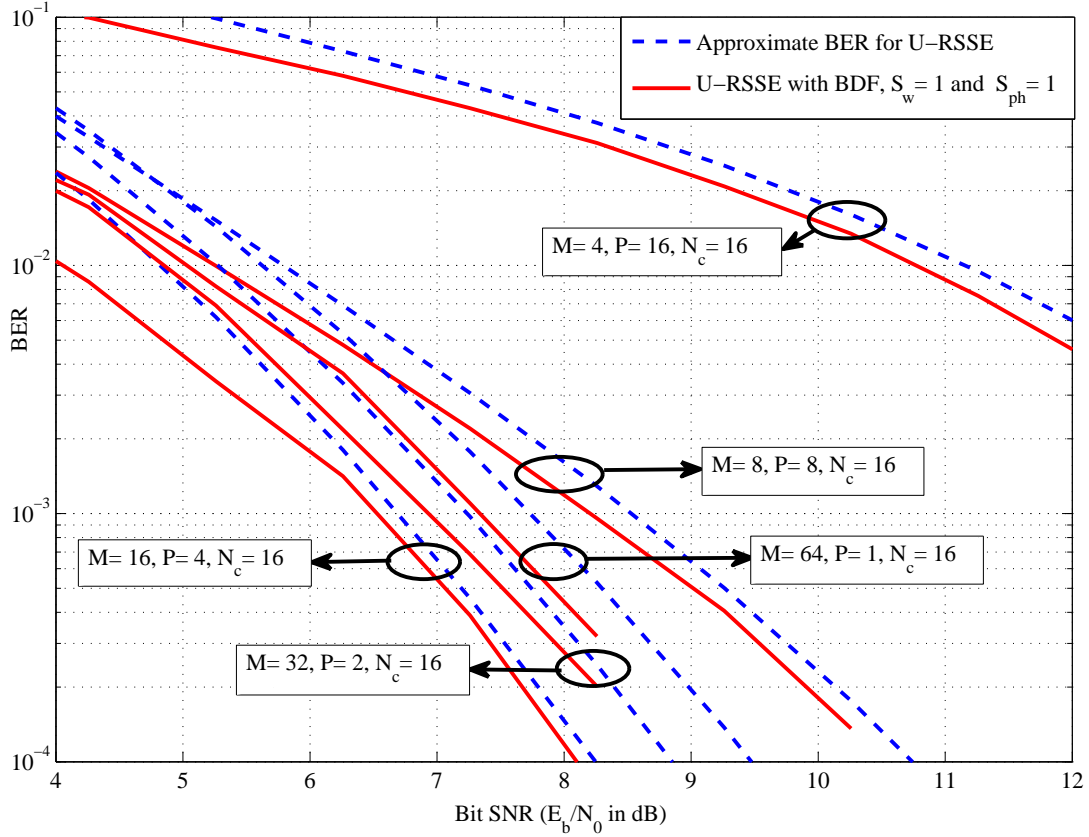


Figure 2.10: Performance variation of U-RSSE with BDF ($S_w = S_{ph} = 1$) and one forward and backward iteration in (2.23), and analytical BER approximation in (2.29) with respect to different (M, P) values at $\nu = \frac{\log_2(MP)}{N_c} = \frac{6}{16}$, $N_c = 16$. Channel is composed of $L_c = 32$ independent Rayleigh taps with exponentially decaying power delay profile

The certain advantage of the proposed Ungerboeck type equalization scheme seen in fading channels will begin to disappear for channels with significant

correlation between multi-path taps leading to a large bias value. In this case, the excellent performance cannot be sustained without compromising complexity since the effect of the anti-causal part of the Ungerboeck ISI will be much worse for static channels with significant correlation among resolvable taps. In Fig. 2.11, the performance of the U-RSSE-BDF MAP detector for the MCS scheme with $M = 4, P = 4, N_c = 8$ values is exhibited. The channel is taken as static square-root-raised-cosine (RRC) type low pass filter with roll-off factor 0.3. The cutoff frequency of the baseband channel is set to $\frac{B}{2}$, and the performance of the U-RSSE receiver is obtained for different $\frac{W}{B}$ ratios. Random signaling waveforms are generated at each packet transmission such that each of them is composed of N_c chips, randomly selected from the QPSK alphabet without any optimization. For large $\frac{W}{B}$ values, the Ungerboeck ISI is so severe that error events with longer duration become more troublesome, thus one cannot claim a close performance to MFB even with the use of optimal MLSE receiver. Nevertheless, the MFBs are also demonstrated for comparison. By increasing the number of states, one can keep the bias at reasonable values, and remarkable performance enhancements can be attained.

For channels with higher $\frac{W}{B}$ values, it is necessary to increase the complexity (number of states in RSSE) in order to confine the pre-cursor ISI to moderate values for the first iteration. Alternatively, one can consider the cycle free message passing algorithm over the Ungerboeck type Factor Graph based on the equivalent model by assuming that the state vectors and variables are Gaussian. This reduces the computational complexity considerably when compared to finite alphabet case. Then, one can eliminate the bias (estimating the pre-cursor Ungerboeck ISI) by using the Gaussian message passing at the first iteration. Afterwards, the URSSE-BDF for MCS can operate in subsequent iterations to attain a near optimum performance.

Furthermore, for higher $\frac{W}{B}$ values, there is significant envelope modulation, and the static channel degrades the correlation properties of the signaling waveforms substantially, thus it would be better to optimize signaling waveforms so as to reach smaller bias values. It would be better to adapt signaling waveforms to the varying channel characteristics which have a great effect on the bias value

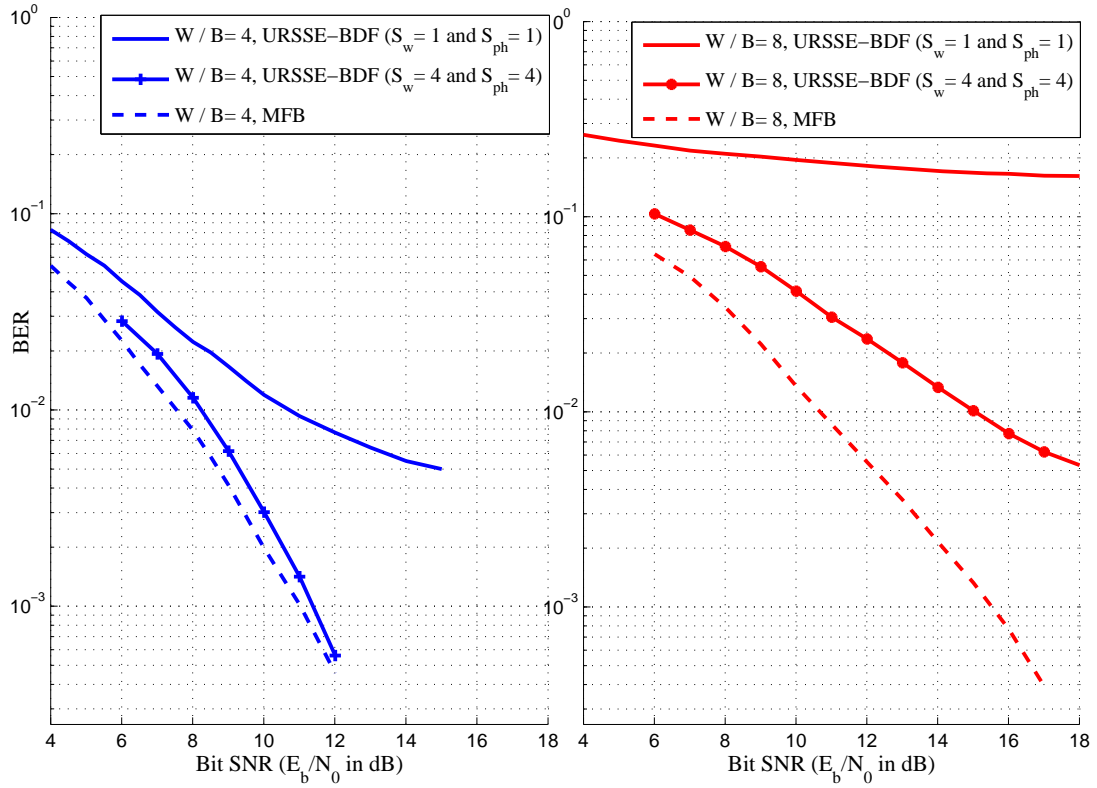


Figure 2.11: Performance for the MCS scheme ($M = 4, P = 4, N_c = 8$) with random codes transmitted through a static channel, RRC type low-pass filter with cut-off at $\frac{B}{2}$ and roll-off factor 0.3, $\frac{W}{B} = 4$ and 8.

predicted by the analysis. However, these are beyond the scope of this thesis. For this type of channels, there exist more efficient equalization techniques to restrict the pre-cursor ISI based on pre-filtering and channel shortening in [60], and reduced complexity detectors based on M-BCJR algorithm working with mismatched filtered channel observations [61] for severe static ISI channels introduced by faster-than-Nyquist (FTN) signaling scenarios.

In Fig 2.12, the performance improvement that can be attained by using a higher number of signaling waveform (increasing M) at the same spectral efficiency is shown for the static channel with $\frac{W}{B} = 6$. The MCS scheme $M = 16, P = 4, N_c = 12$ shows superior performance to that of the scheme $M = 4, P = 4, N_c = 8$, since the bias reduction is more remarkable for larger M values due to the increase in modulation interval (T) at the same spectral efficiency.

2.6.2 Extrinsic Information Transfer (EXIT) Chart Behaviour of the U-RSSE

Although the results have been obtained without outer channel coding, the proposed URSSE-BDF can be utilized as the equalization and demodulation stage supplying bit APPs to a SISO outer decoder. In this case, the extrinsic information transfer (EXIT) chart [62, 63] is useful to analyze the convergence behaviour of the iterative MAP decoding, and to compare the behaviour of the proposed scheme with MFB. In order to obtain EXIT curves, the hard tentative decisions of the MCS symbols (leading to pre-cursor ISI and MCI) are obtained from the SISO decoder modeled by a priori test channel supplying the bit log likelihood ratios (LLR) of the information bits. Then, the forward and backward URSSE stages supplies the extrinsic information after compensating the bias (induced by anti-causal part of the Ungerboeck channel) by utilizing the tentative decisions of MCS symbols. Before providing the details of the EXIT curves for the proposed Ungerboeck receiver, it is better to give some introductory informations about the EXIT chart.

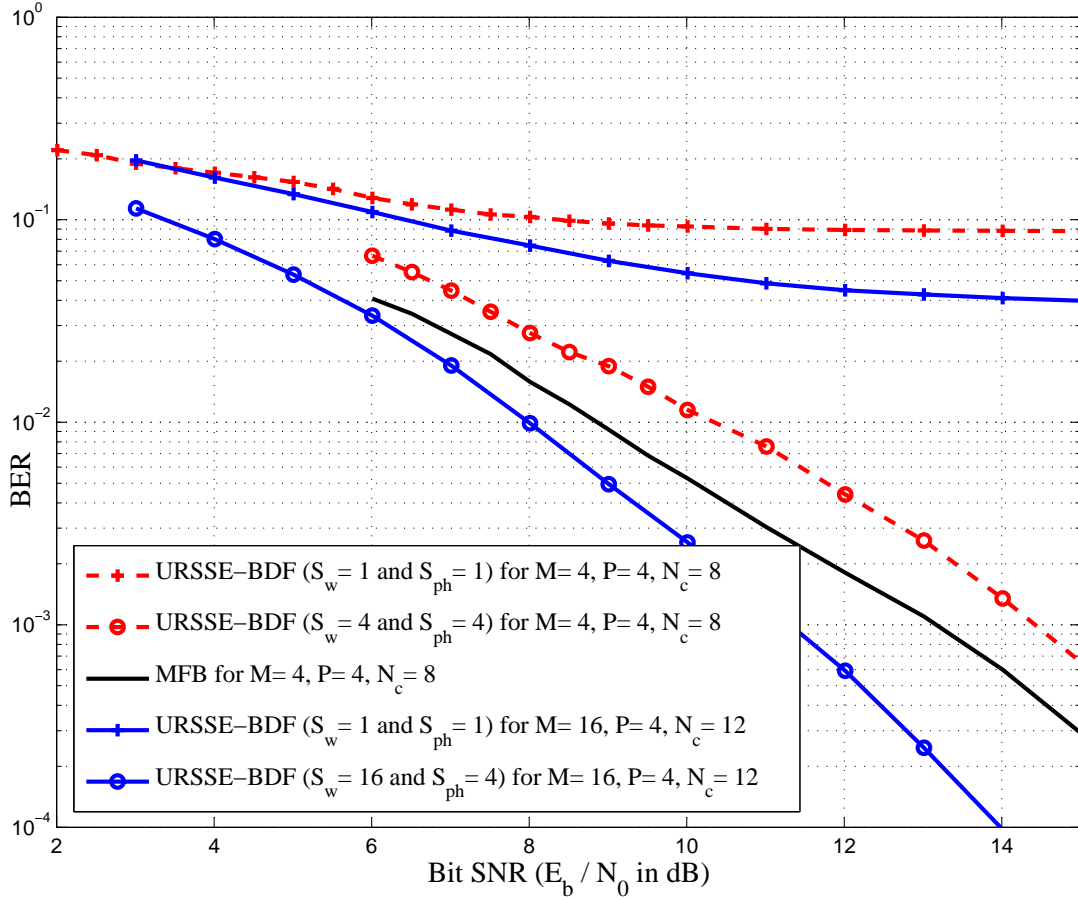


Figure 2.12: Performance for the MCS schemes ($M = 4, P = 4, N_c = 8$) and ($M = 16, P = 4, N_c = 12$) with random codes transmitted through a static channel, RRC type low-pass filter with cut-off at $\frac{B}{2}$ and roll-off factor 0.3, $\frac{W}{B} = 6$.

2.6.2.1 The EXIT Chart

We wish to measure the mutual information between information bits, which after encoding are transmitted over a noisy channel, and the LLR of these bits (soft output) after decoding. The decoder receives not only the transmitted values normalized by the channel state information but also a priori knowledge in the form of LLR values from the other serial or parallel decoding engine. Due to the nonlinearity of the decoder, the LLR distribution of the output is in general unknown and no longer Gaussian. However, by invoking the ergodicity theorem, namely, that the expectation can be replaced by the time average, we can measure the mutual information from a large number of samples even for non-Gaussian or unknown distributions. The mutual information can be calculated by time averaging and assuming that the LLRs have a symmetric distributions satisfying the consistency condition [63], which is feasible for many practical receivers. The EXIT curves, then, shows the mutual information of the constituent decoder number one versus the mutual information of the other constituent decoder (number two) which is modeled by the test channel providing a priori LLRs of the information bits. In other words, the vertical axis (I_E) of the EXIT chart shows the mutual information between the extrinsic LLRs provided by the decoder number one and the information bits. The horizontal axis (I_A) shows the mutual information of the a priori LLRs provided by the decoder number two (test channel) and the information bits. Both range between 0 and 1. Only the extrinsic LLR values are used as output, meaning that the a priori input value is subtracted from the full (APP) soft output value. This avoids propagation of already known information [63].

2.6.2.2 Simulation Results

In Fig. 2.13, the average mutual information between the extrinsic information provided by the proposed URSSE-BDF and the information bits (I_E) versus the mutual information of the a priori channel (I_A) is computed by Monte-Carlo simulation for the fading channel composed of 128 Rayleigh fading taps ($L_c = 128$) chosen from an exponentially decaying power delay profile at $E_b/N_0 = 0$

dB. The MCS schemes with $M = 4, P = 4, N_c = 8$ and $M = 16, P = 4, N_c = 12$ are investigated. Also, the EXIT curve for the PCR is obtained for comparison. It is seen that the proposed URSSE-BDF achieves the performance predicted by MFB as the information obtained from the a priori channel improves. Since the PCR does not take the bias into account, it fails to attain MFB even with perfect a priori knowledge.

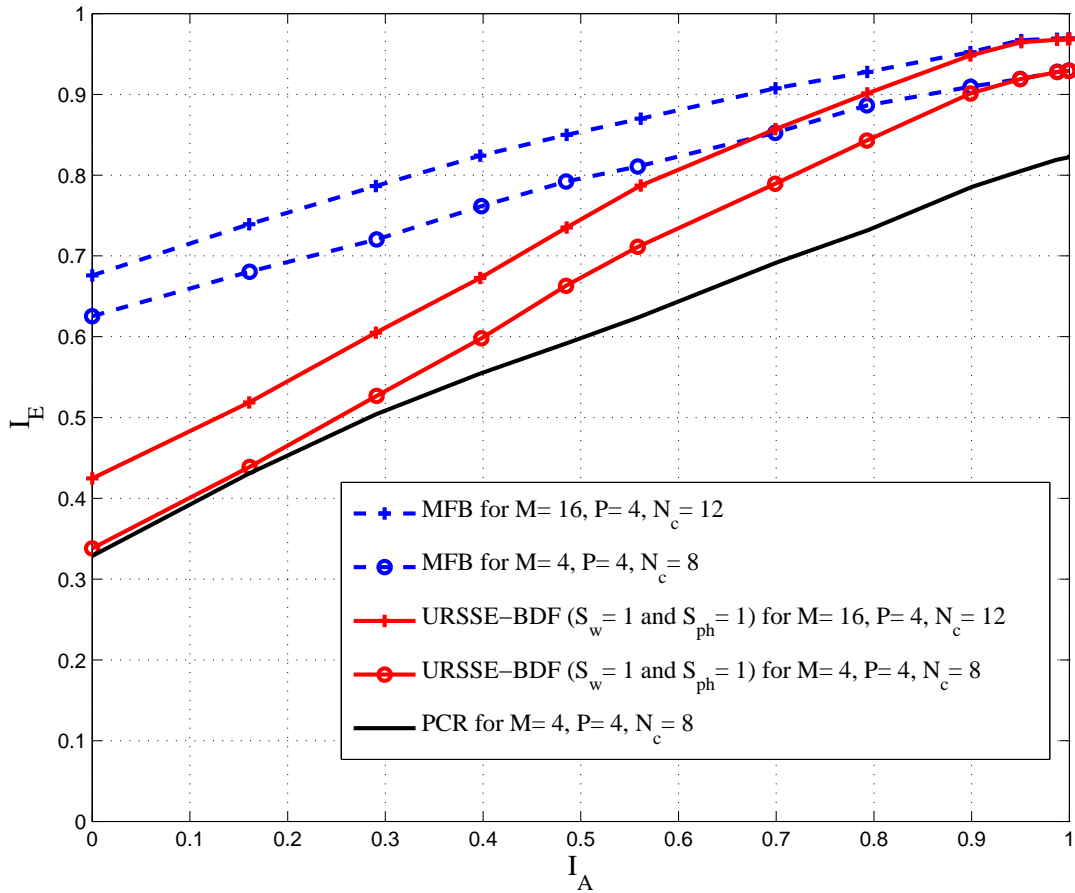


Figure 2.13: An EXIT chart at $\frac{E_b}{N_0} = 0$ dB, showing extrinsic vs. a priori information for block containing 200 MCS symbols. The channel is composed of $L_c = 128$ independent Rayleigh taps with exponentially decaying power delay profile. MCS waveforms for $(M = 4, P = 4, N_c = 8)$ and $(M = 16, P = 4, N_c = 12)$ are obtained by truncating Kasami Sequences.

As to the case of RRC static channel with $W/B = 6$ illustrated in Fig 2.14, the URSSE-BDF ($J_I = J_\theta = 0, S_{total} = 1$) provides very poor extrinsic information

at $I_A = 0$ due to the much larger bias value compared to fading channel even though it attains MFB at $I_A = 1$. Thus, the number of states should be increased to keep bias at reasonable level at $I_A = 0$, thus URSSE-BDF ($J_I = J_\theta = 1, S_{total} = 16$) is shown to achieve the MFB with the help of iterative processing as confirmed by Fig 2.11. Furthermore, the average mutual information at the detector output for the proposed scheme after one forward and backward URSSE self-iterations to cancel bias factor before supplying bit APPs at $I_A = 0$ is shown for fading channel in Fig 2.15. It is observed that PCR fails to achieve MFB due to the untreated bias.

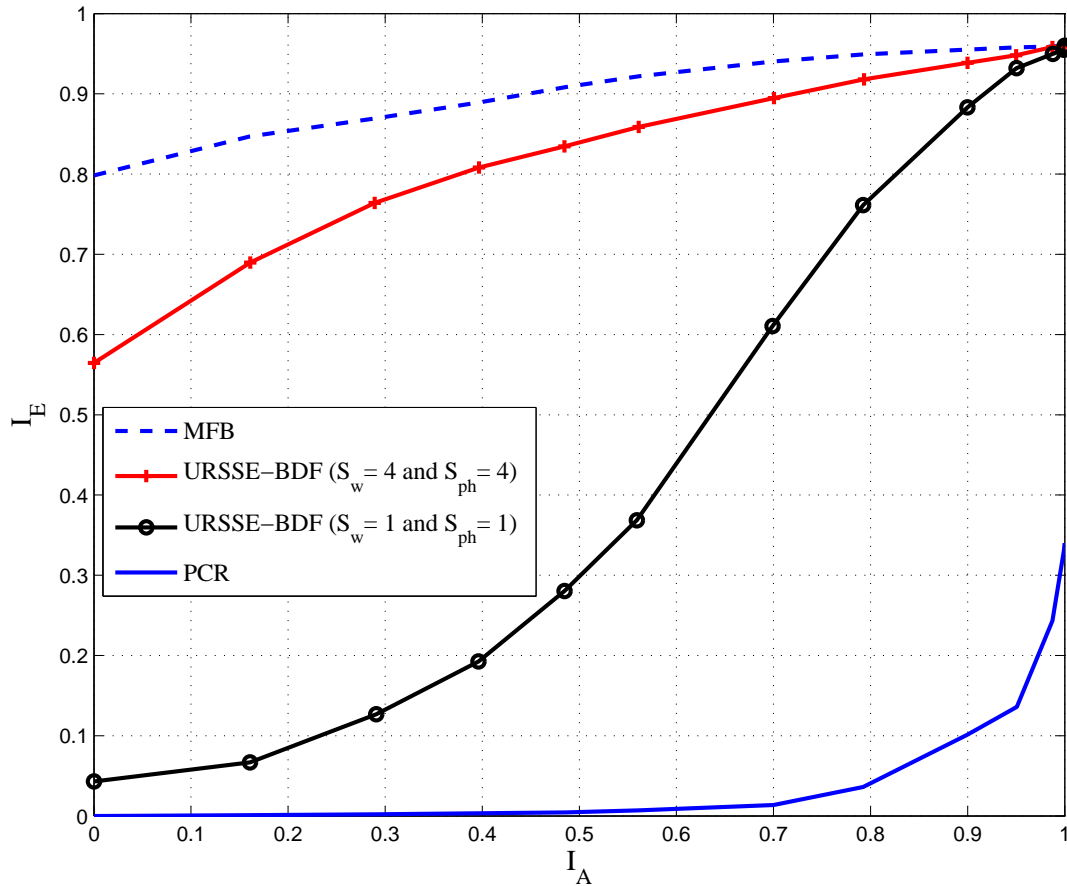


Figure 2.14: An EXIT chart at $\frac{E_b}{N_0} = 5$ dB, showing extrinsic vs. a priori information for block containing 200 MCS symbols ($M = 4, P = 4, N_c = 8$). The channel is a static RRC low-pass filter with cut-off at $\frac{B}{2}$ and roll-off factor 0.3, and $\frac{W}{B}$ is set to 6. MCS waveforms for ($M = 4, P = 4, N_c = 8$) have chips randomly selected from the QPSK alphabet at each packet transmission.

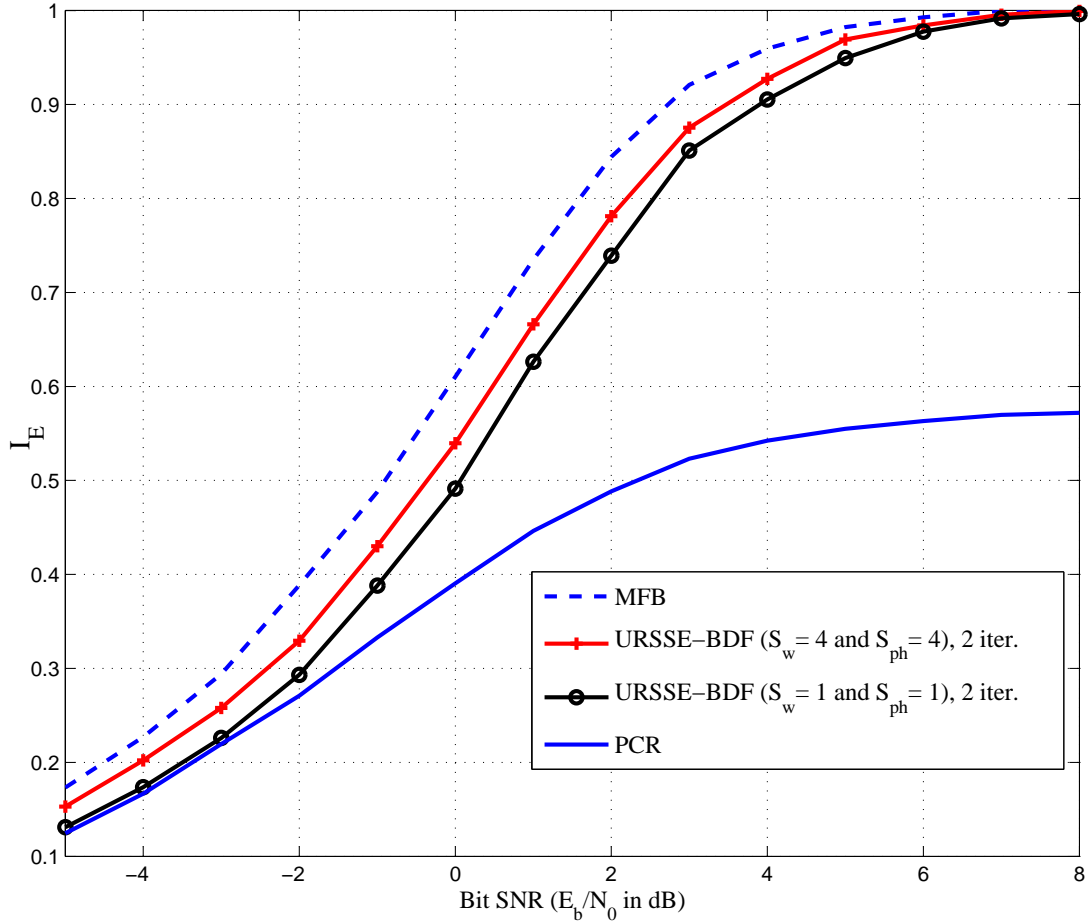


Figure 2.15: Average mutual information at the detector output in the case of $I_A = 0$ for the MCS scheme ($M = 4, P = 4, N_c = 8$). The channel is composed of $L_c = 128$ independent Rayleigh taps with exponentially decaying power delay profile. MCS waveforms for ($M = 4, P = 4, N_c = 8$) are obtained by truncating Kasami Sequences.

To sum up, the conclusions drawn from the BER curves obtained for different MCS schemes also hold for the mutual information indicated by EXIT curves.

2.7 Conclusions

In this chapter, we first propose a highly efficient receiver architecture for MCS based on a symbol rate operating bidirectional U-RSSE with BDF which yields a near optimum performance in relation to the MFB. The symbol rate BDF is utilized during U-RSSE to remove the effects of post- and pre-cursor ISI and MCI components at the output of a correlator bank by taking the non-ideal waveform correlations and multi-path channel into account. Second, a probability of error analysis is carried out to develop insight on the efficiency of the proposed structure and the selection of system parameters. Also, a tight analytical approximation for BER of the proposed receiver structure is derived.

It is seen that the proposed symbol rate U-RSSE with BDF can attain the MFB at significantly reduced complexity for multi-path channels with very large delay spread. Thus, MCS is shown to be an effective spread spectrum modulation technique at low transmission power with the use of the proposed receiver structure. Furthermore, the conducted analysis can be regarded as a useful design tool which helps one decide on modulation related parameters and required complexity level for MCS in order to achieve near-optimum performance for given channel statistical properties. The proposed receiver and the associated analysis can be extended for arbitrary constellations per waveform by straightforward procedures.

CHAPTER 3

CUTOFF RATE BASED ERROR PROBABILITY ANALYSIS OF CODED MCS SCHEME FOR FINITE BLOCK-LENGTH REGIME

3.1 Introduction

Performance bounds play a vital role in assessing the quality of a coded system and giving guidelines in code design. In this chapter, we deal with the performance analysis of MCS based transmission where outer channel coding is utilized. Our aim is to relate the performance of the coded MCS system over multipath fading channel to the modulation related parameters such as number of signaling waveforms (M), number of phase levels in each waveform (P), auto- and cross-correlations between them, bandwidth expansion factor (N_c), and the statistical properties of the stochastic channel with Gaussian distributed taps. Thus, it turns out that one can exploit this corresponding analysis to attain a remarkable performance improvement of the Ungerboeck type receivers by a proper choice of the signaling parameters for coded MCS transmission in a similar manner to the *bias* and BER analysis given in Chapter 2. However, it is well known that the analysis of the exact error probability of a coded system is prohibitively complicated. Instead of using a specific coding structure in MCS transmission, we adopt a probabilistic approach, which is based on randomly selected codes chosen from the MCS alphabet, to simplify the analysis.

This approach corresponds to an important benchmark known as the *cutoff rate* [7], which is widely used to assess achievable rates of coded modulation

schemes over a finite state channel with equiprobable inputs chosen from a finite alphabet. Cutoff rate approach is utilized as an alternative measure to constrained Shannon channel capacity for finite constellations because of its analytical tractability. Channel capacity of bandlimited AWGN channels with discrete-valued input and continuous-valued output signals was provided in [64]. However, this constrained capacity is not analytical, which limits its usage in practical system design contrary to the cutoff rate. Moreover, cutoff rate measure accounts also for a mismatched metric employed in the receiver, and demonstrates the achievable reliability of the given coded modulation scheme in terms of an error probability exponent with a given block length of the code (packet length) [65]. Therefore, we adopt cutoff rate as our performance measure of the studied coded MCS scheme, and obtain an approximate upper bound for the packet (or block) error probability with a given finite block length when the practical Ungerboeck type receiver architecture with near-optimum performance (in terms of MFB) is utilized.

3.2 Cutoff Rate Analysis of Coded MCS Scheme

We start with some definitions related to the structure of the coded MCS scheme based on the equivalent vector symbol model given in (2.8). We consider that k bits are desired to be transmitted by each codeword. Then, the codeword matrix for the i^{th} codeword can be defined as

$$\mathbf{X}_i \triangleq [\mathbf{x}_0^i, \mathbf{x}_1^i, \dots, \mathbf{x}_{N-1}^i]_{M \times N} \quad (3.1)$$

where $\mathbf{x}_n^i = \mathbf{c}_n^i e^{j\theta_n^i} \in \mathfrak{X}$ with cardinality $|\mathfrak{X}| = MP$ is the equivalent MCS symbol in (2.8). This leads to the codeword $\mathbf{X}_i \in \mathfrak{X}^N$ for $i = 1, \dots, 2^k$. The coded modulation scheme \mathfrak{X}^N is constructed such that 2^k information sequences are selected randomly from $(MP)^N$ different waveforms. A total of $N_{total} = N_c \times N$ complex dimensions are utilized for the transmission of one codeword. The desired bit rate, $R_b = \frac{k}{T_0}$ bits/sec and $D = \frac{N_{total}}{T_0}$ dimensions/sec are defined for the packet duration T_0 . Then, $R = \frac{R_b}{D}$ is the ratio showing the communication rate in bits per dimension (or channel use). R can be deemed as the desired spectral efficiency in bps/Hz or transmission rate in bits/dimension. The differ-

ence codeword matrix, namely, $\mathbf{D}^{ij} = \mathbf{X}_i - \mathbf{X}_j$ to be used for cutoff rate analysis can be defined as

$$\mathbf{D}^{ij} \triangleq [\mathbf{d}_0^{ij}, \mathbf{d}_1^{ij}, \dots, \mathbf{d}_{N-1}^{ij}]_{M \times N} \quad (3.2)$$

where $\mathbf{d}_n^{ij} = \mathbf{x}_n^i - \mathbf{x}_n^j \in \mathfrak{D}$ with cardinality $|\mathfrak{D}| = (MP)^2$, and $\mathbf{D}^{ij} \in \mathfrak{D}^N$.

Based on the discrete time equivalent model for MCS in (2.8), the packet error rate (PER), averaged over all possible codebook's performances, can be obtained for a given total dimension $N_{total} = N_c N$ and the given transmission rate R to the channel (in bits/dimension), when the proposed Ungerboeck type processing is employed at the receiver, as

$$\overline{P_e}(\mathbf{h}) \leq 2^{-N_{total}(R_c(\mathbf{h})-R)} \quad (3.3)$$

in Appendix D where $R_c(\mathbf{h})$ is the cutoff rate obtained for a given channel vector \mathbf{h} and waveform's auto- and cross-correlation matrices $\{\mathbf{R}_g^{i,j}(n)\}_{i,j}$ as

$$R_c(\mathbf{h}) = -\frac{1}{N_c} \log_2 \left[\frac{1}{|\mathfrak{D}|} \sum_{\forall \mathbf{d}_n \in \mathfrak{D}} \exp \left(-\frac{E_c}{4N_0} \mathbf{d}_n^H \mathbf{H}(0) \mathbf{d}_n \right) \right] \quad (3.4)$$

for $\mathbf{H}(l) = (\mathbf{R}(l))^T$.

Our approach here is different from the cutoff rate calculations in [66–68]. In [66], different bounds on the symmetric binary cutoff rate for a pulse amplitude modulated (PAM) signaling over ISI channels are evaluated. Then, in [67], the results are generalized to multi level discrete inputs. In [68], expected cutoff rate expressions depending on block-length is provided for QAM block coded data transmissions over time-varying ISI channels. The exact cutoff rate [66–68] and constrained capacity expressions [69] for ISI channels, however, are not computationally efficient to be used as a design guideline, and not analytically tractable to be used in error probability analysis. Instead, we simplify the cutoff rate calculation by assuming that the proposed U-RSSE-BDF in Chapter 2 attains a near-optimum performance in terms of MFB by properly setting the modulation and complexity related parameters. This is a reasonable assumption, because the proposed Ungerboeck MAP receiver perfectly removes the ISI and bias, which makes the MFB achievable even without using outer channel coding as can be seen from the simulation results of Chapter 2. Thus, while obtaining

(3.4), we assume that the post- and pre-cursor Ungerboeck ISI are perfectly removed after CMF and code MF operations at the receiver, where the error events with duration other than one are not effective in U-RSSE operation as is the case for the derivations in Appendix C. The obtained cutoff rate expression in (3.4) corresponds to the upper bound derived in [66] for binary inputs. We can express (3.4) more explicitly to show its dependence on signaling waveforms as

$$\begin{aligned}
R_c(\mathbf{h}) &= -\frac{1}{N_c} \log_2 \left[\frac{1}{(MP)^2} \sum_{\forall \mathbf{c}_n^1, \mathbf{c}_n^2 \in A_I} \sum_{\forall \theta_n^1, \theta_n^2 \in A_\theta} \right. \\
&\quad \left. \exp \left(-\frac{E_c}{4N_0} (\mathbf{c}_n^1 e^{j\theta_n^1} - \mathbf{c}_n^2 e^{j\theta_n^2})^H \mathbf{R}^T(0) (\mathbf{c}_n^1 e^{j\theta_n^1} - \mathbf{c}_n^2 e^{j\theta_n^2}) \right) \right] \\
&= -\frac{1}{N_c} \log_2 \left[\frac{1}{MP} + \frac{1}{M^2P} \sum_{\Omega_1} \exp \left(-\frac{E_c}{4N_0} [R_{I_1, I_1}(0) + R_{I_2, I_2}(0) \right. \right. \\
&\quad \left. \left. - 2 \operatorname{Re} \left\{ e^{-j\frac{2\pi}{P}p} R_{I_1, I_2}(0) \right\} \right) \right] + \frac{1}{M^2P} \sum_{\Omega_2} \exp \left(-\frac{E_c}{N_0} \sin^2 \left(\frac{\pi}{P}p \right) R_{I_1, I_1}(0) \right) \right] \\
&= -\frac{1}{N_c} \log_2 \left[\frac{1}{MP} + \frac{1}{M^2P} \sum_{\Omega_1} \exp \left(-\frac{E_c}{4N_0} \mathbf{h}^H \mathbf{T}_1^{(I_1, I_2, p)} \mathbf{h} \right) \right. \\
&\quad \left. + \frac{1}{M^2P} \sum_{\Omega_2} \exp \left(-\frac{E_c}{4N_0} \mathbf{h}^H \mathbf{T}_2^{(I_1, p)} \mathbf{h} \right) \right] \tag{3.5}
\end{aligned}$$

where the sets Ω_1 , Ω_2 , and the matrices $\mathbf{T}_1^{(I_1, I_2, p)}$, $\mathbf{T}_2^{(I_1, p)}$ are defined in (2.30) and (2.31), respectively. Since the cutoff rate is a function of instantaneous channel gains, it changes depending on fading conditions. Block fading channel (BFC) or quasi static channel model is assumed such that the channel response does not vary during a block transmission period. Thus, we evaluate the performance bounds for PER given in (3.3) in an average sense by taking the expectation over the fading multipath channel. Also, the mean value of the cutoff rate for MCS will be calculated to exhibit the achievable ergodic rates. For the calculation of average PER, it is more convenient to express (3.5) in the following form

$$R_c(\mathbf{h}) = -\frac{1}{N_c} \log_2 \left(\frac{1}{MP} + \frac{\gamma(\mathbf{h})}{M^2P} \right), \tag{3.6}$$

where

$$\begin{aligned}\gamma(\mathbf{h}) &\triangleq \sum_{i=1}^J \xi_i(\mathbf{h}), \quad J = |\Omega_1| + |\Omega_2| = M(MP - 1) \quad \text{and} \\ \xi_i(\mathbf{h}) &= \exp\left(-\frac{E_c}{4N_0} \mathbf{h}^H \mathbf{A}_i \mathbf{h}\right) \quad \text{for } \mathbf{A}_i \in \left\{ \mathbf{T}_1^{(I_1, I_2, p)}, \mathbf{T}_2^{(I_1, p)} \mid I_1, I_2, p \in \Omega_1 \text{ or } \Omega_2 \right\}\end{aligned}\tag{3.7}$$

3.3 Performance Analysis based on MGF Generation of Cutoff Rate for Coded MCS

3.3.1 LBA Bound (Optimum Bound) based on Cutoff Rate

In this part, instead of direct expectation of (3.3) over \mathbf{h} , the limit-before-average (LBA) technique [32, 33] is exploited to obtain tight PER bounds. Since the standard union technique is used in Appendix D to obtain (3.3) for a given instantaneous cutoff rate, it may be substantially loose especially in quasi static fading and may even diverge. In this case, the importance of dominant error events is lost as the union bound continues to grow as more error events are counted in. To prevent this, LBA is helpful in the general framework of Gallager bounds [70], which are primarily used as the performance bounding technique in the context of space-time coding with a given weight spectrum in BFC [59]. Then, LBA can be applied to our PER expression in (3.3) as

$$\begin{aligned}PER &\leq E_{\mathbf{h}} \left\{ \min(1, \overline{P}_e(\mathbf{h})) \right\} = E_{\mathbf{h}} \left\{ \min(1, 2^{-N_{\text{total}}(R_c(\mathbf{h})-R)}) \right\} \\ &= \mathbb{P}\{\mathbf{h} \in \mathfrak{R}^O\} + \int_{\overline{\mathfrak{R}^O}} \overline{P}_e(\mathbf{h}) p(\mathbf{h}) d\mathbf{h}\end{aligned}\tag{3.8}$$

where $\mathfrak{R}^O \triangleq \left\{ \mathbf{h} \mid R_c(\mathbf{h}) < R \right\}$ is the optimum Gallager region, selected as a subset in the space of fading coefficients, which includes the events when all fading gains are relatively small, i.e., the channel is in deep fade. We call this event as *outage* when the instantaneous cutoff rate is below the desired spectral efficiency. In (3.8), $\overline{\mathfrak{R}^O}$ denotes the complement of \mathfrak{R}^O . It is expected that the union bound will likely diverge in this outage region; but PER is simply bounded by unity in (3.8). The integral in (3.8) accounts for the error events when the channel is not in outage, thus it is related with the reliability exponent depending on the block-length N of the code. Other Gallager's bounding techniques in the

literature such as [70], [59] search for ellipsoidal or spherical regions instead of using optimum Gallager region due to its complicated geometric shape. This is an obstacle of deriving a closed-form bound. On the other hand, we utilize the optimum region, namely, \mathfrak{R}^O in LBA type bounding of PER in (3.8).

3.3.2 Analytical Calculation of the Moments

The moment generating function (MGF) of $\gamma(\mathbf{h})$ in (3.7) is calculated first in order to avoid the computational burden arising from the multidimensional integral in (3.8). Then, the expression in (3.8) can be easily evaluated in a closed-form by using Residue Theorem. The MGF of $\gamma(\mathbf{h})$, namely, $\Phi_\gamma(s)$ can be written as

$$\Phi_\gamma(s) = E_\gamma \{e^{-s\gamma}\} = \sum_{k=0}^{\infty} \frac{E\{\gamma^k\}}{k!} (-1)^k s^k. \quad (3.9)$$

$\Phi_\gamma(s)$ cannot be calculated in a closed form, instead, all finite order moments of γ can be obtained analytically by using (B.9) in Appendix B for a jointly complex Gaussian channel vector \mathbf{h} with distribution $CN(\boldsymbol{\mu}_h, \mathbf{P}_h)$ as

$$\begin{aligned} E\{\gamma^d\} &= E\left\{\left(\sum_{i=1}^J \xi_i\right)^d\right\} = \sum_{\{d_i\}_{i=1}^J \in \sigma_d} \frac{d!}{d_1!d_2! \dots d_J!} E\left\{\prod_{i=1}^J \xi_i^{d_i}\right\}, \\ \sigma_d &= \left\{\forall d_i \geq 0 \mid \sum_i d_i = d\right\} \\ &= \sum_{\{d_i\}_{i=1}^J \in \sigma_d} \frac{d!}{d_1!d_2! \dots d_J!} E\left\{\exp\left(-\frac{E_c}{4N_0} \mathbf{h}^H \sum_{i=1}^J d_i \mathbf{A}_i \mathbf{h}\right)\right\} \\ &= \sum_{\{d_i\}_{i=1}^J \in \sigma_d} \frac{d!}{d_1!d_2! \dots d_J!} \\ &\quad \frac{\exp\left\{-\boldsymbol{\mu}_h^H \left(\mathbf{P}_h^{-1} - \mathbf{P}_h^{-1} \left(\frac{E_c}{4N_0} \sum_{i=1}^J d_i \mathbf{A}_i + \mathbf{P}_h^{-1}\right)^{-1} \mathbf{P}_h^{-1}\right) \boldsymbol{\mu}_h\right\}}{\left|\mathbf{I} + \frac{E_c}{4N_0} \sum_{i=1}^J d_i \mathbf{A}_i \mathbf{P}_h\right|} \end{aligned} \quad (3.10)$$

3.3.3 Moment Based Approximation of MGF

It is possible to approximate $\Phi_\gamma(s)$ or the probability density function (pdf) of γ accurately enough by employing a limited number of exactly specified moments

to calculate (3.8). In the literature, there are various techniques to realize this approximation. One of the useful methods is to use Pade approximation (PA) which creates an approximate pole-zero model of the MGF of a random variable in a rational form [34]. Then, this MGF can be inverted using residues to obtain the corresponding pdf. PA is used for evaluating the outage probability in [71] and the error probability for DS/CDMA systems in [72] based on the MGF construction of simple test statistic. Also, the performance analysis of UWB receivers in multipath channels is realized by approximating the MGF of the SNR via PA expansion in [73].

Another method is that of Gram-Charlier and Edgeworth series [74, 75], which represents the density function as a Gaussian density function plus a sequence of correction terms in Hermite polynomials; the expansion coefficients are directly related to the moments of the random variable. These two approaches are effective to compute outage probability by using moments without explicit knowledge of MGF. There are also numerical methods that calculates outage probability when MGF is available in an explicit form such as [76, 77]. In our problem, by using PA or Gram-Charlier approach, we can directly evaluate (3.8) in terms of the moments derived in (3.10). It is seen that moments up to order 2 or 3 is sufficient to calculate $PER < 10^{-3}$.

3.3.4 Packet Error Rate Calculation for Coded MCS Scheme

We adopt PA approach [34] to approximate $\Phi_\gamma(s)$, then the PER in (3.8) can be obtained by inverting the characteristic function and residue theorem as follows

$$\begin{aligned}
PER(E_c/N_0) &\leq \mathbb{P}\{\gamma \geq \tau\} + \mathbb{P}\{\gamma < \tau\} E_\gamma \left\{ 2^{-N_{\text{total}}(R_c(\gamma)-R)} \mid \gamma < \tau \right\} \\
&= \int_\tau^\infty p_\gamma(\gamma) d\gamma + \int_0^\tau 2^{-N_{\text{total}}(R_c(\gamma)-R)} p_\gamma(\gamma) d\gamma \\
&= P_{\text{outage}}(R) + \left(\frac{2^{N_c R}}{MP} \right)^N \int_0^\tau \left(1 + \frac{\gamma}{M} \right)^N p_\gamma(\gamma) d\gamma \\
&= 1 - \int_0^\tau \frac{1}{2\pi j} \int_{-j\infty+\epsilon}^{j\infty+\epsilon} \Phi_\gamma(s) e^{s\gamma} ds d\gamma \\
&\quad + \left(\frac{2^{N_c R}}{MP} \right)^N \int_0^\tau \left(1 + \frac{\gamma}{M} \right)^N \frac{1}{2\pi j} \int_{-j\infty+\epsilon}^{j\infty+\epsilon} \Phi_\gamma(s) e^{s\gamma} ds d\gamma \\
&= 1 - \frac{1}{2\pi j} \int_{-j\infty+\epsilon}^{j\infty+\epsilon} [s^{-1}(e^{s\tau} - 1) - \Psi_\tau(s)] \Phi_\gamma(s) ds \quad (3.11) \\
&= 1 - \sum_{k=1}^K \text{Residue} \left\{ [s^{-1}(e^{s\tau} - 1) - \Psi_\tau(s)] \Phi_\gamma(s), s_k < 0 \right\}
\end{aligned}$$

where

$$\begin{aligned}
\tau(M, P, N_c, R) &= M(MP2^{-N_c R} - 1), \\
\Psi_\tau(s) &= \left(\frac{2^{N_c R}}{MP} \right)^N \int_0^\tau \left(1 + \frac{\gamma}{M} \right)^N e^{s\gamma} d\gamma, \\
p_\gamma(\gamma) &= \frac{1}{2\pi j} \int_{-j\infty+\epsilon}^{j\infty+\epsilon} \Phi_\gamma(s) e^{s\gamma} ds, \quad \epsilon > 0, \\
P_{\text{outage}}(R) &= \mathbb{P}\{\mathfrak{R}^O\} = 1 - \mathbb{P}\{\gamma < \tau\} = 1 - \frac{1}{2\pi j} \int_{-j\infty+\epsilon}^{j\infty+\epsilon} \frac{e^{s\tau} - 1}{s} \Phi_\gamma(s) ds \\
&= 1 - \sum_{k=1}^K \text{Residue} \left\{ s^{-1}(e^{s\tau} - 1) \Phi_\gamma(s), s_k < 0 \right\}. \quad (3.12)
\end{aligned}$$

In (3.11) and (3.12), by noting that $\epsilon > 0$ such that the integration path is chosen in the right half plane, s_k is the k^{th} of the K distinct negative poles of $\Phi_\gamma(s)$ (obtained by PA method) since $[s^{-1}(e^{s\tau} - 1) - \Psi_\tau(s)]$ has no poles in the entire complex s -plane. For a function in the form as shown in the curly bracket of (3.11) and (3.12), the residue at a pole $s_k = a$ of order m is defined as

$$\text{Residue} \{f(s), s_k = a\} = \frac{1}{(m-1)!} \frac{d^{(m-1)}}{ds^{(m-1)}} [(s-a)^m f(s)] \Big|_{s=a}. \quad (3.13)$$

This analysis technique can be applied to any coded scheme provided that the MGF of γ can be characterized in terms of a convergent Pade expansion.

3.4 Ergodic Cutoff Rate Calculation for Coded MCS Scheme

Additionally, the ergodic cutoff rate can be calculated by using the Taylor series expansion in terms of the moments of γ in (3.10) as

$$\begin{aligned}
\overline{R}_c &= E\{R_c(\mathbf{h})\} = \frac{1}{N_c} \log_2(MP) - \frac{1}{N_c} E\left\{\log_2\left(1 + \frac{1}{M}\gamma(\mathbf{h})\right)\right\} \\
&= \frac{1}{N_c} \log_2(MP) - \frac{\log_2(e)}{N_c} \sum_{d=1}^{\infty} \frac{(-1)^{(d-1)} E\{\gamma^d\}}{M^d d} \\
&= \frac{1}{N_c} \log_2(MP) - \frac{\log_2(e)}{N_c} \sum_{d=1}^{\infty} \left[\frac{(-1)^{(d-1)}}{M^d} \sum_{\{d_i\}_{i=1}^J \in \sigma_d} \frac{(d-1)!}{d_1! d_2! \dots d_J!} \right. \\
&\quad \left. \frac{\exp\left\{-\boldsymbol{\mu}_h^H \left(\mathbf{P}_h^{-1} - \mathbf{P}_h^{-1} \left(\frac{E_c}{4N_0} \sum_{i=1}^J d_i \mathbf{A}_i + \mathbf{P}_h^{-1}\right)^{-1} \mathbf{P}_h^{-1}\right) \boldsymbol{\mu}_h\right\}}{\left|\mathbf{I} + \frac{E_c}{4N_0} \sum_{i=1}^J d_i \mathbf{A}_i \mathbf{P}_h\right|} \right]
\end{aligned} \tag{3.14}$$

Truncation of the series expansion at moment order 3 is sufficient since the moments of γ decay rapidly as can be seen from the determinant expression in (3.10). Finally, the expressions obtained for PER and ergodic cutoff rate given in (3.11) and (3.14) appears as a useful tool in assessing the quality of a any coded scheme in the general MCS format for given statistical properties of the multipath channel and signaling parameters. Also, it gives some design guidelines on the selection of system parameters and signaling waveforms for a performance enhancement of reduced state Ungerboeck type receivers.

3.5 Multidimensional Signaling Waveform Design Guidelines for MCS Scheme based on Cutoff Rate

Alternatively, one can use instantaneous and ergodic cutoff rate measures in (3.5) and (3.14) to optimize system performance via a proper selection of a modulation scheme and its corresponding waveforms. First, one can obtain eigendecomposition for the $L_c \times L_c$ symmetric Toeplitz cross correlation matrices

$\{\mathbf{R}_g^{i,j}(0)\}_{i,j}$ as

$$\mathbf{R}_g^{i,j}(0) = \mathbf{Q}\Lambda^{i,j}\mathbf{Q}^H, \quad i, j = 1, \dots, M, \quad (3.15)$$

where $\Lambda^{i,j}$ is the diagonal matrix with nonnegative entries $\lambda_k^{i,j}$'s, $k = 1, \dots, L_c$, and \mathbf{Q} is $L_c \times L_c$ unitary matrix composed of eigenvectors of $\mathbf{R}_g^{i,j}(0)$. For large values of L_c , \mathbf{Q} converges to Discrete Fourier Transform (DFT) matrix of size L_c , and $\lambda_k^{i,j}$'s converge to the DFT of $\{r_g^{i,j}(nT_c)\}_n$. By making the transformation $\mathbf{h}' = \mathbf{Q}^H\mathbf{h}$, one get the following equivalent form of $\gamma(\mathbf{h})$ in (3.6) as

$$\begin{aligned} \gamma(\mathbf{h}) = & \sum_{I_1=1}^M \sum_{I_2=1, I_2 \neq I_1}^M \sum_{p=0}^{P-1} \exp \left(-\frac{E_c}{4N_0} \sum_{m=0}^{L_c-1} |h'_m|^2 [\lambda_m^{I_1, I_1} + \lambda_m^{I_2, I_2} \right. \\ & \left. - 2 \operatorname{Re} \left\{ e^{j\frac{2\pi}{P}p} \lambda_m^{I_1, I_2} \right\} \right] \Big) + \sum_{I_1=1}^M \sum_{p=0}^{P-1} \exp \left(-\frac{E_c}{N_0} \sin^2 \left(\frac{\pi}{P}p \right) \sum_{m=0}^{L_c-1} |h'_m|^2 \lambda_m^{I_1, I_1} \right). \end{aligned} \quad (3.16)$$

Then, for a known channel response at the transmitter, the following metric can be utilized to improve instantaneous cutoff rate in (3.5)

$$\begin{aligned} \beta_{min} = & \min_{I_1, I_2, p \in \Omega_1 \text{ or } \Omega_2} \left\{ \sum_{m=0}^{L_c-1} |h'_m|^2 [\lambda_m^{I_1, I_1} + \lambda_m^{I_2, I_2} \right. \\ & \left. - 2 \operatorname{Re} \left\{ e^{j\frac{2\pi}{P}p} \lambda_m^{I_1, I_2} \right\} \right], 4 \sin^2 \left(\frac{\pi}{P}p \right) \sum_{m=0}^{L_c-1} |h'_m|^2 \lambda_m^{I_1, I_1} \right\}. \end{aligned} \quad (3.17)$$

Similarly, for known statistical properties of the channel, namely, \mathbf{P}_h at the transmitter, the ergodic cutoff rate in (3.14) can be maximized by maximizing the following metric

$$\beta_{min} = \min_{I_1, I_2, p \in \Omega_1 \text{ or } \Omega_2} \left\{ \left| \mathbf{I} + \frac{E_c}{4N_0} \mathbf{T}_1^{(I_1, I_2, p)} \mathbf{P}_h \right|, \left| \mathbf{I} + \frac{E_c}{4N_0} \mathbf{T}_2^{(I_1, p)} \mathbf{P}_h \right| \right\}. \quad (3.18)$$

Thus, the signaling waveforms can be optimized to get auto- and cross-correlation matrices that maximizes β_{min} .

3.6 Case Study: Ideal Signaling Waveforms

When ideal signaling waveforms with equal energy and $R_{i,j}(n) = \|\mathbf{h}\|^2 E_s \delta_{i,j} \delta_n$ $\forall i, j = 1, \dots, M$ are assumed to be used for coded MCS transmission, one can

find an approximation for outage probability by using the most dominant terms at high SNR $\left(\frac{E_s}{N_0}\right)$, and using the MGF of $\|\mathbf{h}\|^2$ obtained by (B.9) in Appendix B. Then, the cutoff rate and the corresponding asymptotic outage probability can be expressed as

$$R_c^{\text{ideal}}(\mathbf{h}) = \frac{1}{N_c} \log_2 \left[\frac{M}{(M-1) \exp\left(-\frac{E_s \|\mathbf{h}\|^2}{2N_0}\right) + \frac{1}{P} \sum_{p=0}^{P-1} \exp\left(-\frac{E_s \|\mathbf{h}\|^2}{N_0} \sin^2\left(\frac{\pi p}{P}\right)\right)} \right] \quad (3.19)$$

and

$$\begin{aligned} P_{\text{outage}}^{\text{asympt}}(R) &= \mathbb{P} \{ R_c^{\text{ideal}}(\mathbf{h}) < R \} \\ &\approx \mathbb{P} \left\{ \frac{1}{N_c} \log_2 \left[\frac{MP}{1 + \alpha \exp\left(-\beta_{\min} \frac{E_s}{N_0} \|\mathbf{h}\|^2\right)} \right] < R \right\} \\ &= \mathbb{P} \left\{ \frac{E_s}{N_0} \|\mathbf{h}\|^2 < \frac{1}{\beta_{\min}} \ln \left[\frac{\alpha}{(MP)2^{-N_c R} - 1} \right] \right\} \\ &= \sum_{k=1}^K \text{Residue} \left\{ s^{-1}(e^{s\kappa} - 1) \right. \\ &\quad \left. \frac{\exp \left\{ -\boldsymbol{\mu}_h^H \left(\mathbf{P}_h^{-1} - \mathbf{P}_h^{-1} \left(s \frac{E_s}{N_0} \mathbf{I} + \mathbf{P}_h^{-1} \right)^{-1} \mathbf{P}_h^{-1} \right) \boldsymbol{\mu}_h \right\}}{\left| \mathbf{I} + s \frac{E_s}{N_0} \mathbf{P}_h \right|}, s_k < 0 \right\}. \end{aligned} \quad (3.20)$$

where

$$\begin{aligned} \beta_{\min} &= \begin{cases} \frac{1}{2}, & \alpha = (M-1)P & \text{if } P < 4 \\ \frac{1}{2}, & \alpha = (M-1)P + 2 & \text{if } P = 4 \\ \sin^2\left(\frac{\pi}{P}\right), & \alpha = 2 & \text{if } P > 4 \end{cases} \\ \kappa &= \frac{1}{\beta_{\min}} \ln \left[\frac{\alpha}{(MP)2^{-N_c R} - 1} \right] \end{aligned} \quad (3.21)$$

As $SNR \rightarrow \infty$, $R_c^{\text{ideal}} \rightarrow \frac{1}{N_c} \log_2(MP)$ and if $R < R_c^{\text{ideal}}$, $P_{\text{outage}}^{\text{asympt}}(R)$ goes to 0 with a decay rate in the order of L_c . Therefore, we can say that the total multipath diversity order L_c is achieved by this MCS scheme.

3.7 Performance Results

In this part, our aim is to use the analytical expressions of cutoff rate and the PER expressions in (3.11) useful to evaluate performance in multi-path fading channel in order to find achievable rates with given PER constraint for different modulation parameters, namely, M, P, N_c in coded MCS. Each waveform is composed of N_c chips by truncating the full-length Kasami codes [1] as in Chapter 2, although one can utilize different approaches to obtain MCS waveforms with better distance and correlation properties.

In Fig. 3.1, cutoff rates of different MCS schemes evaluated by (3.5) are exhibited for AWGN channel along with the unconstrained cutoff rate corresponding to Gaussian alphabet [7] shown for comparison. One can observe that it is better to increase the length of signaling interval, i.e., MCS symbol duration, by keeping the uncoded spectral efficiency at $\nu = \frac{\log_2(MP)}{N_c} = 0.1$ (larger M), which results in grater achievable rates. This result is also confirmed by the BER simulations in Chapter 2 saying that increasing the number of MCS waveforms brings performance improvement when the spectral efficiency (ν) is held constant.

In Fig. 3.2 and 3.4, PER is fixed at 10^{-2} and the achievable rates (R) calculated from (3.3) for different coded MCS schemes are shown. It is seen that for a given uncoded spectral efficiency (fixed N_c), there is a suitable (M, P) pair that yields the best performance. MCS with $P = 4$ usually attain the highest achievable rate due to the larger error event distances. In Fig. 3.3 and 3.5, similar conclusions can be drawn for multi-path fading scenario where Rayleigh Suburban channel [7] with exponentially decaying power delay profile is assumed. In this case, the achievable rates (R) are calculated by using (3.11) where PA [34] is used to approximate MGF in rational form with 2 poles and a single zero, which produces a very accurate model as validated by Monte Carlo simulations.

In Fig. 3.6, the packet duration (N_{total}) and uncoded spectral efficiency $\nu = \frac{\log_2(MP)}{N_c} = 0.125$ are kept constant for a targeted PER at 10^{-2} by using (3.11). It is seen that higher rates can be attained for MCS schemes with larger bandwidth

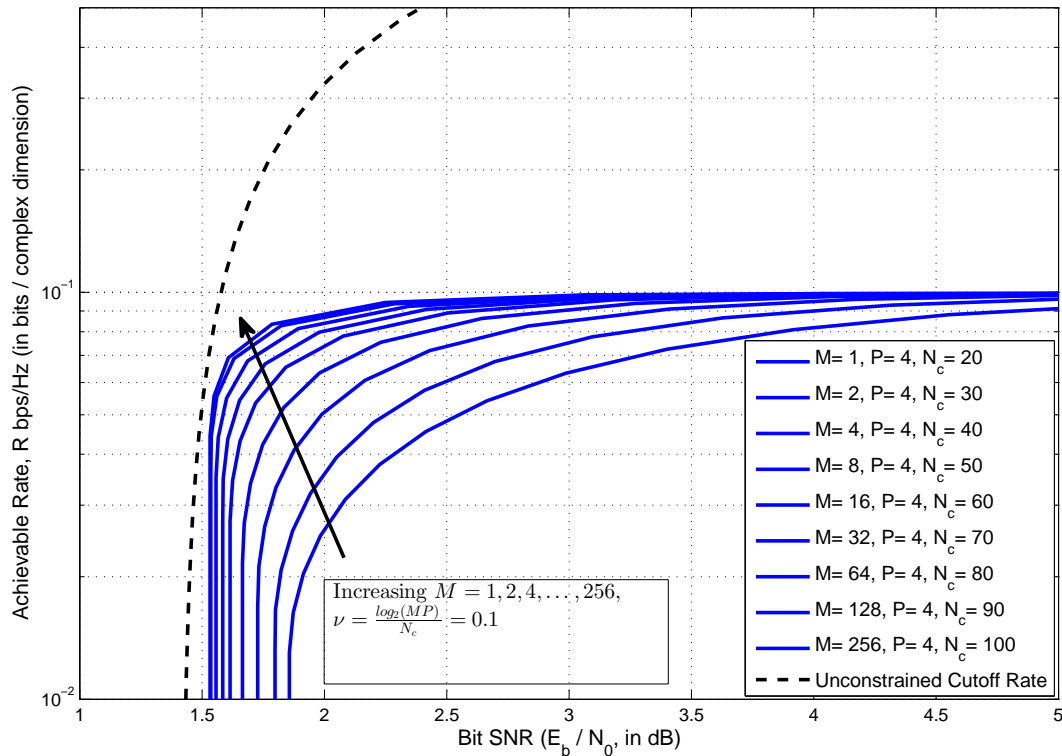


Figure 3.1: Cutoff Rates for AWGN channel, Truncated Kasami Codes are used

expansion (N_c) by increasing M .

In Fig. 3.7, similarly, N_{total} is kept constant. Suitable (M, P, N_c) values yielding higher rates can be determined in this case.

In Fig. 3.8, for different uncoded spectral efficiencies at fixed PER, the achievable rates are demonstrated for different MCS schemes in AWGN channel and fading scenario. The gap between the achievable rates of ideal and the selected MCS waveforms are also shown for comparison. Depending on the operational SNR_c value, one can use an adaptively modulated MCS scheme. Also, one may use the truncated Kasami codes studied here or search for better codes.

In Fig. 3.9, the variation of the achievable rates as a function of the channel length (L_c) is shown for different SNR_c values by using (3.11) for MCS with $(16, 4, 24)$. It is seen that the effective channel length, for which the proposed scheme behaves as if the channel is AWGN, depends on the operational SNR_c level.

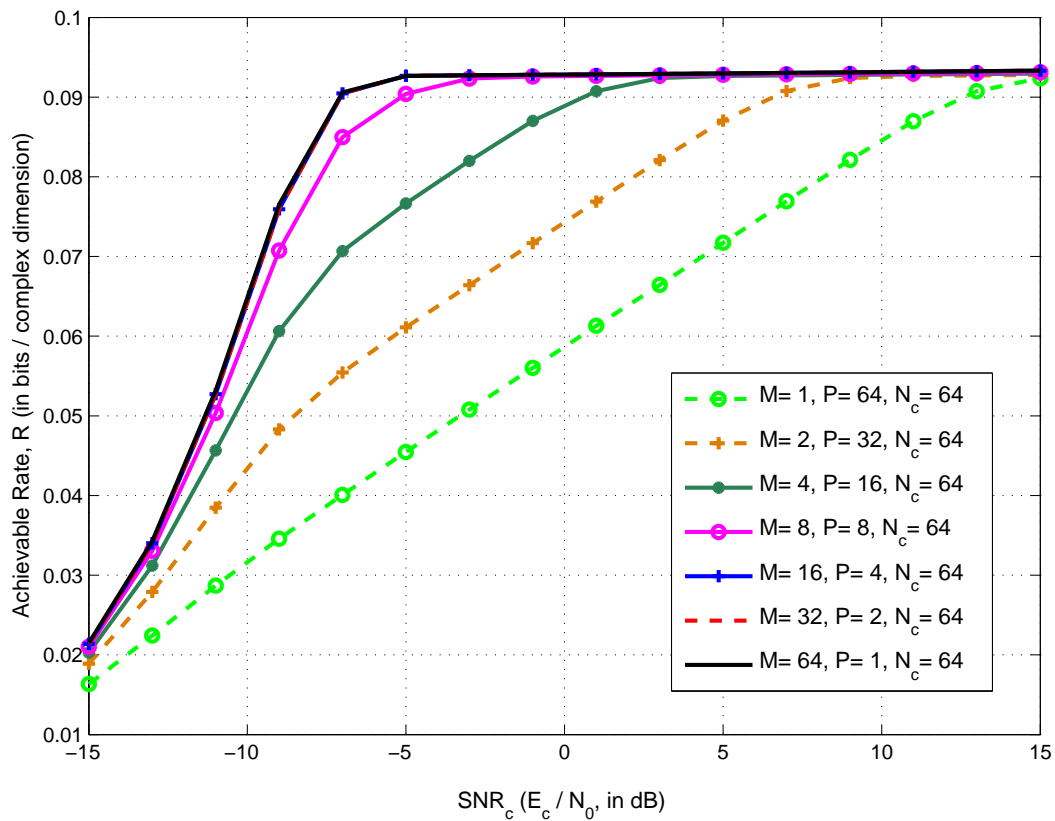


Figure 3.2: AWGN, $N=100$, $\text{PER}=0.01$, $N_c = 64$, $\frac{\log_2(MP)}{N_c} = \frac{6}{64}$

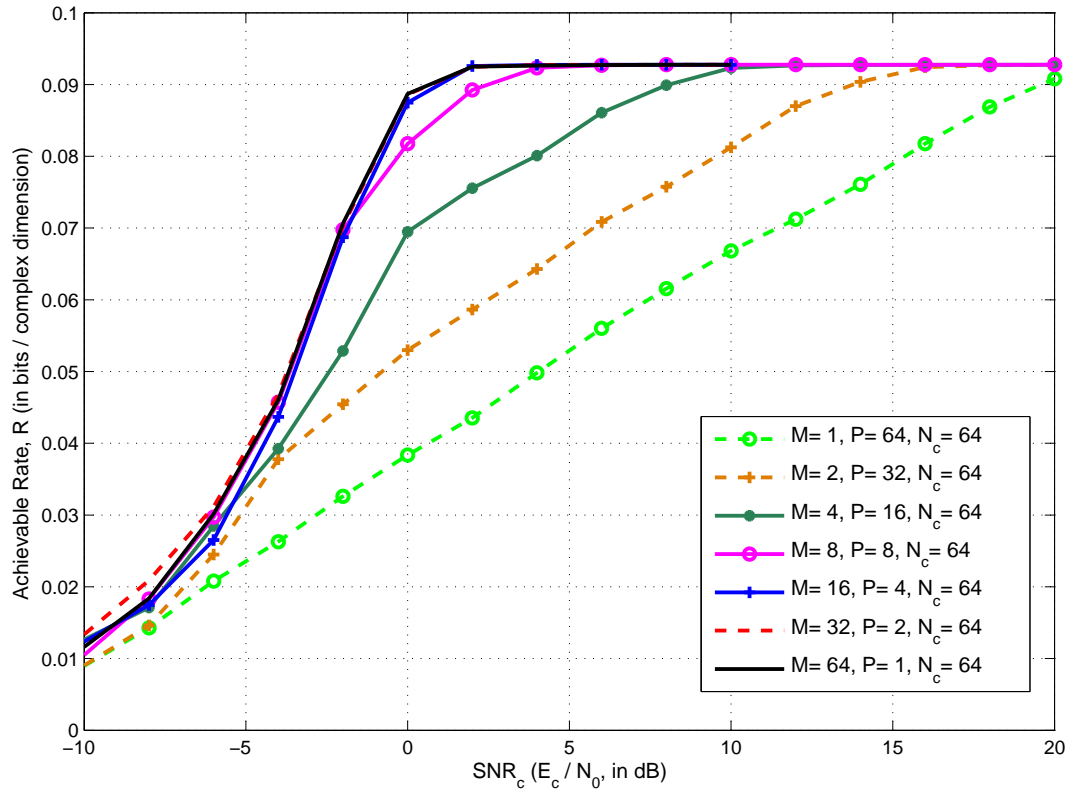


Figure 3.3: Rayleigh Suburban Channel, $L_c = 8$, $N=100$, $\text{PER}=0.01$, $N_c = 64$, $\frac{\log_2(MP)}{N_c} = \frac{6}{64}$

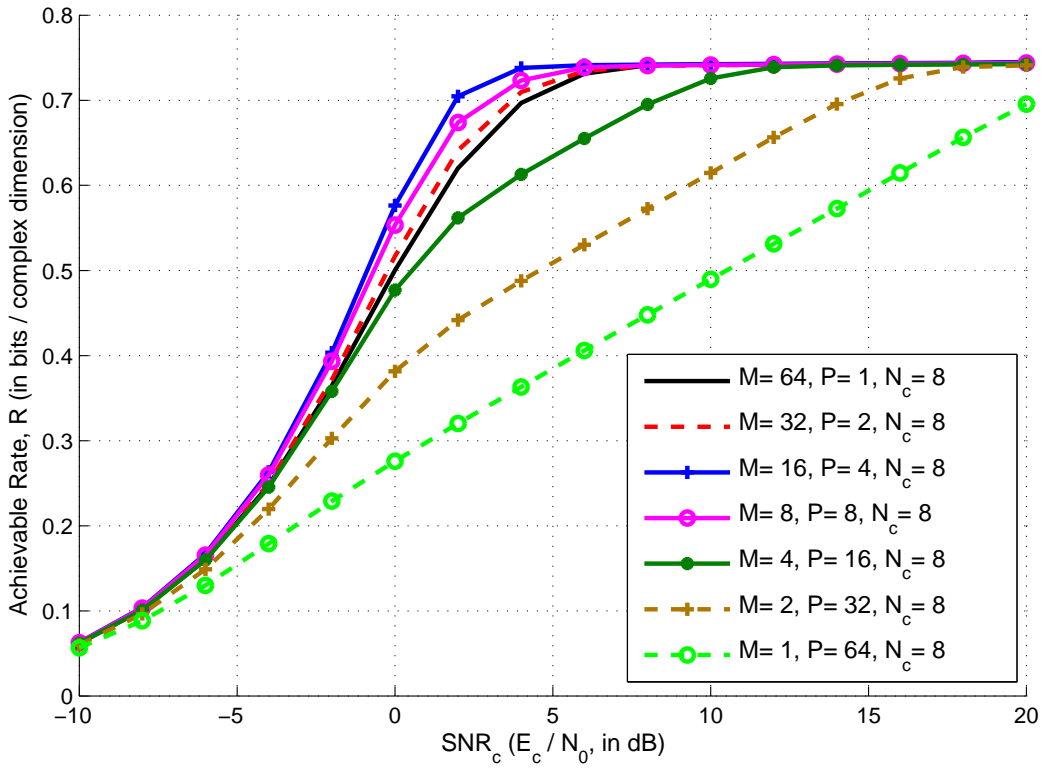


Figure 3.4: AWGN, $N=100$, $\text{PER}=0.01$, $N_c = 8$, $\frac{\log_2(MP)}{N_c} = \frac{3}{4}$

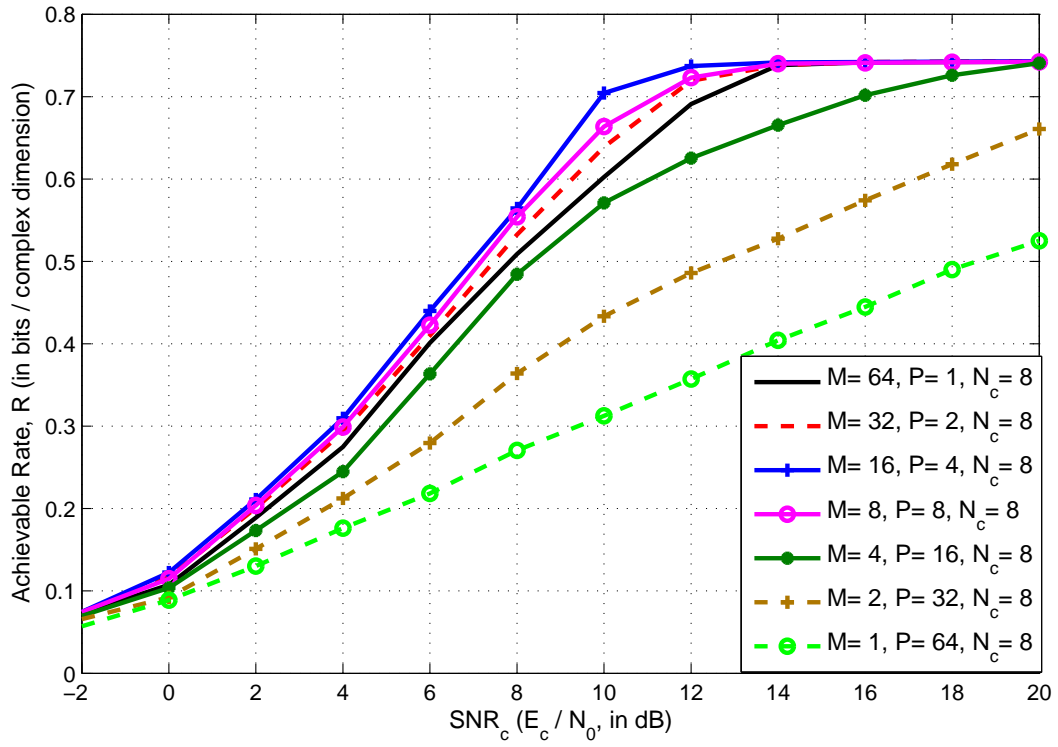


Figure 3.5: Rayleigh Suburban Channel, $L_c = 8$, $N=100$, $\text{PER}=0.01$, $N_c = 8$, $\frac{\log_2(MP)}{N_c} = \frac{3}{4}$

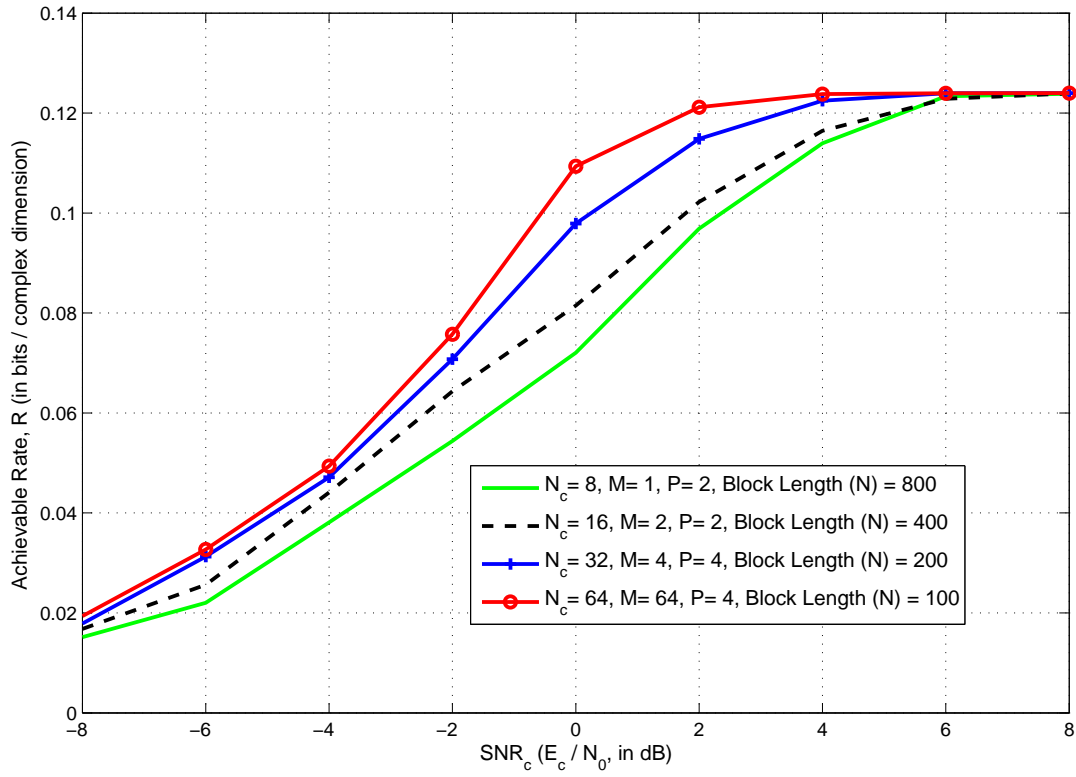


Figure 3.6: Rayleigh Suburban Channel, $L_c = 8$, PER=0.01, Constant Packet Duration $N_{total} = N_c \times N = 6400$, $\frac{\log_2(MP)}{N_c} = \frac{1}{8}$

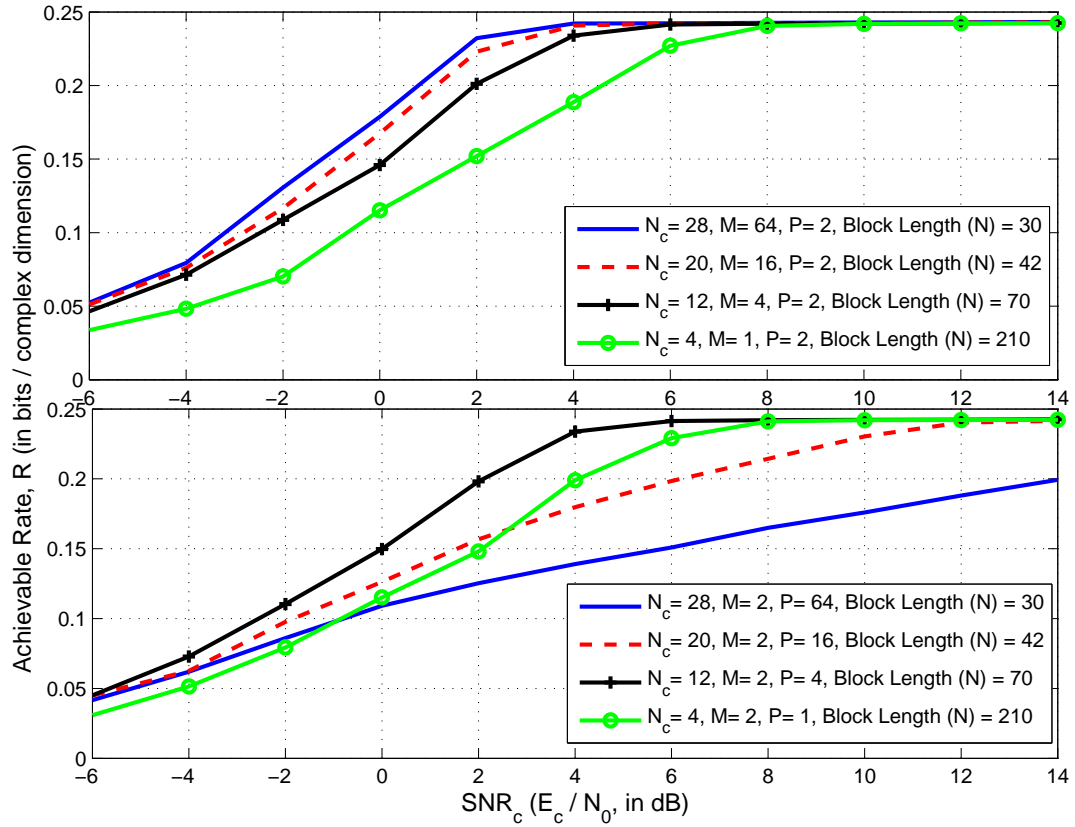


Figure 3.7: Rayleigh Suburban Channel, $L_c = 16$, PER=0.01, Constant Packet Duration $N_{total} = N_c \times N = 840$, $\frac{\log_2(MP)}{N_c} = \frac{1}{4}$

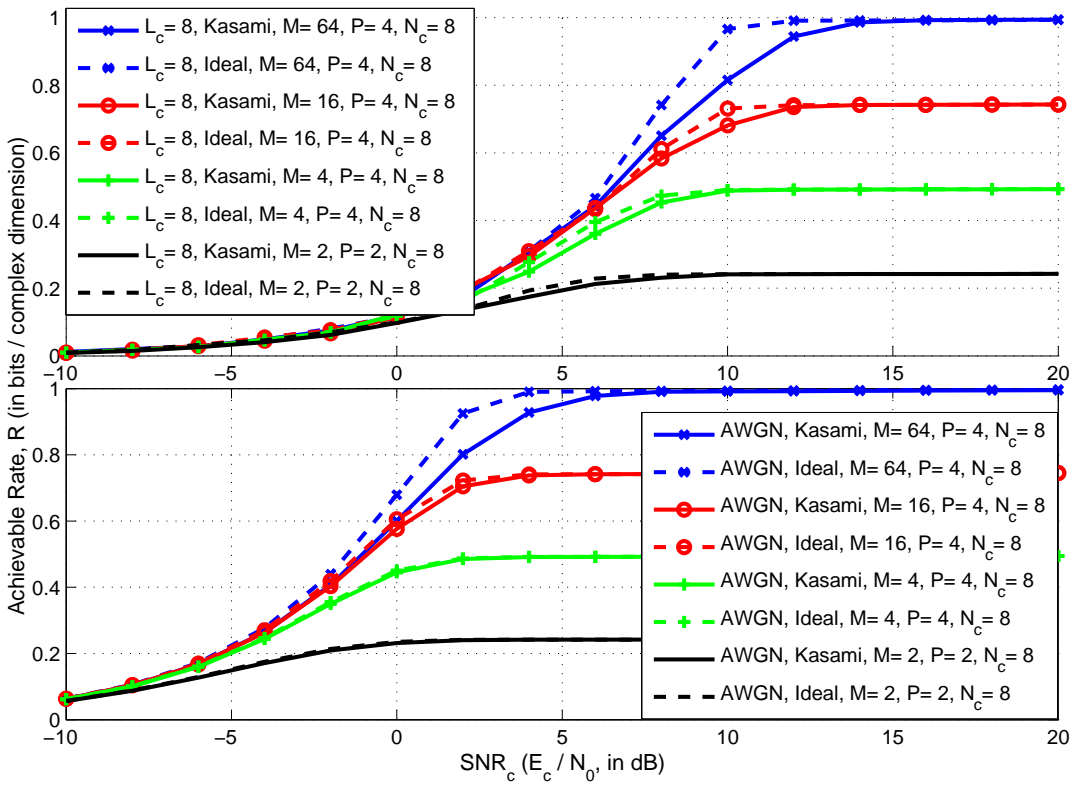


Figure 3.8: Rayleigh Suburban Channel, $L_c = 8$, $\text{PER}=0.01$, $N=100$, $\frac{\log_2(MP)}{N_c} \in \{0.25, 0.5, 0.75, 1\}$

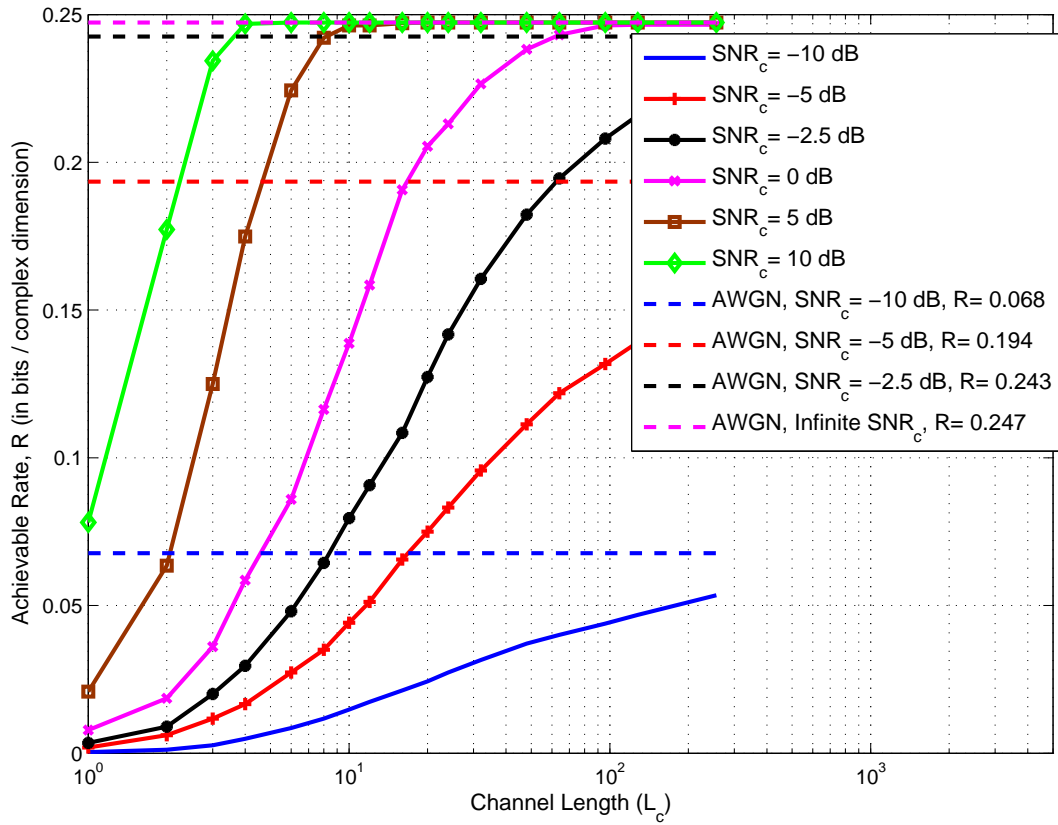


Figure 3.9: Rayleigh Suburban Channel, PER=0.01, $N=100$, $N_c = 24$, $M = 16$ and $P = 4$, $\frac{\log_2(MP)}{N_c} = \frac{1}{4}$

In Fig. 3.10, the effect of finite block length (N) on the success of the MCS scheme (8, 4, 32) is exhibited. Due to the effect of error exponent in (3.8), the PER is dominated by the second term, which accounts for the error events when the channel is not in outage, up to some N value.

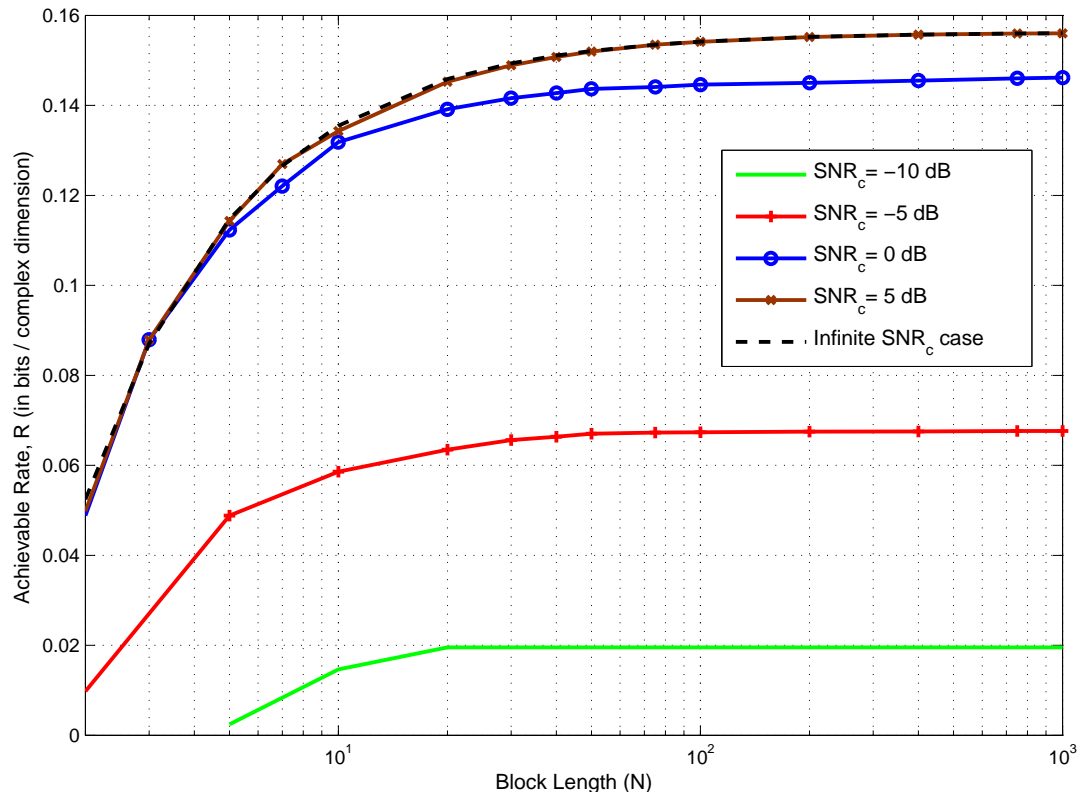


Figure 3.10: Rayleigh Suburban Channel, $L_c = 16$, $\text{PER}=0.01$, $N_c = 32$, $M = 8$ and $P = 4$, $\frac{\log_2(MP)}{N_c} = \frac{5}{32}$

3.8 Conclusions

In this chapter, the upper PER bound of the proposed Ungerboeck MAP receiver in Chapter 2 with a given finite block length is obtained based on the cutoff rate measure analytically. The PER analysis is fulfilled by resorting to the limit-before-average technique in order to tighten the bounds in quasi static fading,

and approximating the MGF of the instantaneous cutoff rate by employing a limited number of exactly specified moments with Pade approximation. This cutoff rate based analysis of the coded MCS transmission brings a significant insight by demonstrating how the modulation related parameters, like bandwidth expansion ratio, number of signaling waveforms, outer channel coding rate etc., are optimized to improve the performance of Ungerboeck type processing while taking the multi-path channel characteristics into account.

CHAPTER 4

A GENERIC REDUCED COMPLEXITY UNGERBOECK TYPE MAP RECEIVER FOR MULTIPLE ACCESS CHANNEL (MAC)

4.1 Introduction

In this chapter, we generalize the reduced state Ungerboeck type MAP receiver with bias correction for MCS proposed in Chapter 2 to a multi-user scenario. First, the generalized symbol rate unwhitened Ungerboeck type vector-matrix signal model is obtained for MCS in multiple access channel (MAC). Then, based on this equivalent discrete-time model, an Ungerboeck type factorization of the likelihood function is constructed, and the iterative reduced state Ungerboeck type multi-user MAP detector, which has linear complexity in the number of interfering users, is proposed by applying the sum-product algorithm (SPA) framework to the resultant Ungerboeck type factor graph (FG). The proposed soft-output iterative receiver can be seen as an extended version of U-RSSE-BDF architecture in Chapter 2 adapted to MAC. Before going into the details of the proposed structure, it is better to give some motivation behind searching for an efficient soft-input-soft-output (SISO) multi-user detection algorithm for the channel of interest, and to mention the related literature.

The literature addressing the suboptimal SISO detection algorithms is huge and an exhaustive survey is not provided here. Nevertheless, it is important to discuss some of the notable works related to iterative SISO multi user detection (MUD) algorithms. Among the abundant literature, most of the recent schemes

are iterative. First, an optimum MUD with exponential complexity in the number of users based on ML criterion was derived for the general asynchronous CDMA systems in [78]. To reduce the complexity, interference cancellation (IC) based algorithms were proposed for CDMA systems. Based on the Gaussian assumption of the interfering signals, linear MMSE based soft IC type MUD algorithms are developed mainly in [79–81] which have quadratic complexity in the number of users. A reduced complexity version is also described by neglecting the correlation between the matched filtered received samples, which results in linear complexity [80, 81] for CDMA systems. Similarly, FG based SISO detection with the help of Gaussian message passing with reference to linear MMSE in Forney type channel (whitened channel) is studied in [82], [83]. Alternatively, joint RSSE type equalization based on set partitioning preceded by channel shortening is proposed for MIMO ISI channels in [84], and for downlink CDMA systems [85]. In [86], bank of RAKE correlators followed by symbol rate decision feedback is proposed for multi code CDMA systems. Finally, a chip rate graphical MUD algorithm using belief propagation for CDMA is proposed based on Forney type FG [87].

For Interleave-division multiple access (IDMA) based systems, turbo MUD algorithm, which is based on soft IC after RAKE type processing, is proposed in [88]. FG based iterative MUD algorithm which has a complexity linear in the number of users for spread spectrum multi-h CPM schemes is described in [89,90]. As to the time-frequency packing [91], where the adjacent signals in time and frequency are allowed to overlap in order to increase spectral efficiency as in CDMA, Faster-Than-Nyquist (FTN) signaling [92] and MCS, symbol by symbol receiver with soft IC based on the Gaussian assumption of the interfering signals [91], and mismatched Ungerboeck type processing based on channel shortening and Gaussian assumption [93], [94], [95] are developed.

FG based equalization techniques based on Ungerboeck observation model are proposed for MIMO ISI channel in [96,97]. They still have computational burden or rely on Gaussian approximation. In [22], [96,97] factorization of the likelihood function is realized without using state variables composing of post-cursor ISI part of the channel, which results in many cycles in FG especially for channels

with long memory, and it is known that the existence of cycles in the FG cannot lead to an algorithm for exact MAP symbol detection [56]. However, there is still a performance gap between the studied equalizer structures and the optimal one when complexity is constrained to be low especially for more general channel model with long memory and non-sparse structure, and modulation types. Thus, there is a need for searching more efficient receiver structures with near optimum performance for the general MCS type modulation in MAC especially with very long memory. In the light of this motivation, our contribution is to obtain an efficient MUD by using the FG and the SPA framework developed based on a general MAC model for MCS.

In this chapter, first we propose an alternative factorization which includes state variables leading to post-cursor Ungerboeck ISI for each user separately so that the number of cycles is kept limited to the number of users only not to the length of the channel memory. Then, the resultant FG is two dimensional, namely, time and user space based on a more general observation model for MCS, where the reduced trellis equalization with decision feedback and MUD are jointly realized. RSSE with BDF is utilized to limit the number of states and to compensate the bias together with the use of MUD based on Ungerboeck factorization.

The proposed receiver here confirms and includes many previous works by changing several system parameters generalized to MCS format. It actually appears as the unification of bidirectional U-RSSE recursions in [37] (Chapter 2) applied to each user for ISI compensation and the mitigation of multi-user interference (MUI) fulfilled by the SPA similar to the one in [22] based on the obtained Ungerboeck type FG. The bias, induced by the use of reduced state equalization per user, is compensated (during the construction of surviving paths of each user) by using the tentative decisions obtained in the previous RSSE recursion. The main advantage of the proposed structure is that one can adjust the complexity level depending on the modulation, number of users, and the statistics of the channels. Furthermore, the receiver architecture operates on unwhitened observations without need of any computationally expensive operations like whitening, pre-filtering (requiring matrix inversions) and resorting to the Gaussian approximation, since these operations are problematic especially

for channels with long memory and time varying environments where the use of adaptive algorithms is indispensable [18]. In addition to this practically important features, the proposed MUD exhibits a close performance to the MFB (where all ISI, MCI and MUI components are removed for each user) even without channel coding as shown in the simulation results.

4.2 System Model

In this chapter, we generalize the reduced state Ungerboeck type receiver architecture presented in Chapter 2 to a multi-user scenario. We deal with the multiple access channel (MAC) where MCS scheme is adopted for each user. That is to say, a total of K users are assumed to be present in the MAC where M distinct signaling waveforms are assigned to each user as done in MCS scheme. Each user selects one of these waveforms for transmission at each signaling interval by applying phase modulation with cardinality P on them. Then, the baseband equivalent of the transmitted signal by n^{th} user can be written as

$$x_n(t) = \sum_{k=0}^{N-1} g_{I_k^n}^n(t - kT) e^{j\theta_k^n} \text{ for } I_k^n \in \{1, \dots, M\}, \quad (4.1)$$

where $\{g_i^n(t)\}$, $i = 1, \dots, M$, $n = 1, \dots, K$ is the i^{th} signaling waveform belonging to n^{th} user. The $\{I_k^n, \theta_k^n\}$ pair denotes the k^{th} transmitted MCS symbol for n^{th} user, where I_k^n is the index of the transmitted waveform within $A_I = \{1, \dots, M\}$, and θ_k^n from $A_\theta = \{\frac{2\pi}{P}(i-1)\}_{i=1}^P$ is the phase information for n^{th} user at k^{th} signaling interval. The properties of the MCS scheme, and the properties of the corresponding waveforms $g_i^n(t)$'s are the same as in the single user case explained in Chapter 2. One data block of each user consists of N MCS symbols.

Each user is assumed to have a quasi-static channel having a baseband equivalent response $h_n(t)$, then the received baseband waveform at the access point can be written as

$$r(t) = \sum_{n=1}^K h_n(t) * x_n(t) + n(t) = \sum_{n=1}^K \sum_{k=0}^{N-1} s_{I_k^n}^n(t - kT) e^{j\theta_k^n} + n(t) \quad (4.2)$$

where $s_i^n(t) = g_i^n(t) * h_n(t)$ for $i = 1, \dots, M$, $n = 1, \dots, K$. The general multipath MAC model is assumed, where the channel responses are static over a block duration, and include a user delay, which accounts for user-asynchronous transmissions due to imperfect network synchronization and the near-far effect.

4.3 Ungerboeck type MLSE Receiver for MCS in MAC

In this section, we first derive the optimal MLSE based detector based on Ungerboeck observation model as a generalization of the previous work in Chapter 2 from single user case to MAC. To start with, we define the following sequences to be detected for n^{th} user:

$$\mathbf{I}_N^n = \{I_0^n, I_1^n, \dots, I_{N-1}^n\} \text{ for } I_k^n \in A_I, \quad \Theta_N^n = \{\theta_0^n, \theta_1^n, \dots, \theta_{N-1}^n\} \text{ for } \theta_k^n \in A_\theta. \quad (4.3)$$

4.3.1 Optimum ML Multi-User Detection for MCS

The optimal ML rule that maximizes the likelihood of the received signal $r(t)$ during one block duration can be obtained as

$$\begin{aligned} \{\hat{\mathbf{I}}_N^n, \hat{\Theta}_N^n\}_{n=1}^K = & \operatorname{argmax}_{\{\mathbf{I}_N^n, \Theta_N^n\}_{n=1}^K} \left(2 \operatorname{Re} \left\{ \sum_n \sum_k e^{-j\theta_k^n} r_k^n(I_k^n) \right\} \right. \\ & \left. - \sum_{n_1} \sum_{n_2} \sum_{k_1} \sum_{k_2} R_{I_{k_1}^{n_1}, I_{k_2}^{n_2}}^{(n_1, n_2)}(k_2 - k_1) e^{j(\theta_{k_1}^{n_1} - \theta_{k_2}^{n_2})} \right) \end{aligned} \quad (4.4)$$

where

$$r_k^n(i) \triangleq \int_{T_0} r(t) (s_i^n(t - kT))^* dt = r(t) * h_n^*(-t) * (g_i^n(-t))^* \Big|_{t=kT} \quad (4.5)$$

$$R_{i,j}^{(m,n)}(k) \triangleq \int_{T_0} s_i^m(t) (s_j^n(t - kT))^* dt = s_i^m(t) * (s_j^n(-t))^* \Big|_{t=kT}. \quad (4.6)$$

In (4.4), by using similar arguments as in Chapter 2, it is practically reasonable to assume that $R_{i,j}^{(m,n)}(k)$ is nonzero only for some finite k values for $|k| < L$ due to the finite delay spreads of the MAC. Eqn. (4.4) indicates that $\{r_k^n(i)\}$ become the sufficient statistics to decide on $\{\hat{\mathbf{I}}_N^n, \hat{\Theta}_N^n\}_{n=1}^K$. Thus, the complexity

of the optimal MUD is in the order of $O((MP)^{KL})$ which can not be afforded in practical scenarios.

4.3.2 Discrete Time Equivalent MAC Model for MCS

In this part, the discrete time equivalent model for MAC with MCS scheme is developed by using the MF outputs sampled at symbol rate, namely, $\{r_k^n(i)\}$. This model will be useful for deriving the reduced state implementation of (4.4), and for performance analysis. The equivalent channel vector for the n^{th} user can be expressed as $\mathbf{h}_n = [h_0^{(n)}, \dots, h_{L_c-1}^{(n)}]^T$ at the Nyquist rate $W \approx \frac{1}{T_c}$. After symbol synchronization and CMF for n^{th} user together with code MF operations at rate W , $R_{i,j}^{(m,n)}(l)$ in (4.6) can be calculated as

$$R_{i,j}^{(m,n)}(l) = \mathbf{h}_n^H \mathbf{G}_{i,j}^{(m,n)}(l) \mathbf{h}_m \quad (4.7)$$

where $\mathbf{G}_{i,j}^{(m,n)}(l)$ is an $L_c \times L_c$ Toeplitz matrix exhibiting the waveform correlations at different delays so that $(k_1, k_2)^{\text{th}}$ element of the Toeplitz matrix is $r_{g,i,j}^{m,n}(lT + (k_1 - k_2)T_c)$. Here, $r_{g,i,j}^{m,n}(t)$ is the cross-correlation function between i^{th} signaling waveform of m^{th} user and the j^{th} waveform of n^{th} user, which is given by $r_{g,i,j}^{m,n}(t) = g_i^m(t) * (g_j^n(-t))^*$.

MF outputs of each user in (4.5), yielding the sufficient statistics, can be modeled by using (4.2) and (4.6) as

$$\mathbf{r}_k^n = \sum_{m=1}^K \sum_{l=-(L-1)}^{L-1} [\mathbf{R}^{(m,n)}(l)]^T \mathbf{c}_{k-l}^m e^{j\theta_{k-l}^m} + \mathbf{v}_k^n, \quad (4.8)$$

for $k = 0, \dots, N-1$ and $n = 1, \dots, K$, where

- $\mathbf{r}_k^n = [r_k^n(1), \dots, r_k^n(M)]^T$ are the MF outputs for n^{th} user at time $t = kT$,
- $\mathbf{R}^{m,n}(l)$ is the $M \times M$ sampled cross-correlation matrix of the signaling waveforms of m^{th} and n^{th} user passing through the MAC with $(i, j)^{\text{th}}$ element $R_{i,j}^{m,n}(l) = s_i^m(t) * (s_j^n(-t))^* \Big|_{t=lT}$ given in (4.6),
- The variable L denotes the effective channel length in terms of symbol period,

- \mathbf{c}_k^n is the equivalent vector symbol of MCS modulation defined in (2.8).
- \mathbf{v}_k^n is the noise vector sequence for n^{th} user with $E\{\mathbf{v}_k^n (\mathbf{v}_{k-l}^m)^H\} = [\mathbf{R}^{m,n}(l)]^T N_0$.
- The equivalent MCS symbol with phase information to be detected can be defined for n^{th} user as $\mathbf{x}_k^{(n)} = \mathbf{c}_k^n e^{j\theta_k^n}$.

The model in (4.8) provides a general description for many different communication schemes employing general MCS format in linear channels impaired by AWGN with the proper selection of M , P and N_c . For example, CDMA [7] and IDMA [88], [98], which is a kind of spread spectrum multiple access scheme where bandwidth expansion is fully exploited for forward error correction code other than spreading, spectrally efficient time-frequency packing techniques based on the superposition of uniformly time and frequency shifted replicas of a base pulse [91], [93] including frequency division multiplexing (FDM) based multi-user scenario, recently proposed OFDM index modulation [99], and with the help of Laurent decomposition spread spectrum scheme based on continuous phase modulation (CPM) exploiting the sequence of modulation indices of a multi-h CPM as a frequency hopping (FH) sequence [89] yield a discrete-time equivalent models which are the special cases of the general model in (4.8) with proper choices of M, P, N_c, K, L values.

4.4 Ungerboeck Type 2–D Factor Graph Construction for MCS in MAC

In this part, two dimensional FG is obtained as a generalization of the FG/SPA framework given in Chapter 2 for single user case to MAC based on the unwhitened observations of the MF outputs. This general FG construction will be helpful in deriving the reduced complexity multi-user MAP detector in the next section. First of all, we provide some vector and matrix definitions which simplify the ML metric of the optimal MUD in (4.4) based on Ungerboeck observation model:

$$\mathbf{a}_k^{(n)} \triangleq [(\mathbf{x}_0^{(n)})^T, (\mathbf{x}_1^{(n)})^T, \dots, (\mathbf{x}_k^{(n)})^T]^T, \quad \mathbf{y}_k^{(n)} \triangleq [(\mathbf{r}_0^n)^T, (\mathbf{r}_1^n)^T, \dots, (\mathbf{r}_k^n)^T]^T, \quad (4.9)$$

and

$$\Psi_k^{(m_1, m_2)} \triangleq \begin{bmatrix} \mathbf{H}^{(m_1, m_2)}(0) & \cdots & \mathbf{H}^{(m_1, m_2)}(-k) \\ \mathbf{H}^{(m_1, m_2)}(1) & \cdots & \mathbf{H}^{(m_1, m_2)}(-k+1) \\ \vdots & \ddots & \vdots \\ \mathbf{H}^{(m_1, m_2)}(k) & \cdots & \mathbf{H}^{(m_1, m_2)}(0) \end{bmatrix}_{M(k+1) \times M(k+1)}, \quad (4.10)$$

where $\mathbf{H}^{(m_1, m_2)}(l) = (\mathbf{R}^{m_1, m_2}(l))^T$, and $\Psi_k^{(m_2, m_1)} = \left(\Psi_k^{(m_1, m_2)}\right)^H$ since $\mathbf{R}^{m_2, m_1}(l) = (\mathbf{R}^{m_1, m_2}(-l))^H$. Also, the following matrix is defined to be used in error probability analysis:

$$\Phi_k^{(m_1, m_2)} \triangleq \begin{bmatrix} \mathbf{H}^{(m_1, m_2)}(-k-1) & \cdots & \mathbf{H}^{(m_1, m_2)}(-k-L+1) \\ \mathbf{H}^{(m_1, m_2)}(-k) & \cdots & \mathbf{H}^{(m_1, m_2)}(-k-L+2) \\ \vdots & \ddots & \vdots \\ \mathbf{H}^{(m_1, m_2)}(-1) & \cdots & \mathbf{H}^{(m_1, m_2)}(-L+1) \end{bmatrix}_{M(k+1) \times M(L-1)} \quad (4.11)$$

By using (4.9) and (4.10), the Ungerboeck type ML decision metric in (4.4) up to $(k+1)^{th}$ signaling interval can be expressed as

$$\Lambda_{k+1} \left(\left\{ \mathbf{I}_{k+1}^n, \boldsymbol{\Theta}_{k+1}^n \right\}_{n=1}^K \right) = 2 \operatorname{Re} \left\{ \sum_m \left(\mathbf{a}_k^{(m)} \right)^H \mathbf{y}_k^{(m)} \right\} - \sum_{m_1} \sum_{m_2} \left(\mathbf{a}_k^{(m_2)} \right)^H \Psi_k^{(m_1, m_2)} \mathbf{a}_k^{(m_1)}. \quad (4.12)$$

The number of states for each user can be reduced with the help of U-RSSE algorithm proposed in Chapter 2. Thus, it is assumed that a total of $M^{J_I^m}$ and $P^{J_\theta^m}$ states are used for I_k^m and θ_k^m respectively. The reduced state vector of m^{th} user at time k can be defined as

$$S_k^m = \left[I_{k-1}^m \quad \cdots \quad I_{k-J_I^m}^m, \theta_{k-1}^m \quad \cdots \quad \theta_{k-J_\theta^m}^m \right], \quad m = 1, \dots, K. \quad (4.13)$$

By using the definition in (4.13) and the symmetry of $\Psi_k^{(m_1, m_2)}$, one can express (4.12) as the sum of accumulated Ungerboeck metrics in time and user domain

as

$$\begin{aligned}
\Lambda_N &= \sum_{k=0}^{N-1} (\Lambda_{k+1} - \Lambda_k) \\
&= \sum_{k=0}^{N-1} \left(\sum_{n=1}^K [f_k^n(\mathbf{r}_k^n, I_k^n, \theta_k^n) - g_k^n(I_k^n, \theta_k^n, S_k^n)] \right. \\
&\quad \left. - \sum_{m=1, m < n}^K p_k^{m,n}(I_k^m, \theta_k^m, S_k^m, I_k^n, \theta_k^n, S_k^n) \right) \quad (4.14)
\end{aligned}$$

where

$$f_k^n(\cdot) \triangleq 2 \operatorname{Re} \left\{ r_k^n(I_k^n) e^{-j\theta_k^n} \right\} - R_{I_k^n, I_k^n}^{(n,n)}(0), \quad (4.15)$$

$$g_k^n(\cdot) \triangleq 2 \operatorname{Re} \left\{ e^{-j\theta_k^n} \sum_{l=1}^{L-1} R_{I_{k-l}^n, I_k^n}^{(n,n)}(l) e^{j\theta_{k-l}^n} \right\} \quad (4.16)$$

$$\begin{aligned}
p_k^{m,n}(\cdot) &\triangleq 2 \operatorname{Re} \left\{ R_{I_k^m, I_k^n}^{(m,n)}(0) e^{j(\theta_k^m - \theta_k^n)} + e^{-j\theta_k^n} \sum_{l=1}^{L-1} R_{I_{k-l}^m, I_k^n}^{(m,n)}(l) e^{j\theta_{k-l}^m} \right. \\
&\quad \left. + e^{-j\theta_k^m} \sum_{l=1}^{L-1} R_{I_{k-l}^n, I_k^m}^{(n,m)}(l) e^{j\theta_{k-l}^n} \right\}. \quad (4.17)
\end{aligned}$$

In order to compute $g_k^n(\cdot)$ in (4.16) and $p_k^{m,n}(\cdot)$ in (4.17), $\left\{ \hat{I}_l^n(S_k^n) \right\}_{l=0}^{k-(J_I^n+1)}$ and $\left\{ \hat{\theta}_l^n(S_k^n) \right\}_{l=0}^{k-(J_\theta^n+1)}$, which are the sequences of state dependent conditional symbol decisions in the surviving path of S_k^n in U-RSSE of n^{th} user, are used. Then the joint APP of the transmitted symbols, and states for each user can be factored as follows:

$$\begin{aligned}
&P \left(\{I_k^n, \theta_k^n, S_k^n\}_{\forall k,n} \mid \{\mathbf{r}_k^n\}_{\forall k,n} \right) \\
&\propto P \left(\{\mathbf{I}_N^n, \boldsymbol{\Theta}_N^n\}_{\forall n} \right) P \left(\{S_k^n\}_{\forall k,n} \mid \{\mathbf{I}_N^n, \boldsymbol{\Theta}_N^n\}_{\forall n} \right) P \left(\{\mathbf{r}_k^n\}_{\forall k,n} \mid \{I_k^n, \theta_k^n, S_k^n\}_{\forall k,n} \right) \\
&\propto \exp \left\{ \frac{\Lambda_N}{N_0} \right\} \prod_{n=1}^K P(S_0^n) \prod_{k=0}^{N-1} P(\{I_k^n, \theta_k^n\}) p(S_{k+1}^n \mid S_k^n, I_k^n, \theta_k^n) \\
&= \prod_{k=0}^{N-1} \prod_{n=1}^K P(S_0^n) \phi_k^n(\mathbf{r}_k^n, I_k^n, \theta_k^n) \psi_k^n(I_k^n, \theta_k^n, S_k^n) T_k^n(I_k^n, \theta_k^n, S_k^n, S_{k+1}^n) \\
&\quad P(\{I_k^n, \theta_k^n\}) \prod_{m=1, m < n}^K \kappa_k^{m,n}(I_k^m, \theta_k^m, S_k^m, I_k^n, \theta_k^n, S_k^n) \quad (4.18)
\end{aligned}$$

where

$$\phi_k^n(\cdot) \triangleq \exp \left\{ \frac{f_k^n(\cdot)}{N_0} \right\}, \quad \psi_k^n(\cdot) \triangleq \exp \left\{ -\frac{g_k^n(\cdot)}{N_0} \right\}, \quad \kappa_k^{m,n}(\cdot) \triangleq \exp \left\{ -\frac{p_k^{m,n}(\cdot)}{N_0} \right\} \quad (4.19)$$

and $T_k^n (I_k^n, \theta_k^n, S_k^n, S_{k+1}^n)$ is the trellis indicator function for n^{th} user.

The resulting 2–D FG based on the Ungerboeck MAC model in (4.8) is shown in Fig. 4.1. Only the connections between n^{th} and m^{th} user are demonstrated for convenience. The obtained graph can be seen as the generalization of the FG for MCS scheme in Ungerboeck ISI channels in Chapter 2 to the Ungerboeck type MAC. The graph in Fig. 4.1 has cycles of length 6. Since cycles are present, the SPA applied to this graph is iterative and leads to an approximate computation of the marginal symbol APPs. However, it is known that having cycles with length greater than 4 is sufficient to obtain very good approximations to the actual APPs [22].

In Fig. 4.1, instead of representing MCS symbol variables alone, we merge the symbol and state variable in order to increase the cycle length in the graph.¹

4.5 A Reduced Complexity Ungerboeck type Multi-User MAP Receiver for MCS

Based on the FG shown in Fig. 4.1, a novel reduced complexity MAP detector is proposed as generalization of U-RSSE-BDF in Chapter 2 to the multi-user scenario. By using the SPA framework, the following rules for message updating

¹ This operation preserves all the information of the original graph, and known as stretching in the literature [56], [54].

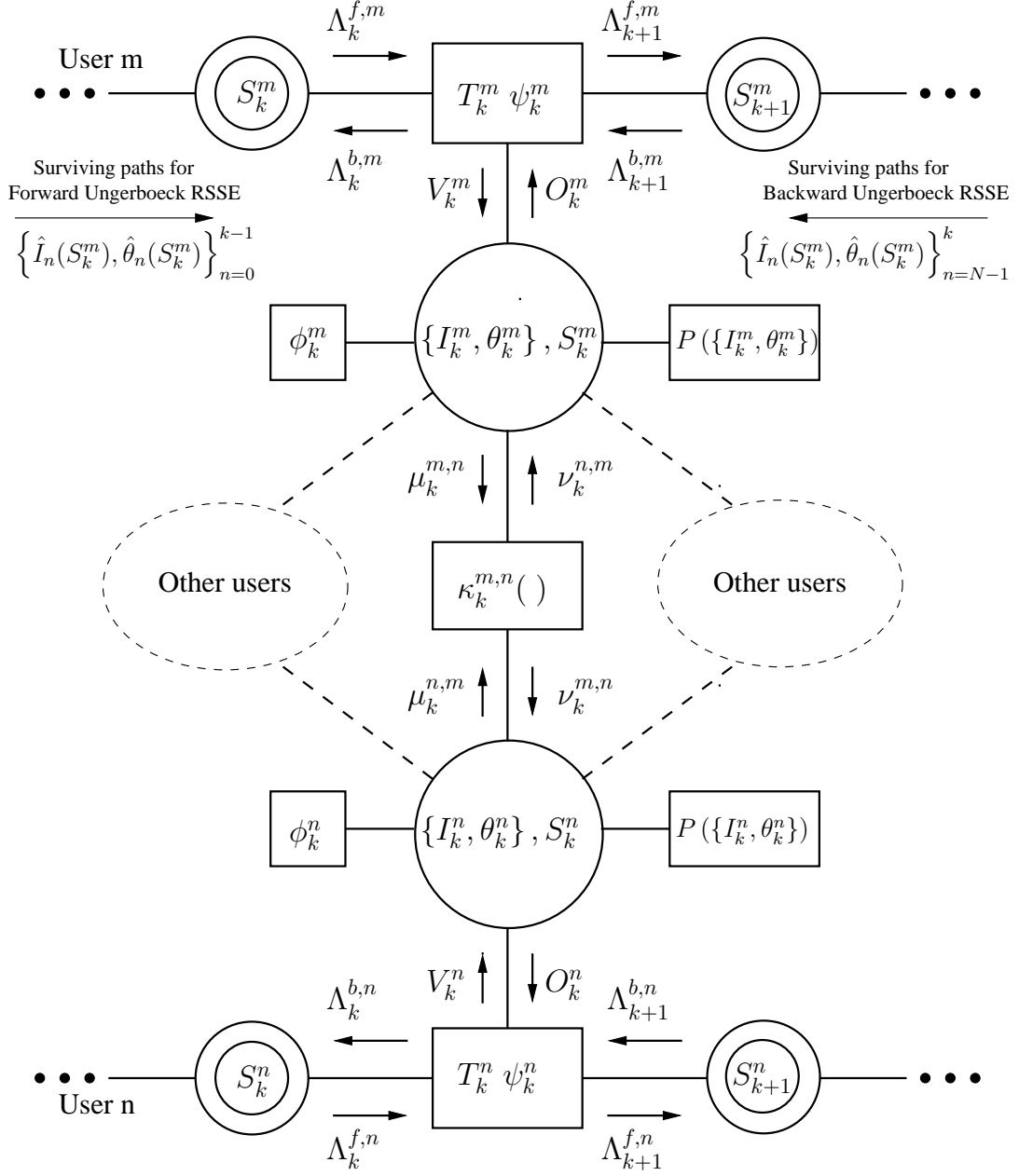


Figure 4.1: FG corresponding to the joint APP in (4.18) for MCS

are obtained:

$$\Lambda_{k+1}^{f,m}(S_{k+1}^m) = \sum_{\sim\{S_{k+1}^m\}} \Lambda_k^{f,m}(S_k^m) T_k^m(\cdot) \psi_k^m(\cdot) O_k^m(I_k^m, \theta_k^m, S_k^m) \quad (4.20)$$

$$\Lambda_k^{b,m}(S_k^m) = \sum_{\sim\{S_k^m\}} \Lambda_{k+1}^{b,m}(S_{k+1}^m) T_k^m(\cdot) \psi_k^m(\cdot) O_k^m(I_k^m, \theta_k^m, S_k^m) \quad (4.21)$$

$$V_k^m(I_k^m, \theta_k^m, S_k^m) = \Lambda_k^{f,m}(S_k^m) \Lambda_{k+1}^{b,m}(S_{k+1}^m) T_k^m(\cdot) \psi_k^m(\cdot) \quad (4.22)$$

$$O_k^m(I_k^m, \theta_k^m, S_k^m) = P(\{I_k^m, \theta_k^m\}) \phi_k^m(\cdot) \left[\prod_{l=1, l \neq m}^K \nu_k^{l,m}(I_k^m, \theta_k^m, S_k^m) \right] \quad (4.23)$$

$$\nu_k^{n,m}(I_k^m, \theta_k^m, S_k^m) = \sum_{\{I_k^n, \theta_k^n\}, S_k^n} \mu_k^{n,m}(I_k^n, \theta_k^n, S_k^n) \kappa_k^{m,n}(\cdot) \quad (4.24)$$

$$\mu_k^{m,n}(I_k^m, \theta_k^m, S_k^m) = \frac{V_k^m(I_k^m, \theta_k^m, S_k^m) O_k^m(I_k^m, \theta_k^m, S_k^m)}{\nu_k^{n,m}(I_k^m, \theta_k^m, S_k^m)}. \quad (4.25)$$

It is seen that the resultant Ungerboeck type FG contains the cycle free FG given in Chapter 2. Actually, without considering MUI, the corresponding FG per user is the same as the reduced state graph in Chapter 2. Therefore, this is an extended graph of MCS detection taking the MUI into account. In (4.23), $\nu_k^{n,m}(\cdot)$ actually fulfills the soft IC operation that tries to cancel the effect of n^{th} user on m^{th} user's signal during the bidirectional U-RSSE operation of m^{th} user realized by the upper part of the graph. This soft estimate of the MUI in m^{th} user signal, stemming from the n^{th} user, namely, $\nu_k^{n,m}(\cdot)$ in (4.24) is calculated by using the probabilities $\mu_k^{n,m}(\cdot)$ in (4.25). In Ungerboeck type processing, the node $\kappa_k^{n,m}(\cdot)$ just propagates approximated APPs between interfering nodes, after the averaging operation in (4.24). The product of the messages, $V_k^m(\cdot) O_k^m(\cdot)$ is proportional to the approximated APP $P(\{I_k^m, \theta_k^m\} | \{\mathbf{r}_l^n\}_{\forall l, n})$ for m^{th} user.

4.5.1 Message Schedule

This proposed algorithm can be seen as the unification of the reduced state Ungerboeck type MAP detection based on bidirectional U-RSSE in Chapter 2 and the soft output graph based multi-user detection with linear complexity in the number of users in [22]. We call this algorithm as multi-user U-RSSE-BDF (MU-RSSE-BDF), where U-RSSE is responsible for removing self ISI, MCI and MUI with the help of BDF at each time k .

Due to the existence of cycles in the considered 2-D Ungerboeck type FG for MAC in Fig. 4.1, there is not a unique schedule for the operation of SPA. We utilize a *serial schedule*, similar to the one in [22], to update the messages while using SPA. All messages $\{\nu_k^{n,m}\}$ and $\{\mu_k^{n,m}\}$ should be initialized to the same positive value where the choice of this value is irrelevant [56]. First, the messages are updated in user domain, then the forward and backward messages in time domain, namely, $\Lambda_k^{f,m}(\cdot)$ and $\Lambda_k^{b,m}(\cdot)$ are updated by using bidirectional RSSE recursions in an iterative fashion as follows:

- At time k , for a given $V_k^m(\cdot)$, forward recursion in user domain is defined as the following sequence of steps, to be serially executed for each user index m from 1 to K :
 - Update the messages $\{\nu_k^{n,m}\}_{m>n}$;
 - Update the term $O_k^m(\cdot)$;
 - Update the messages $\{\mu_k^{m,n}\}_{m<n}$.
- The backward recursion can also be defined as to be serially executed for each user index m from K down to 1:
 - Update the messages $\{\nu_k^{n,m}\}_{m<n}$;
 - Update the term $O_k^m(\cdot)$;
 - Update the messages $\{\mu_k^{m,n}\}_{m>n}$.

Finally, forward recursion part of the serially scheduled SPA in time domain from $k = 0$ to $k = N - 1$ can be formalized by the following steps:

- 1) run the forward recursion in user domain to update $O_k^m(\cdot)$ at time k ;
- 2) run the backward recursion in user domain to update $O_k^m(\cdot)$ at time k ;
- 3) update forward and backward messages in time domain, namely, $\Lambda_{k+1}^{f,m}(\cdot)$ and $\Lambda_k^{b,m}(\cdot)$;
- 4) $k = k + 1$, update $V_{k+1}^m(\cdot)$ for each user;
- 5) if the stopping criterion is not satisfied go to step 1.

Then, the backward recursion in time domain can be executed from $k = N - 1$ to 0 in a similar manner. We will only consider stopping criteria based on the number of self-iterations, which is the number of times that forward and backward recursions in time domain are executed. Due to the presence of serial recursions, the proposed SPA is characterized by a latency that linearly increases with the value of KN .

4.5.2 Bias Compensation

By using a similar methodology given in Chapter 2, the surviving path construction of the states of the m^{th} user can be obtained by using the analysis to be given in Section 4.6 as

$$\left\{ \hat{I}_{k-J_I^m}^m(S_{k+1}^m), \hat{\theta}_{k-J_\theta^m}^m(S_{k+1}^m) \right\} = \arg \max_{\left\{ I_{k-J_I^m}^m, \theta_{k-J_\theta^m}^m \right\}} \left[N_0 \ln \left(\Lambda_k^{f,m}(S_k^m) \psi_k^m(\cdot) O_k^m(\cdot) \right) - \beta_{k-J_\theta^m}^m(S_k^m) \right] \quad (4.26)$$

where the bias correction term for the m^{th} user is

$$\beta_{k-J_\theta^m}^m(S_k^m) = 2 \operatorname{Re} \left\{ \sum_{n=1}^K \mathbf{h}_n^H \left[\sum_{l_1=k-L+2}^{k-J_I^m} \sum_{l_2=k-l_1+1}^{L-1} \mathbf{G}_{\hat{I}_{l_1}^m(S_k^m), \tilde{I}_{l_1+l_2}^m}^{(m,n)}(l_2) \right. \right. \\ \left. \left. e^{j(\hat{\theta}_{l_1}^m(S_k^m) - \tilde{\theta}_{l_1+l_2}^n)} + \sum_{l_1=k-J_I^m+1}^{k-J_\theta^m} \sum_{l_2=k-l_1+1}^{L-1} \mathbf{G}_{I_{l_1}^m(S_k^m), \tilde{I}_{l_1+l_2}^n}^{(m,n)}(l_2) e^{j(\hat{\theta}_{l_1}^m(S_k^m) - \tilde{\theta}_{l_1+l_2}^n)} \right] \mathbf{h}_m \right\} \quad (4.27)$$

The bias of the m^{th} user in MAC is calculated by using the hard tentative decisions about future symbols $\{\tilde{I}_k^m, \tilde{\theta}_k^m\}_{\forall m,k}$ (obtained from previous iterations) yielding anticausal ISI, MCI and MUI part of the Ungerboeck channel. Finally, the marginal MCS symbol APPs of m^{th} user can be calculated by means of the following completion based on FG in Fig. 4.1 and by using the bias correction term $\beta_k^m(\cdot)$ in (4.29)

$$P \left(\{I_k^m, \theta_k^m\} \mid \{\mathbf{r}_l^n\}_{\forall l,n} \right) = \sum_{S_k^m} \left[V_k^m(\cdot) O_k^m(\cdot) \exp \left\{ -\frac{1}{N_0} \beta_k^m(\cdot) \right\} \right] \quad (4.28)$$

where

$$\beta_k^m(I_k^m, \theta_k^m, S_k^m) = 2 \operatorname{Re} \left\{ \sum_{n=1}^K \sum_{l_1=k-L+\min\{J_I^m, J_\theta^m\}+2}^k \sum_{l_2=k-l_1+\min\{J_I^m, J_\theta^m\}+1}^{L-1} R_{I_{l_1}^m(S_k^m), \tilde{l}_{l_1+l_2}}^{(m,n)}(l_2) e^{j(\theta_{l_1}^m(S_k^m) - \tilde{\theta}_{l_1+l_2}^n)} \right\} \quad (4.29)$$

and the corresponding MAP symbol detection rule for the m^{th} user is

$$\left\{ \hat{I}_k^m, \hat{\theta}_k^m \right\} = \arg \max_{\{I_k^m, \theta_k^m\}} P \left(\{I_k^m, \theta_k^m\} \mid \{\mathbf{r}_l^n\}_{\forall l, n} \right). \quad (4.30)$$

4.5.3 Computational Complexity

The complexity of MU-RSSE-BDF is linear in the number of users, since it basically requires the operation of U-RSSE-BDF for each user. By using a similar argument as in Chapter 2, we can say that the computational complexity is on the order of $O(\frac{1}{N_c} \sum_{n=1}^K M^{J_I^n+1} P^{J_\theta^n+1})$.

4.6 Error Probability Analysis for Reduced Trellis Ungerboeck type MUD

4.6.1 Generalized Bias Analysis for MCS in MAC

In this section, we provide the extension of the analysis given in Appendix B to MAC. Let $\mathbf{x}_k^{(n)} \triangleq \mathbf{c}_k^n e^{j\theta_k^n}$ be the equivalent vector symbol of multi-user MCS with modulated phase in (4.8). We define $\{\mathbf{x}_{k,1}^{(n)}\}_{k=0}^{N-1}$ as the transmitted sequence of vector symbols belonging to path-1 for n^{th} user, and $\{S_{k,1}^n\}_{k=0}^{N-1}$ is the corresponding sequence of states in the reduced trellis for path-1 for n^{th} user. Similarly, $\{\mathbf{x}_{k,2}^{(n)}\}_{k=0}^{N-1}$ is defined as a hypothetical sequence of vector symbols for path-2 of n^{th} user that the receiver erroneously decides on instead of path-1 and $\{S_{k,2}^n\}_{k=0}^{N-1}$ is the sequence of states in the reduced trellis of path-2 that diverges from the correct sequence of states of path-1 at time $l = 0$ and remerges with it at a later time $l = k + 1$ such that

$$S_{0,1}^n = S_{k,2}^n, \text{ and } S_{k+1,1}^n = S_{k+1,2}^n, \quad (4.31)$$

which implies

$$\begin{aligned} I_{l,1}^{(n)} &= I_{l,2}^{(n)} \text{ for } l = k, \dots, k - J_I^n + 1, \\ \theta_{l,1}^{(n)} &= \theta_{l,2}^{(n)} \text{ for } l = k, \dots, k - J_\theta^n + 1. \end{aligned} \quad (4.32)$$

By using the equivalent model in (4.8), the symbol time sampled matched filter outputs up to time k in (4.9) can be written by using (4.10) and (4.11) as

$$\mathbf{y}_k^{(n)} = \sum_m \Psi_k^{(m,n)} \mathbf{a}_{k,1}^{(m)} + \sum_m \Phi_k^{(m,n)} \mathbf{a}_{k,*}^{(m)} + \boldsymbol{\eta}_k^{(n)}, \quad n = 1, \dots, K \quad (4.33)$$

where

$$\begin{aligned} \mathbf{a}_{k,1}^{(n)} &\triangleq [(\mathbf{x}_{0,1}^{(n)})^T, (\mathbf{x}_{0,1}^{(n)})^T, \dots, (\mathbf{x}_{k,1}^{(n)})^T]^T, \\ \mathbf{a}_{k,2}^{(n)} &\triangleq [(\mathbf{x}_{0,2}^{(n)})^T, (\mathbf{x}_{0,2}^{(n)})^T, \dots, (\mathbf{x}_{k,2}^{(n)})^T]^T, \\ \mathbf{a}_{k,*}^{(n)} &\triangleq [(\mathbf{x}_{k+1,1}^{(n)})^T, (\mathbf{x}_{k+2,1}^{(n)})^T, \dots, (\mathbf{x}_{k+L-1,1}^{(n)})^T]^T \\ \boldsymbol{\eta}_k^{(n)} &\triangleq [(\mathbf{v}_0^n)^T, (\mathbf{v}_1^n)^T, \dots, (\mathbf{v}_k^n)^T]^T \end{aligned} \quad (4.34)$$

and, the error vector for n^{th} user can be defined as

$$\mathbf{e}_{1 \rightarrow 2}^{(n)} \triangleq \mathbf{a}_{k,2}^{(n)} - \mathbf{a}_{k,1}^{(n)} \triangleq [(\mathbf{e}_{0,1 \rightarrow 2}^{(n)})^T, (\mathbf{e}_{1,1 \rightarrow 2}^{(n)})^T, \dots, (\mathbf{e}_{k,1 \rightarrow 2}^{(n)})^T]^T. \quad (4.35)$$

An error event occurs if the accumulated metric on path-2 is greater than that on path-1 at time $k + 1$ when the paths merge. By using the metric rule for MCS in (4.12), one can obtain the probability of this error event in MU-RSSE with error-free decision feedback. The pairwise error probability (PEP) that corresponds to decision on path-2 when the sequence of path-1 is sent can be

written as

$$\begin{aligned}
& \mathbb{P} \left\{ \left\{ \mathbf{a}_{k,1}^{(n)} \right\}_{n=1}^K \rightarrow \left\{ \mathbf{a}_{k,2}^{(n)} \right\}_{n=1}^K \right\} = \\
& \mathbb{P} \left\{ \Lambda_{k+1} \left(\left\{ \mathbf{a}_{k,2}^{(n)} \right\}_{n=1}^K \right) > \Lambda_{k+1} \left(\left\{ \mathbf{a}_{k,1}^{(n)} \right\}_{n=1}^K \right) \mid \left\{ \mathbf{a}_{k,1}^{(n)} \right\}_{n=1}^K \text{ is sent} \right\} \\
& = \mathbb{P} \left\{ 2 \operatorname{Re} \left\{ \sum_m \left(\mathbf{a}_{k,2}^{(m)} - \mathbf{a}_{k,1}^{(m)} \right)^H \mathbf{y}_k^{(m)} \right\} > \sum_{m_1} \sum_{m_2} \left(\mathbf{a}_{k,2}^{(m_2)} \right)^H \boldsymbol{\Psi}_k^{(m_1, m_2)} \mathbf{a}_{k,2}^{(m_1)} \right. \\
& \quad \left. - \sum_{m_1} \sum_{m_2} \left(\mathbf{a}_{k,1}^{(m_2)} \right)^H \boldsymbol{\Psi}_k^{(m_1, m_2)} \mathbf{a}_{k,1}^{(m_1)} \mid \mathbf{y}_k^{(n)} = \sum_m \boldsymbol{\Psi}_k^{(m, n)} \mathbf{a}_{k,1}^{(m)} \right. \\
& \quad \left. + \sum_m \boldsymbol{\Phi}_k^{(m, n)} \mathbf{a}_{k,*}^{(m)} + \boldsymbol{\eta}_k^{(n)}, n = 1, \dots, K \right\} \\
& = \mathbb{P} \left\{ \sum_m 2 \operatorname{Re} \left\{ \left(\mathbf{e}_{1 \rightarrow 2}^{(m)} \right)^H \boldsymbol{\eta}_k^{(m)} \right\} > \sum_{m_1} \sum_{m_2} \left(\mathbf{e}_{1 \rightarrow 2}^{(m_1)} \right)^H \boldsymbol{\Psi}_k^{(m_2, m_1)} \mathbf{e}_{1 \rightarrow 2}^{(m_2)} \right. \\
& \quad \left. - \sum_{m_1} \sum_{m_2} 2 \operatorname{Re} \left\{ \left(\mathbf{e}_{1 \rightarrow 2}^{(m_1)} \right)^H \boldsymbol{\Phi}_k^{(m_2, m_1)} \mathbf{a}_{k,*}^{(m_2)} \right\} \right\}. \tag{4.36}
\end{aligned}$$

Then, one can obtain PEP in the following form

$$\begin{aligned}
& \mathbb{P} \left\{ \left\{ \mathbf{a}_{k,1}^{(n)} \right\}_{n=1}^K \rightarrow \left\{ \mathbf{a}_{k,2}^{(n)} \right\}_{n=1}^K \right\} = \\
& Q \left(\frac{d^2 \left(\left\{ \mathbf{e}_{1 \rightarrow 2}^{(m)} \right\}_{m=1}^K \right) + \gamma \left(\left\{ \mathbf{e}_{1 \rightarrow 2}^{(m)} \right\}_{m=1}^K, \left\{ \mathbf{a}_{k,*}^{(m)} \right\}_{m=1}^K \right)}{\sqrt{2N_0 d^2 \left(\left\{ \mathbf{e}_{1 \rightarrow 2}^{(m)} \right\}_{m=1}^K \right)}} \right) \tag{4.37}
\end{aligned}$$

where

$$\begin{aligned}
d^2 \left(\left\{ \mathbf{e}_{1 \rightarrow 2}^{(m)} \right\}_{m=1}^K \right) &= \sum_{m_1} \sum_{m_2} \left(\mathbf{e}_{1 \rightarrow 2}^{(m_1)} \right)^H \boldsymbol{\Psi}_k^{(m_2, m_1)} \mathbf{e}_{1 \rightarrow 2}^{(m_2)}, \tag{4.38} \\
\gamma \left(\left\{ \mathbf{e}_{1 \rightarrow 2}^{(m)} \right\}_{m=1}^K, \left\{ \mathbf{a}_{k,*}^{(m)} \right\}_{m=1}^K \right) &= - \sum_{m_1} \sum_{m_2} 2 \operatorname{Re} \left\{ \left(\mathbf{e}_{1 \rightarrow 2}^{(m_1)} \right)^H \boldsymbol{\Phi}_k^{(m_2, m_1)} \mathbf{a}_{k,*}^{(m_2)} \right\} \\
&= -2 \operatorname{Re} \left\{ \sum_{m_1} \sum_{m_2} \sum_{l_1=k-L+2}^{k-\min\{J_I^{m_1}, J_\theta^{m_1}\}} \sum_{l_2=k-l_1+1}^{L-1} \left(\mathbf{e}_{l_1, 1 \rightarrow 2}^{(m_1)} \right)^H \mathbf{H}^{(m_2, m_1)}(-l_2) \mathbf{x}_{l_1+l_2, 1}^{(m_2)} \right\}
\end{aligned}$$

by noting that $\mathbf{e}_{l, 1 \rightarrow 2}^n = 0$ for $l = k, \dots, k - \min\{J_I^n, J_\theta^n\} + 1$ from (4.32) and taking $J_I^n \geq J_\theta^n$.

The variance of the bias term can be calculated by using the similar analysis technique for the single user case given in Appendix B and assuming that only

one user has erroneous decision as

$$\begin{aligned}
E\{|\gamma|^2\} &= \frac{1}{K} \sum_{n_1=1}^K \sum_{n_2=1}^K \frac{2}{M^2 [MP - 1 + \mathbf{1}\{J_I^{n_1} > J_\theta^{n_1}\} (P - 1)]} \\
&\left[\sum_{l=J_I^{n_1}+1}^{L-1} \sum_{m_1=1}^M \sum_{m_2=1, m_2 \neq m_1}^M \sum_{p=0}^{P-1} \sum_{n=1}^M \left| \mathbf{h}_{n_2}^H \mathbf{A}_{n_1, n_2, l}^{(m_1, m_2, p, n)} \mathbf{h}_{n_1} \right|^2 + \right. \\
&\left. \sum_{l=J_\theta^{n_1}+1}^{L-1} \sum_{m_1=1}^M \sum_{p=1}^{P-1} \sum_{n=1}^M (1 + \mathbf{1}\{J_I^{n_1} > J_\theta^{n_1}\} \mathbf{1}\{l > J_I^{n_1}\}) \left| \mathbf{h}_{n_2}^H \mathbf{B}_{n_1, n_2, l}^{(m_1, p, n)} \mathbf{h}_{n_1} \right|^2 \right] \quad (4.39)
\end{aligned}$$

where

$$\begin{aligned}
\mathbf{A}_{n_1, n_2, l}^{(m_1, m_2, p, n)} &= \mathbf{G}_{m_1, n}^{(n_1, n_2)}(l) - e^{-j\frac{2\pi}{P}p} \mathbf{G}_{m_2, n}^{(n_1, n_2)}(l), \\
\mathbf{B}_{n_1, n_2, l}^{(m_1, p, n)} &= 2\sqrt{\sin^2\left(\frac{\pi}{P}p\right)} \mathbf{G}_{m_1, n}^{(n_1, n_2)}(l) \quad (4.40)
\end{aligned}$$

and $\mathbf{G}_{m_1, m_2}^{(n_1, n_2)}(l)$ is an $L_c \times L_c$ Toeplitz matrix comprised of the waveform correlations at different delays as given in (4.7).

4.6.2 Approximate Bit Error Probability for MU-RSSE with BDF

Assuming that all input sequences are equally likely and weight one error events dominate the others, BER of the n^{th} user can be calculated by using similar

analysis tools in Appendix C and (4.37):

$$P_b^{(n)} \leq E_{\{\mathbf{h}_m\}} \left\{ \sum_{\forall \{\mathbf{e}_{1 \rightarrow 2}^{(m)}\}_m \mid \mathbf{e}_{1 \rightarrow 2}^{(n)} \neq \mathbf{0}} \frac{w_b(\mathbf{e}_{1 \rightarrow 2}^{(n)})}{\log_2(MP)} \mathbb{P} \left(\left\{ \mathbf{a}_{k,1}^{(m)} \right\}_{m=1}^K \right) \right. \\ \left. \mathbb{P} \left\{ \left\{ \mathbf{e}_{1 \rightarrow 2}^{(m)} \right\}_{m=1}^K \mid \{\mathbf{h}_m\} \right\} \right\} \quad (4.41)$$

$$\approx E_{\{\mathbf{h}_m\}} \left\{ \sum_{\forall \{\mathbf{e}_{k,1 \rightarrow 2}^{(m)}\}_m \mid \mathbf{e}_{k,1 \rightarrow 2}^{(n)} \neq \mathbf{0}} \frac{w_b(\mathbf{e}_{k,1 \rightarrow 2}^{(n)})}{\log_2(MP)} \frac{1}{(MP)^K} \right. \\ \left. \mathbb{P} \left\{ \left\{ \mathbf{x}_{k,1}^{(m)} \right\}_{m=1}^K \rightarrow \left\{ \mathbf{x}_{k,2}^{(m)} \right\}_{m=1}^K \mid \{\mathbf{h}_m\} \right\} \right\} \\ \approx \sum_{q=1}^Q \frac{1}{2K} \frac{1}{(MP)^K} \frac{w_b(\mathbf{e}_{k,1 \rightarrow 2}^{(n)})}{\log_2(MP)} \sum_{\forall \{\mathbf{e}_{k,1 \rightarrow 2}^{(m)}\}_m \mid \mathbf{e}_{k,1 \rightarrow 2}^{(n)} \neq \mathbf{0}} E_{\{\mathbf{h}_m\}} \left\{ \exp \left[\frac{-1}{4 \sin^2(\frac{\pi}{2K}q)} \right. \right. \\ \left. \left. \frac{E_c}{N_0} \sum_{m_1=1}^K \sum_{m_2=1}^K \mathbf{h}_{m_2}^H \mathbf{F} \left(\mathbf{e}_{k,1 \rightarrow 2}^{(m_1)}, \mathbf{e}_{k,1 \rightarrow 2}^{(m_2)}, \left\{ \mathbf{G}_{i,j}^{(m_1, m_2)}(0) \right\}_{i,j} \right) \mathbf{h}_{m_1} \right] \right\}. \quad (4.42)$$

The expectation in (4.42) can be calculated by using (B.9), where the matrix $\mathbf{F}(\cdot)$ accounts for all error event distances as in (2.31). One can further simplify the BER calculation by assuming that only one user have erroneous decision. This corresponds to the case that MUI is perfectly canceled by the proposed MU-RSSE-BDF. Then, the BER for n^{th} user can be reduced to the the following form which is similar to the expression for the case of single user MCS transmission in (2.29):

$$P_b^{(n)} \approx \sum_{q=1}^Q \frac{1}{2K} \frac{1}{(MP)} \frac{w_b(\mathbf{e}_{k,1 \rightarrow 2}^{(n)})}{\log_2(MP)} \sum_{\forall \mathbf{e}_{k,1 \rightarrow 2}^{(n)} \mid \mathbf{e}_{k,1 \rightarrow 2}^{(n)} \neq \mathbf{0}} \\ E_{\mathbf{h}_n} \left\{ \exp \left[\frac{-1}{4 \sin^2(\frac{\pi}{2K}q)} \frac{E_c}{N_0} \mathbf{h}_n^H \mathbf{F} \left(\mathbf{e}_{k,1 \rightarrow 2}^{(n)}, \left\{ \mathbf{G}_{i,j}^{(n,n)}(0) \right\}_{i,j} \right) \mathbf{h}_n \right] \right\}. \quad (4.43)$$

4.7 Simulation Results

As to the performance of the proposed iterative MUD (MU-RSSE-BDF), we use randomly selected MCS waveforms from the QPSK alphabet without any

optimization. In Fig. 4.2, the performance variation of the proposed receiver is demonstrated while increasing the number of self iterations. Multiple access channels are assumed to be independent of each other and Rayleigh distributed with suburban exponentially decaying power delay profile [7] with $L_c = 64$. Self iterations help the MUD improve its performance due to the cycles in FG, and also the bias can be compensated more accurately with the help of iterative processing.

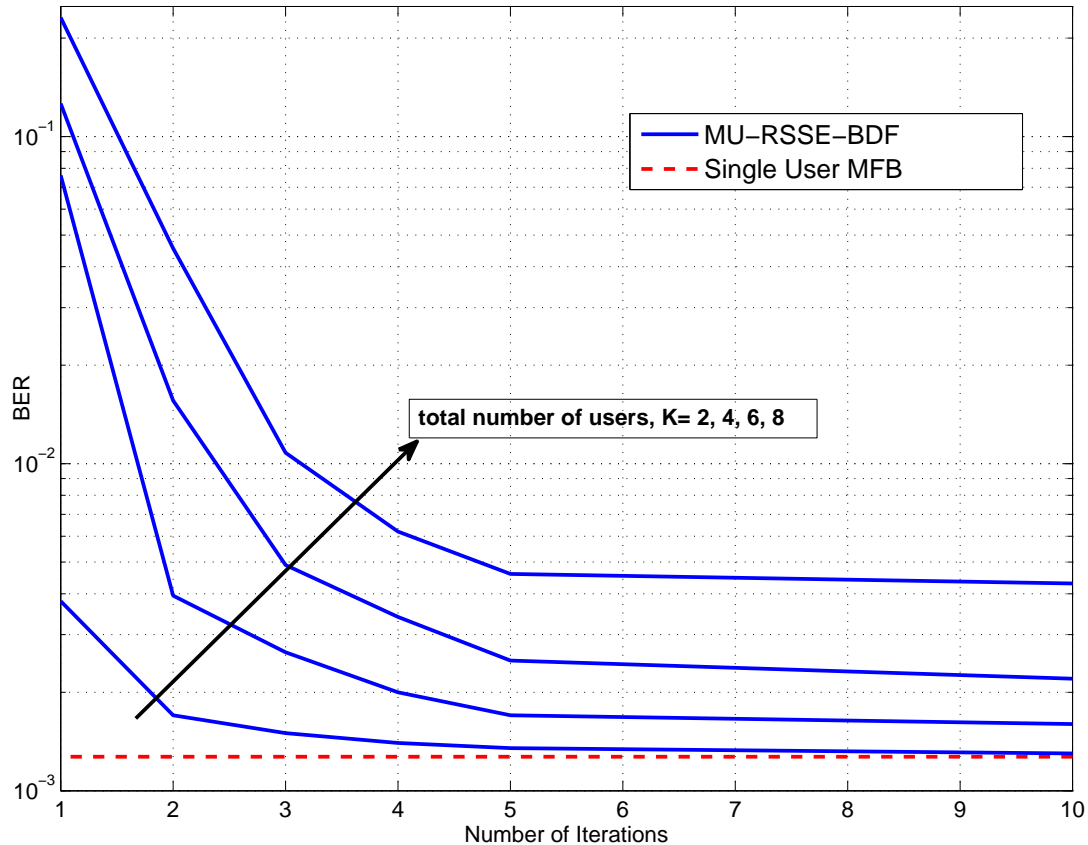


Figure 4.2: $M = 4$, $P = 4$, $N_c = 16$, $L_c = 64$ Rayleigh distributed taps exponentially decaying power delay profile for MAC, $J_I^n = 0$ and $J_\theta^n = 0$, $SNR_c = \frac{E_c}{N_0} = 0$ dB

In Fig. 4.3, the BER of the MCS scheme with $(4, 4, 16)$ is shown for different number of users (K). This performance is remarkable for the selected parameters since there is no outer channel code used to help iterative processing, whereas

the self iterations of MUD improve the quality of soft decisions only, and also the MCS waveforms are not optimized in MAC. Nevertheless, the performance loss compared to MFB even with this remarkably reduced complexity is similar to the reference benchmark algorithms in [79], [22], [88] for MUD at the operational spectral efficiencies chosen. Therefore, this generalized MUD structure appears as an important candidate for the reduced complexity SISO decoding of MAC channels with the use of spectrally efficient MCS scheme by extending the reduced state Ungerboeck type MAP receiver in Chapter 2 to the MUD enhanced with the SPA for MUI mitigation.

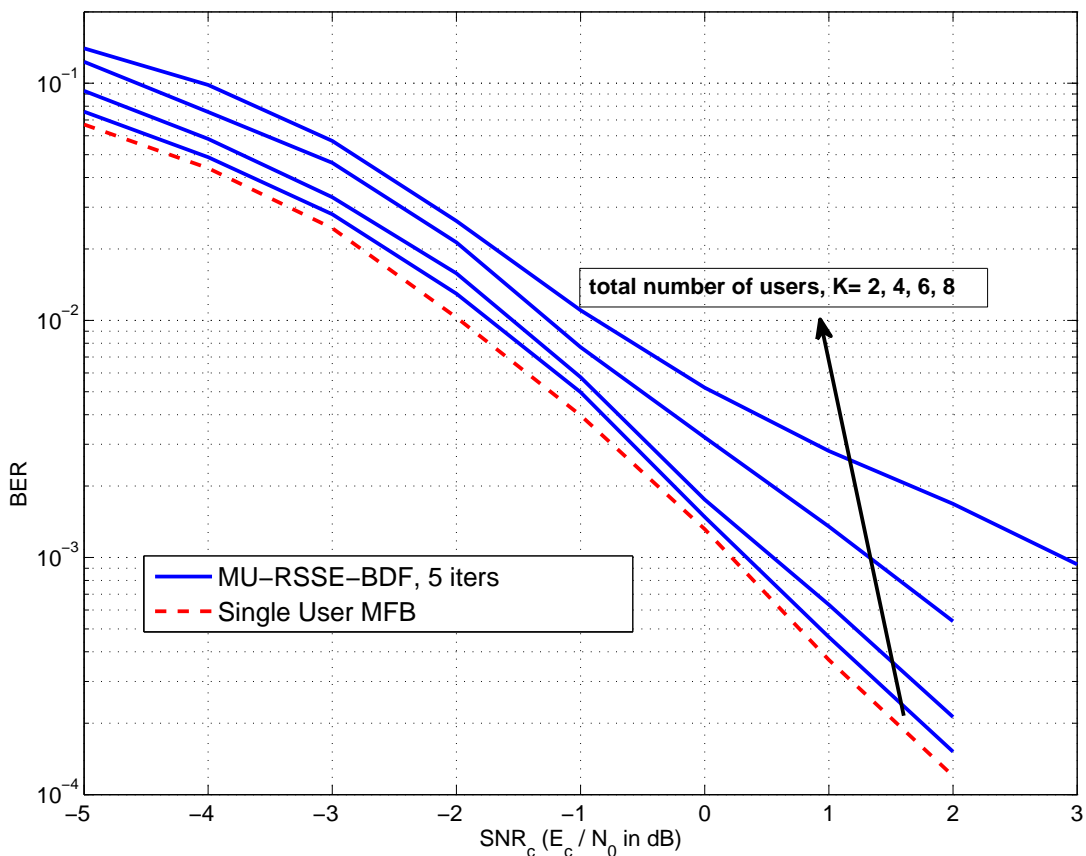


Figure 4.3: $M = 4$, $P = 4$, $N_c = 16$, $L_c = 64$ Rayleigh distributed taps exponentially decaying power delay profile for MAC, $J_I^n = 0$ and $J_\theta^n = 0$

4.8 Conclusions

In this chapter, we generalized the proposed reduced state Ungerboeck MAP receiver in Chapter 2 to be exploited in MAC at symbol rate by using an Ungerboeck type factorization of pdf's. The resultant soft output iterative MUD, which has linear complexity in the number of interfering users, is actually the unification of bidirectional Ungerboeck RSSE recursions in [37] (Chapter 2) applied to each user separately for ISI and MCI compensation and the use of SPA framework for soft MUI mitigation. Similar to the bias correction technique in Chapter 2, the bias, induced by the the use of RSSE per user, is analytically found and can also be compensated with the help of iterative BDF which is instrumental in eliminating the post- and pre-cursor ISI, MCI and MUI for MCS. The proposed MUD exhibits a close performance to the reference MFB even without outer channel coding at significantly lowered complexity in dense multi-path environment.

CHAPTER 5

CONCLUSION AND FUTURE WORKS

The main focus in this thesis is to propose an efficient receiver structure realizing SISO detection, which is directly applied to unwhitened observations after CMF and code MFs, for a general class of modulation format called MCS. This type of modulation can be represented as selection of one out of M waveforms per signaling interval to which an additional phase modulation is applied. It allows the use of non-orthogonal signaling waveforms to attain higher spectral efficiencies, and many modulation schemes can be put into this framework. In this thesis, we investigate generic suboptimal receiver architectures, without need of computationally expensive operations like whitening, pre-filtering, channel shortening etc., based on the Ungerboeck model for MCS in highly dispersive channels.

First, a reduced state implementation of the Ungerboeck type MAP receiver is proposed for MCS by forming the Ungerboeck type FG and applying SPA framework substantiated with bidirectional RSSE recursions, where BDF is instrumental in eliminating the post- and pre-cursor ISI and multi code interference. Second, an error probability analysis, helping the designer improve the receiver's performance for uncoded MCS scheme is carried out. The conducted analysis indicates a bias term, originating from the anticausal part of the Ungerboeck channel, and its statistical properties for a stochastic channel with Gaussian distributed taps in MCS are determined. A PER analysis based on cutoff rate by using the MGF for coded MCS transmission in multi-path fading channels is provided. These analyses lead to significant insight on the selection of system parameters and clearly demonstrate the high performance

and the efficiency of the proposed scheme by proper choice of the signaling parameters. They can be exploited to determine how to transport data optimally in highly dispersive channels for MCS when the reduced complexity Ungerboeck type receiver is employed.

Finally, the reduced trellis Ungerboeck MAP receiver is extended to MAC by unifying the forward and backward RSSE recursions with bias correction applied to each user for ISI and MCI compensation, and the use of SPA for the mitigation of MUI based on the obtained Ungerboeck type FG. The resultant soft output iterative MUD has linear complexity in the number of interfering users. The proposed receiver architectures exhibit almost optimal performance with reference to MFB at significantly reduced complexity especially for channels with large dispersion. The computational complexity of the proposed detection algorithms can be arranged flexibly depending on the modulation related parameters and channel statistics by using the analytical tools developed. The obtained results justify the utilization of MCS, allowing simultaneous use of a common channel by multiple users, as an effective modulation technique for extremely dispersive channels at low transmit power.

To sum up, the developed MCS transmission model provides a general description for many communication schemes in linear channels impaired by AWGN. The proposed receiver architectures here confirms, compares many previous works, and complements reduced complexity Ungerboeck structure by changing several system parameters generalized to MCS format with the help of the provided analytical tools. Although phase modulation is applied to each signaling waveform throughout the thesis work, quite a standard procedure will be utilized in order to extend the proposed Ungerboeck receiver and the associated analysis techniques for arbitrary constellations per waveform.

As a future study, an adaptive form of the algorithm and the corresponding analysis can be considered for time varying media by incorporating the timing synchronization, adaptive channel estimation and tracking into the Ungerboeck type MAP detection. Also, the robustness issue of the Ungerboeck based reception against channel estimation errors, Doppler effects, synchronization errors

can be studied. Non-coherent versions of the proposed algorithms, taking these issues into account, can be developed.

REFERENCES

- [1] A. Goldsmith, *Wireless Communications*. Cambridge University Press, 2005.
- [2] P. Enge and D. Sarwate, "Spread-spectrum multiple-access performance of orthogonal codes: Linear receivers," *IEEE Trans. Commun.*, vol. 35, no. 12, pp. 1309–1319, Dec. 1987.
- [3] K. Pahlavan and M. Chase, "Spread-spectrum multiple-access performance of orthogonal codes for indoor radio communications," *IEEE Trans. Commun.*, vol. 38, no. 5, pp. 574–577, May 1990.
- [4] M. Chase and K. Pahlavan, "Performance of DS-CDMA over measured indoor radio channels using random orthogonal codes," *IEEE Trans. Veh. Technol.*, vol. 42, no. 4, pp. 617–624, Nov. 1993.
- [5] E. K. Hong, K. J. Kim, and K. C. Whang, "Performance evaluation of DS-CDMA system with M-ary orthogonal signaling," *IEEE Trans. Veh. Technol.*, vol. 45, no. 1, pp. 57–63, Feb. 1996.
- [6] M. B. Pursley and T. C. Royster, "High-rate direct-sequence spread spectrum with error-control coding," *IEEE Trans. Commun.*, vol. 54, no. 9, pp. 1693–1702, Sept. 2006.
- [7] J. G. Proakis, *Digital Communications 4th Edition*. McGRAW-HILL, 2001.
- [8] J. Rossler, L. H. Lampe, W. Gerstacker, and J. Huber, "Decision-feedback equalization for CDMA downlink," in *Proc. 2002 IEEE Veh. Technol. Conf.*, vol. 2, pp. 816–820.
- [9] M. Pursley and T. Royster, "Properties and performance of the IEEE 802.11b complementary-code-key signal sets," *IEEE Trans. Commun.*, vol. 57, no. 2, pp. 440–449, Feb. 2009.
- [10] K. Takizawa and R. Kohno, "Low-complexity Rake reception and equalization for MBOK DS-UWB systems," in *Proc. IEEE Global Telecommun. Conf. (GLOBECOM)*, vol. 2, Nov. 2004, pp. 1249–1253.
- [11] J. K. Hwang, Y. L. Chiu, and R. L. Chung, "Efficient bidirectional decision-feedback receiver for MBOK direct sequence," *IEEE Trans. Signal Process.*, vol. 56, no. 3, pp. 1167–1177, Mar. 2008.
- [12] C. He, J. Huang, and Z. Ding, "A variable-rate spread-spectrum system for underwater acoustic communications," *IEEE J. Ocean. Eng.*, vol. 34, no. 4, pp. 624–633, Oct. 2009.
- [13] J. Jeganathan, A. Ghrayeb, L. Szczecinski, and A. Ceron, "Space shift keying modulation for MIMO channels," *IEEE Trans. Wireless Commun.*, vol. 8, no. 7, pp. 3692–3703, July 2009.

- [14] K. C. Hwang and K. B. Lee, "Performance analysis of low processing gain DS/CDMA systems with random spreading sequences," *IEEE Commun. Lett.*, vol. 2, no. 12, pp. 315–317, Dec. 1998.
- [15] J. Forney, G., "Maximum-likelihood sequence estimation of digital sequences in the presence of intersymbol interference," *IEEE Trans. Inf. Theory*, vol. 18, no. 3, pp. 363–378, May 1972.
- [16] G. Ungerboeck, "Adaptive maximum-likelihood receiver for carrier-modulated data-transmission systems," *IEEE Trans. Commun.*, vol. 22, no. 5, pp. 624–636, May 1974.
- [17] G. E. Bottomley and S. Chennakeshu, "Unification of MLSE receivers and extension to time-varying channels," *IEEE Trans. Commun.*, vol. 46, no. 4, pp. 464–472, Apr. 1998.
- [18] A. Hafeez and W. E. Stark, "Decision feedback sequence estimation for unwhitened ISI channels with applications to multiuser detection," *IEEE J. Sel. Areas Commun.*, vol. 16, no. 9, pp. 1785–1795, Dec. 1998.
- [19] A. Duel-Hallen and C. Heegard, "Delayed decision-feedback sequence estimation," *IEEE Trans. Commun.*, vol. 37, no. 5, pp. 428–436, May 1989.
- [20] M. V. Eyuboglu and S. U. H. Qureshi, "Reduced-state sequence estimation for coded modulation of intersymbol interference channels," *IEEE J. Sel. Areas Commun.*, vol. 7, no. 6, pp. 989–995, Aug. 1989.
- [21] W. Gerstacker, R. Muller, and J. Huber, "Iterative equalization with adaptive soft feedback," *IEEE Trans. Commun.*, vol. 48, no. 9, pp. 1462–1466, Sept. 2000.
- [22] G. Colavolpe, D. Fertonani, and A. Piemontese, "SISO detection over linear channels with linear complexity in the number of interferers," *IEEE J. Sel. Topics Signal Process.*, vol. 5, no. 8, pp. 1475–1485, Dec. 2011.
- [23] F. Rusek and A. Prlja, "Optimal channel shortening for MIMO and ISI channels," *IEEE Trans. Wireless Commun.*, vol. 11, no. 2, pp. 810–818, Feb. 2012.
- [24] F. Rusek and D. Fertonani, "Bounds on the information rate of intersymbol interference channels based on mismatched receivers," *IEEE Trans. Inf. Theory*, vol. 58, no. 3, pp. 1470–1482, Mar. 2012.
- [25] A. Radosevic, D. Fertonani, T. M. Duman, J. G. Proakis, and M. Stojanovic, "Bounds on the information rate for sparse channels with long memory and i.u.d. inputs," *IEEE Trans. Commun.*, vol. 59, no. 12, pp. 3343–3352, Dec. 2011.
- [26] F. Rusek, M. Loncar, and A. Prlja, "A comparison of Ungerboeck and Forney models for reduced-complexity ISI equalization," in *Proc. IEEE Global Telecommun. Conf. (GLOBECOM)*, Nov. 2007, pp. 1431–1436.
- [27] M. Loncar and F. Rusek, "On reduced-complexity equalization based on Ungerboeck and Forney observation models," *IEEE Trans. Signal Process.*, vol. 56, no. 8, pp. 3784–3789, Aug. 2008.
- [28] G. Colavolpe and A. Barbieri, "On MAP symbol detection for ISI channels using the Ungerboeck observation model," *IEEE Commun. Lett.*, vol. 9, no. 8, pp. 720–722, Aug. 2005.

- [29] B. D. Woerner and W. E. Stark, "Trellis-coded direct-sequence spread-spectrum communications," *IEEE Trans. Commun.*, vol. 42, no. 12, pp. 3161–3170, Dec. 1994.
- [30] N. Merhav, G. Kaplan, A. Lapidoth, and S. Shamai Shitz, "On information rates for mismatched decoders," *IEEE Trans. Inf. Theory*, vol. 40, no. 6, pp. 1953–1967, 1994.
- [31] L. R. Bahl, J. Cocke, F. Jelinek, and J. Raviv, "Optimal decoding of linear codes for minimizing symbol error rate," *IEEE Trans. Inf. Theory*, vol. 20, pp. 284–287, Mar. 1974.
- [32] E. Malkamaki and H. Leib, "Evaluating the performance of convolutional codes over block fading channels," *IEEE Trans. Inf. Theory*, vol. 45, no. 5, pp. 1643–1646, 1999.
- [33] H. Bouzekri and S. L. Miller, "Distance spectra and performance bounds of space-time trellis codes over quasi-static fading channels," *IEEE Trans. Inf. Theory*, vol. 50, no. 8, p. 1820–1831, 2004.
- [34] H. Amindavar and J. A. Ritcey, "Pade approximations of probability density functions," *IEEE Trans. Aerosp. Electron. Syst.*, vol. 30, no. 2, pp. 416–424, 1994.
- [35] V. V. Veeravalli and A. Mantravadi, "The coding-spreading tradeoff in CDMA systems," *IEEE J. Sel. Areas Commun.*, vol. 20, no. 2, pp. 396–408, Feb. 2002.
- [36] M. Agarwal, K. Datta, and A. K. Chaturvedi, "Optimal bandwidth allocation to coding and spreading in DS-CDMA systems using LMMSE front-end detector," *IEEE Trans. Wireless Commun.*, vol. 4, no. 6, pp. 2636–2641, Nov. 2005.
- [37] G. M. Guvensen, Y. Tanik, and A. O. Yilmaz, "A reduced-state Ungerboeck type MAP receiver with bidirectional decision feedback for M-ary quasi orthogonal signaling," *IEEE Trans. Commun.*, vol. 62, no. 2, pp. 552–566, Feb. 2014.
- [38] B. H. Kim, "Bidirectional iterative ISI canceller for high-rate DSSS/CCK communications," *IEEE J. Sel. Areas Commun.*, vol. 24, no. 1, pp. 171–180, Jan. 2006.
- [39] Y. Lee and H. Park, "A RAKE receiver with an ICI/ISI equalizer for a CCK modem," *IEEE Trans. Veh. Technol.*, vol. 58, no. 1, pp. 198–206, Jan. 2009.
- [40] Y. Kim and J. Moon, "CCK demodulation via symbol decision feedback equalizer," *IEEE Commun. Lett.*, vol. 8, no. 10, pp. 620–622, Oct. 2004.
- [41] K. Tang, L. B. Milstein, and P. H. Siegel, "MLSE receiver for direct-sequence spread-spectrum systems on a multipath fading channel," *IEEE Trans. Commun.*, vol. 51, no. 7, pp. 1173–1184, July 2003.
- [42] C. Unger, R. Irmer, and G. P. Fettweis, "On interpath interference suppression by MLSE detection in DS/SS systems," in *Proc. IEEE Int. Symp. on Personal, Indoor and Mobile Radio Commun. (PIMRC)*, vol. 1, Sept. 2003, pp. 740–744.

- [43] S. Tantikovit and A. U. H. Sheikh, "Joint multipath diversity combining and MLSE equalization (RAKE-MLSE receiver) for WCDMA systems," in *Proc. IEEE 51st Veh. Technol. Conf. (VTC)*, vol. 1, 2000, pp. 435–439.
- [44] Y. P. E. Wang, J. F. Chen, S. J. Grant, and G. E. Bottomley, "MLSE and MAP detectors for high-data-rate DS-SS reception in dispersive channels," in *Proc. IEEE 60th Veh. Technol. Conf. (VTC)*, vol. 2, Sept. 2004, pp. 963–967.
- [45] C. Jonietz, W. H. Gerstacker, and R. Schober, "Transmission and reception concepts for WLAN IEEE 802.11b," *IEEE Trans. Wireless Commun.*, vol. 5, no. 12, pp. 3375–3381, Dec. 2006.
- [46] C. Jonietz, W. Gerstacker, and R. Schober, "Sphere constrained detection of complementary code keying signals transmitted over frequency-selective channels," *IEEE Trans. Wireless Commun.*, vol. 8, no. 9, pp. 4656–4667, Sept. 2009.
- [47] W. Gerstacker and R. Schober, "Equalization concepts for EDGE," *IEEE Trans. Wireless Commun.*, vol. 1, no. 1, pp. 190–199, Jan. 2002.
- [48] W. Gerstacker, F. Obernosterer, R. Meyer, and J. Huber, "On prefilter computation for reduced-state equalization," *IEEE Trans. Wireless Commun.*, vol. 1, no. 4, pp. 793–800, Oct. 2002.
- [49] W. Koch and A. Baier, "Optimum and sub-optimum detection of coded data disturbed by time-varying intersymbol interference (applicable to digital mobile radio receivers)," in *Proc. 1990 IEEE Global Telecommun. Conf.*, vol. 3, pp. 1679–1684.
- [50] G. Colavolpe, G. Ferrari, and R. Raheli, "Reduced-state BCJR-type algorithms," *IEEE J. Sel. Areas Commun.*, vol. 19, no. 5, pp. 848–859, 2001.
- [51] D. Fertonani, A. Barbieri, and G. Colavolpe, "Reduced-complexity BCJR algorithm for turbo equalization," *IEEE Trans. Commun.*, vol. 55, no. 11, pp. 2279–2287, Nov. 2007.
- [52] D. N. Liu and M. P. Fitz, "Iterative MAP equalization and decoding in wireless mobile coded OFDM," *IEEE Trans. Commun.*, vol. 57, no. 7, pp. 2042–2051, 2009.
- [53] J. R. Barry, E. A. Lee, and D. G. Messerschmitt, *Digital Communication*. Springer, Third Edition.
- [54] G. Colavolpe and G. Geremi, "On the application of factor graphs and the sum-product algorithm to ISI channels," *IEEE Trans. Commun.*, vol. 53, no. 5, pp. 818–825, May 2005.
- [55] J. Sykora, "Tapped delay line model of linear randomly time-variant WS-SUS channel," *Electronics Letters*, vol. 36, no. 19, pp. 1656–1657, Sept. 2000.
- [56] F. Kschischang, B. Frey, and H. Loeliger, "Factor graphs and the sum-product algorithm," *IEEE Trans. Inf. Theory*, vol. 47, no. 2, pp. 498–519, Feb. 2001.
- [57] C. Laot, A. Glavieux, and J. Labat, "Turbo Equalization: Adaptive equalization and channel decoding jointly optimized," *IEEE J. Sel. Areas Commun.*, vol. 19, no. 9, pp. 1744–1752, Sept. 2001.

- [58] R. Schober, W. H. Gerstacker, and L. H. J. Lampe, "Performance analysis and design of STBCs for frequency-selective fading channels," *Wireless Communications, IEEE Transactions on*, vol. 3, no. 3, pp. 734–744, May 2004.
- [59] C. Ling, K. H. Li, and A. C. Kot, "Performance of space time codes: Gallager bounds and weight enumeration," *IEEE Trans. Inf. Theory*, vol. 54, no. 8, pp. 3592–3610, Aug. 2008.
- [60] A. Modenini, F. Rusek, and G. Colavolpe, "Optimal transmit filters for ISI channels under channel shortening detection," *IEEE Trans. Commun.*, vol. 61, no. 12, pp. 4997–5005, Dec. 2013.
- [61] A. Prlja and J. Anderson, "Reduced-complexity receivers for strongly narrowband intersymbol interference introduced by faster-than-Nyquist signaling," *IEEE Trans. Commun.*, vol. 60, no. 9, pp. 2591–2601, 2012.
- [62] S. Ten Brink, "Convergence of iterative decoding," *Electronics Letters*, vol. 35, no. 10, pp. 806–808, 1999.
- [63] J. Hagenauer, "The EXIT chart—Introduction to extrinsic information transfer in iterative processing," in *Proc. Eur. Signal Process. Conf.*, 2004, p. 1541–1548.
- [64] G. Ungerboeck, "Channel coding with multilevel/phase signals," *IEEE Trans. Inf. Theory*, vol. 28, no. 1, pp. 55–67, Jan. 1982.
- [65] L. Biederman, J. Omura, and P. Jain, "Decoding with approximate channel statistics for bandlimited nonlinear satellite channels," *IEEE Trans. Inf. Theory*, vol. 27, no. 6, pp. 697–707, 1981.
- [66] S. Shamai and A. Dembo, "Bounds on the symmetric binary cutoff rate for dispersive Gaussian channels," *IEEE Trans. Commun.*, vol. 42, no. 1, pp. 39–53, 1994.
- [67] S. Shamai and S. A. Raghavan, "On the generalized symmetric cutoff rate for finite-state channels," *IEEE Trans. Inf. Theory*, vol. 41, no. 5, pp. 1333–1346, 1995.
- [68] E. Baccarelli, "Performance bounds and cutoff rates for data channels affected by correlated randomly time-variant multipath fading," *IEEE Trans. Commun.*, vol. 46, no. 10, pp. 1258–1261, 1998.
- [69] S. Shamai, L. H. Ozarow, and A. D. Wyner, "Information rates for a discrete-time Gaussian channel with intersymbol interference and stationary inputs," *IEEE Trans. Inf. Theory*, vol. 37, no. 6, pp. 1527–1539, 1991.
- [70] X. Wu, H. Xiang, and C. Ling, "New Gallager bounds in block-fading channels," *IEEE Trans. Inf. Theory*, vol. 53, no. 2, pp. 684–694, 2007.
- [71] J. Stokes and J. Ritcey, "A general method for evaluating outage probabilities using Pade approximations," in *Proc. 1998 IEEE Global Telecommun. Conf.*, vol. 3, 1998, pp. 1485–1490.
- [72] J. W. Stokes and J. A. Ritcey, "Performance analysis of DS/CDMA systems with shadowing and flat fading," *Signal processing*, vol. 81, no. 12, pp. 2555–2571, 2001.

- [73] M. Di Renzo, F. Graziosi, and F. Santucci, "A framework for the analysis of UWB receivers in sparse multipath channels with intra-pulse interference via Pade expansion," *IEEE Trans. Commun.*, vol. 56, no. 4, pp. 535–541, April 2008.
- [74] M. G. Kendall and A. Stuart, *The Advanced Theory of Statistics, Vol. 1, Distribution Theory*. London: Griffin, 1987.
- [75] D. D. Murphy and C. C. Murphy, "A Gram-Charlier series method for calculating general signal constellation error probabilities," *IEEE Trans. Commun.*, vol. 60, no. 2, pp. 300–305, 2012.
- [76] M. K. Simon and M. S. Alouini, *Digital Communication over Generalized Fading Channels: A Unified Approach to the Performance Analysis*. John Wiley and Sons, Inc., 2000.
- [77] D. Senaratne and C. Tellambura, "A general numerical method for computing the probability of outage," in *Proc. 2009 IEEE Wireless Commun. and Networking Conf.*, 2009, pp. 1–6.
- [78] S. Verdú, *Multiuser Detection*. Cambridge, U.K.: Cambridge Univ., 1998.
- [79] X. Wang and H. V. Poor, "Iterative (turbo) soft interference cancellation and decoding for coded CDMA," *IEEE Trans. Commun.*, vol. 47, no. 7, pp. 1046–1061, Jul. 1999.
- [80] H. El Gamal and E. Geraniotis, "Iterative multiuser detection for coded CDMA signals in AWGN and fading channels," *IEEE J. Sel. Areas Commun.*, vol. 18, no. 1, pp. 30–41, 2000.
- [81] J. Boutros and G. Caire, "Iterative multiuser joint decoding: Unified framework and asymptotic analysis," *IEEE Trans. Inf. Theory*, vol. 48, no. 7, pp. 1772–1793, 2002.
- [82] H. Loeliger, J. Dauwels, J. Hu, S. Korl, L. Ping, and F. Kschischang, "The factor graph approach to model-based signal processing," *Proc. IEEE*, vol. 95, no. 6, pp. 1295–1322, 2007.
- [83] Q. Guo and L. Ping, "LMMSE turbo equalization based on factor graphs," *IEEE J. Sel. Areas Commun.*, vol. 26, no. 2, pp. 311–319, 2008.
- [84] J. Zhang, A. M. Sayeed, and B. D. Van Veen, "Reduced-state MIMO sequence detection with application to EDGE systems," *IEEE Trans. Wireless Commun.*, vol. 4, no. 3, pp. 1040–1049, 2005.
- [85] N. Benvenuto, R. Sandre, and G. Sostrato, "Reduced-state maximum-likelihood multiuser detection for down-link TD-CDMA systems," *IEEE J. Sel. Areas Commun.*, vol. 20, no. 2, pp. 264–272, Feb. 2002.
- [86] Y. Chiu, J. Hwang, and C. Hsiao, "Efficient multi-stage decision-feedback multiuser detectors for multi-code DS-SS-CDMA system over severe multipath channel," in *Proc. 2009 IEEE Int. Symp. on Personal, Indoor and Mobile Radio Commun. (PIMRC)*, 2009, pp. 3198–3202.
- [87] N. Gu, S. Wu, L. Kuang, Z. Ni, and J. Lu, "Belief propagation-based joint iterative algorithm for detection and decoding in asynchronous CDMA satellite systems," *EURASIP J. Wireless Commun. and Netw.*, vol. 2013, no. 1, pp. 1–14, 2013.

- [88] K. Kusume, G. Bauch, and W. Utschick, "IDMA vs. CDMA: Analysis and comparison of two multiple access schemes," *IEEE Trans. Wireless Commun.*, vol. 11, no. 1, pp. 78–87, 2012.
- [89] N. Mazzali, G. Colavolpe, and S. Buzzi, "CPM-based spread spectrum systems for multi-user communications," *IEEE Trans. Wireless Commun.*, vol. 12, no. 1, pp. 358–367, 2013.
- [90] A. Piemontese, "Advanced low-complexity multiuser receivers," Ph.D. dissertation, Universita di Parma. Dipartimento di Ingegneria dell'Informazione, 2011.
- [91] A. Barbieri, D. Fertonani, and G. Colavolpe, "Time-frequency packing for linear modulations: Spectral efficiency and practical detection schemes," *IEEE Trans. Commun.*, vol. 57, no. 10, pp. 2951–2959, 2009.
- [92] J. B. Anderson, F. Rusek, and V. Owall, "Faster-than-Nyquist signaling," *Proc. IEEE*, vol. 101, no. 8, pp. 1817–1830, 2013.
- [93] A. Piemontese, A. Modenini, G. Colavolpe, and N. Alagha, "Improving the spectral efficiency of nonlinear satellite systems through time-frequency packing and advanced receiver processing," *IEEE Trans. Commun.*, vol. 61, no. 8, pp. 3404–3412, 2013.
- [94] A. Prlja, "Reduced receivers for faster-than-Nyquist signaling and general linear channels," Ph.D. dissertation, Lund University, 2013.
- [95] A. Modenini, "Advanced transceivers for spectrally-efficient communications," Ph.D. dissertation, 2014.
- [96] W. Haselmayr, B. Etxlinger, and A. Springer, "Factor-graph-based soft-input soft-output detection for frequency-selective MIMO channels," *IEEE Commun. Lett.*, vol. 16, no. 10, pp. 1624–1627, 2012.
- [97] —, "Equalization of MIMO-ISI channels based on Gaussian message passing in factor graphs," in *Proc. 2012 IEEE Int. Turbo Codes and Iterative Information Process. Symposium*, 2012, pp. 76–80.
- [98] C. Novak, G. Matz, and F. Hlawatsch, "IDMA for the multiuser MIMO-OFDM uplink: A factor graph framework for joint data detection and channel estimation," *IEEE Trans. Signal Process.*, vol. 61, no. 16, pp. 4051–4066, 2013.
- [99] E. Basar, U. Aygolu, E. Panayirci, and H. V. Poor, "Orthogonal frequency division multiplexing with index modulation," *IEEE Trans. Signal Process.*, vol. 61, no. 22, pp. 5536–5549, Nov. 2013.
- [100] G. M. Guvensen and A. O. Yilmaz, "An upper bound for limited rate feedback MIMO capacity," *IEEE Trans. Wireless Commun.*, vol. 8, no. 6, pp. 2748–2754, June 2009.
- [101] M. Chiani, D. Dardari, and M. K. Simon, "New exponential bounds and approximations for the computation of error probability in fading channels," *IEEE Trans. Wireless Commun.*, vol. 2, no. 4, pp. 840–845, July 2003.
- [102] R. G. Gallager, *Information Theory and Reliable Communication*. New York, Wiley, 1968.

APPENDIX A

ANALYSIS OF THE *BIAS* TERM IN UNGERBOECK TYPE RSSE

Let $\mathbf{x}_n \triangleq \mathbf{c}_n e^{j\theta_n}$ be the equivalent vector symbol of MCS with modulated phase in (2.8). We define $\{\mathbf{x}_n^{(1)}\}_{n=0}^{N-1}$ as the transmitted sequence of vector symbols belonging to path-1 and $\{S_n^{(1)}\}_{n=0}^{N-1}$ is the corresponding sequence of states in the reduced trellis for path-1. Similarly, $\{\mathbf{x}_n^{(2)}\}_{n=0}^{N-1}$ is defined as a hypothetical sequence of vector symbols for path-2 that the receiver erroneously decides on instead of path-1 and $\{S_n^{(2)}\}_{n=0}^{N-1}$ is the sequence of states in the reduced trellis of path-2 that diverges from the correct sequence of states of path-1 at time $n = 0$ and remerges with it at a later time $n = k + 1$ such that

$$S_0^{(1)} = S_0^{(2)}, \text{ and } S_{k+1}^{(1)} = S_{k+1}^{(2)}, \quad (\text{A.1})$$

which implies

$$\begin{aligned} I_n^{(1)} &= I_n^{(2)} \text{ for } n = k, \dots, k - J_I + 1, \\ \theta_n^{(1)} &= \theta_n^{(2)} \text{ for } n = k, \dots, k - J_\theta + 1. \end{aligned} \quad (\text{A.2})$$

By using the equivalent model in (2.8), the symbol time sampled matched filter outputs up to time k can be written as

$$\mathbf{y}_k = \Psi_1^{(k)} \mathbf{b}_1 + \Psi_2^{(k)} \mathbf{b}'_1 + \boldsymbol{\eta}_k, \quad (\text{A.3})$$

where

$$\mathbf{y}_k = [\mathbf{r}_0^T, \mathbf{r}_1^T, \dots, \mathbf{r}_k^T]^T, \quad \boldsymbol{\eta}_k = [\mathbf{v}_0^T, \mathbf{v}_1^T, \dots, \mathbf{v}_k^T]^T, \quad (\text{A.4})$$

$$\mathbf{b}_1 = [(\mathbf{x}_0^{(1)})^T, (\mathbf{x}_1^{(1)})^T, \dots, (\mathbf{x}_k^{(1)})^T]^T, \quad \mathbf{b}'_1 = [(\mathbf{x}_{k+1}^{(1)})^T, (\mathbf{x}_{k+2}^{(1)})^T, \dots, (\mathbf{x}_{k+L-1}^{(1)})^T]^T, \quad (\text{A.5})$$

$$\mathbf{b}_2 = [(\mathbf{x}_0^{(2)})^T, (\mathbf{x}_1^{(2)})^T, \dots, (\mathbf{x}_k^{(2)})^T]^T, \quad (\text{A.6})$$

and the following vector corresponding to the symbol sequence of path-2 can be defined as

$$\begin{aligned} \Psi_1^{(k)} &= \begin{bmatrix} \mathbf{H}(0) & \mathbf{H}(-1) & \cdots & \mathbf{H}(-k) \\ \mathbf{H}(1) & \mathbf{H}(0) & \cdots & \mathbf{H}(-k+1) \\ \vdots & \vdots & \ddots & \vdots \\ \mathbf{H}(k) & \mathbf{H}(k-1) & \cdots & \mathbf{H}(0) \end{bmatrix}_{M(k+1) \times M(k+1)}, \\ \Psi_2^{(k)} &= \begin{bmatrix} \mathbf{H}(-k-1) & \mathbf{H}(-k-2) & \cdots & \mathbf{H}(-k-L+1) \\ \mathbf{H}(-k) & \mathbf{H}(-k-1) & \cdots & \mathbf{H}(-k-L+2) \\ \vdots & \vdots & \ddots & \vdots \\ \mathbf{H}(-1) & \mathbf{H}(-2) & \cdots & \mathbf{H}(-L+1) \end{bmatrix}_{M(k+1) \times M(L-1)} \end{aligned} \quad (\text{A.7})$$

for $0 \leq k \leq N - L$ and $\mathbf{H}(l) = (\mathbf{R}(l))^T$. The vector \mathbf{b}_2 in (A.6) contains the vector symbols of path-2 up to time k . The autocorrelation matrix of $\boldsymbol{\eta}_k$ can be calculated as $E\{\boldsymbol{\eta}_k \boldsymbol{\eta}_k^H\} = N_0 \Psi_1^{(k)}$.

An error event occurs if the accumulated metric on path-2 is greater than that on path-1 at $n = k + 1$ when paths merge. By using the metric rule for MCS in (2.10), one can obtain the probability of this error event in U-RSSE with error-free decision feedback. The pairwise error probability (PEP) that corresponds to decision on \mathbf{b}_2 when \mathbf{b}_1 is sent can be written as

$$\begin{aligned} \mathbb{P}\{\mathbf{b}_1 \rightarrow \mathbf{b}_2\} &= \\ \mathbb{P}\left\{ \sum_{n=0}^k \mu_n (\mathbf{r}_n, I_n^{(2)}, \theta_n^{(2)}, S_n^{(2)}) > \sum_{n=0}^k \mu_n (\mathbf{r}_n, I_n^{(1)}, \theta_n^{(1)}, S_n^{(1)}) \mid \mathbf{b}_1 \text{ is sent} \right\} &= \\ \mathbb{P}\left\{ 2 \operatorname{Re} \{ \mathbf{y}_k^H \mathbf{b}_2 \} - \mathbf{b}_2^H \Psi_1^{(k)} \mathbf{b}_2 > 2 \operatorname{Re} \{ \mathbf{y}_k^H \mathbf{b}_1 \} - \mathbf{b}_1^H \Psi_1^{(k)} \mathbf{b}_1 \mid \mathbf{b}_1 \text{ is sent} \right\} &= \\ \mathbb{P}\left\{ 2 \operatorname{Re} \{ (\mathbf{b}_2 - \mathbf{b}_1)^H \mathbf{y}_k \} > \mathbf{b}_2^H \Psi_1^{(k)} \mathbf{b}_2 - \mathbf{b}_1^H \Psi_1^{(k)} \mathbf{b}_1 \right. \\ &\quad \left. \mid \mathbf{y}_k = \Psi_1^{(k)} \mathbf{b}_1 + \Psi_2^{(k)} \mathbf{b}_1' + \boldsymbol{\eta}_k \right\} = \\ \mathbb{P}\left\{ 2 \operatorname{Re} \{ \mathbf{e}^H \boldsymbol{\eta}_k \} > \mathbf{e}^H \Psi_1^{(k)} \mathbf{e} - 2 \operatorname{Re} \{ \mathbf{e}^H \Psi_2^{(k)} \mathbf{b}_1' \} \right\} & \quad (\text{A.8}) \end{aligned}$$

where the error vector is defined as $\mathbf{e} \triangleq \mathbf{b}_2 - \mathbf{b}_1 = [\mathbf{e}_0^T, \mathbf{e}_1^T, \dots, \mathbf{e}_k^T]^T$, $\mathbf{e}_n = \mathbf{x}_n^{(2)} - \mathbf{x}_n^{(1)}$. In (A.8), $2 \operatorname{Re} \{ \mathbf{e}^H \boldsymbol{\eta}_k \}$ is a zero mean Gaussian r.v. with variance

$2N_0\mathbf{e}^H\Psi_1^{(k)}\mathbf{e}$. Then,

$$\mathbb{P}\{\mathbf{b}_1 \rightarrow \mathbf{b}_2\} = Q\left(\frac{d^2(\mathbf{e}) + \gamma(\mathbf{e}, \mathbf{b}'_1)}{\sqrt{2N_0d^2(\mathbf{e})}}\right) \quad (\text{A.9})$$

$$\begin{aligned} d^2(\mathbf{e}) &= \mathbf{e}^H\Psi_1^{(k)}\mathbf{e}, \\ \text{where } \gamma(\mathbf{e}, \mathbf{b}'_1) &= -2\operatorname{Re}\left\{\mathbf{e}^H\Psi_2^{(k)}\mathbf{b}'_1\right\} = \\ &= -2\operatorname{Re}\left\{\sum_{m=k-L+2}^k\sum_{l=k-m+1}^{L-1}\mathbf{e}_m^H\mathbf{H}(-l)\mathbf{x}_{m+l}^{(1)}\right\} \end{aligned} \quad (\text{A.10})$$

with $Q(x) = \frac{1}{\sqrt{2\pi}}\int_x^\infty \exp\left(-\frac{u^2}{2}\right)du$ and $\mathbf{H}(n) = 0$ for $|n| \geq L$.

As can be observed from (A.9), PEP depends not only the error sequence itself, but also on the so-called *bias* term $\gamma(\mathbf{e}, \mathbf{b}'_1)$ which is also a function of \mathbf{b}'_1 including the future values on path-1. By noting that $\mathbf{e}_n = 0$ for $n = k, \dots, k - \min\{J_I, J_\theta\} + 1$ from (A.2) and taking $J_I \geq J_\theta$, this bias term can be expressed as

$$\begin{aligned} \gamma(\mathbf{e}, \mathbf{b}'_1) &= 2\operatorname{Re}\left\{\sum_{m=k-L+2}^{k-J_I}\sum_{l=k-m+1}^{L-1}\left[R_{I_m^{(1)}, I_{m+l}^{(1)}}(l)e^{j\theta_m^{(1)}} - R_{I_m^{(2)}, I_{m+l}^{(1)}}(l)e^{j\theta_m^{(2)}}\right]e^{-j\theta_{m+l}^{(1)}}\right. \\ &\quad \left. + \sum_{m=k-J_I+1}^{k-J_\theta}\sum_{l=k-m+1}^{L-1}R_{I_m^{(1)}, I_{m+l}^{(1)}}(l)\left[e^{j\theta_m^{(1)}} - e^{j\theta_m^{(2)}}\right]e^{-j\theta_{m+l}^{(1)}}\right\} \end{aligned} \quad (\text{A.11})$$

where $R_{i,j}(m) = \mathbf{h}^H\mathbf{R}_g^{i,j}(m)\mathbf{h}$, $i, j = 1, \dots, M$. From (A.11), one can clearly observe the dependence of the bias term on the post- and pre-cursor ISI and MCI components stemming from the non-ideal cross- and auto-correlations of the signaling waveforms and the multi-path channel. First term in (A.11) includes errors both for I_k and θ_k , but the latter one takes only the phase errors into account. While deciding on tentative decisions to be used in feedback to calculate forward and backward Ungerboeck metrics in (2.22), one could compensate the effect of this bias. To accomplish this, the effect of this bias due to pre-cursor ISI and MCI can be eliminated during Viterbi like survivor path construction for each reduced state (S_k) as in (2.23). This leads to the subtraction of the

following term from the recursively computed path metrics for S_k :

$$\beta_k(S_k) = 2 \operatorname{Re} \left\{ \sum_{m=k-L+\min\{J_I, J_\theta\}+2}^k \sum_{l=k-m+\min\{J_I, J_\theta\}+1}^{L-1} R_{I_m(S_k), \tilde{I}_{m+l}}(l) e^{j\theta_m(S_k)} e^{-j\tilde{\theta}_{m+l}} \right\}. \quad (\text{A.12})$$

$\beta_k(S_k)$ can be seen as the bias correction term at time epoch k based on tentative decisions for future symbols while deciding on tentative decisions $\{\hat{I}_k, \hat{\theta}_k\}$, and S_k shows the dependence of $\beta_k(S_k)$ on past symbols belonging to the surviving path of S_k up to time k , namely, $\{\hat{I}_n(S_k), \hat{\theta}_n(S_k)\}_{n=0}^{k-1}$. The bias correction term also depends on future symbols leading to pre-cursor ISI and MCI, namely, $\{\tilde{I}_n, \tilde{\theta}_n\}_{n=k+\min\{J_I, J_\theta\}+1}^{k+L-1}$ that can be obtained from the previous forward or backward RSSE stages. Future symbols $\{I_{k+1}, \dots, I_{k+\min\{J_I, J_\theta\}}\}$ and $\{\theta_{k+1}, \dots, \theta_{k+\min\{J_I, J_\theta\}}\}$, which are already taken into account by the reduced state Ungerboeck metric in (2.22) due to the symmetry properties of $\mathbf{R}(l)$ at time k , are not utilized in bias correction. If one chooses $J_\theta = J_I = L - 1$ (full state), the bias correction term becomes zero as expected, and the algorithm (2.23) reduces to the optimal ML rule given in (2.4).

APPENDIX B

VARIANCE ANALYSIS OF THE BIAS TERM

First of all, in order to simplify the analysis, we assume that the error events with *weight one* only dominate the performance, i.e., either $\mathbf{e}_{k-J_I} \neq 0$ or $\mathbf{e}_{k-J_\theta} \neq 0$ up to k^{th} time epoch. Then, the bias term in (A.11) can be rewritten by taking $J_I \geq J_\theta$ as

$$\begin{aligned} \gamma(\mathbf{e}_{k-J_I}, \mathbf{e}_{k-J_\theta}, \mathbf{b}'_1) &= -2 \operatorname{Re} \left\{ \sum_{l=J_I+1}^{L-1} \mathbf{e}_{k-J_I}^H \mathbf{H}(l)^H \mathbf{x}_{k-J_I+l}^{(1)} \right. \\ &\quad \left. + \mathbf{1}\{J_I > J_\theta\} \sum_{l=J_\theta+1}^{L-1} \mathbf{e}_{k-J_\theta}^H \mathbf{H}(l)^H \mathbf{x}_{k-J_\theta+l}^{(1)} \right\} \end{aligned} \quad (\text{B.1})$$

where the error event distances, namely, \mathbf{e}_{k-J_I} and \mathbf{e}_{k-J_θ} are defined in Appendix A and $\mathbf{1}\{\cdot\}$ is the indicator function. As can be seen from (A.1)-(A.2) in Appendix A, for $J_I > J_\theta$, $\mathbf{e}_{k-J_I} \neq 0$ event includes both phase and waveform selection errors, but $\mathbf{e}_{k-J_\theta} \neq 0$ event comprises phase error only. Furthermore, these two error events are assumed to be independent. These are reasonable assumptions especially for the *Ungerboeck* model, since the *weight one* error event distance captures the full multi-path power which may not be the case in the *Forney* based RSSE [21].

$E\{|\gamma|^2\}$ can be obtained by averaging over the future input values \mathbf{b}'_1 , all possible error events \mathbf{e} with *weight one* chosen from the set $\Omega_e = \{\text{either } \mathbf{e}_{k-J_I} \neq 0 \text{ or } \mathbf{e}_{k-J_\theta} \neq 0\}$, and the equivalent multi-path channel vector \mathbf{h} . The events $\mathbf{e}_{k-J_I} \neq 0$ and $\mathbf{e}_{k-J_\theta} \neq 0$ are disjoint given Ω_e if $J_I > J_\theta$, then one can express the variance of the bias term as

$$\begin{aligned}
E_{\mathbf{h}, \mathbf{e}, \mathbf{b}'_1} \{|\gamma|^2\} &= 2E \left\{ \left| \sum_{l=J_I+1}^{L-1} \mathbf{e}_{k-J_I}^H \mathbf{H}(l) \mathbf{H}(l)^H \mathbf{x}_{k-J_I+l}^{(1)} + \mathbf{1}\{J_I > J_\theta\} \sum_{l=J_\theta+1}^{L-1} \mathbf{e}_{k-J_\theta}^H \mathbf{H}(l) \mathbf{H}(l)^H \mathbf{x}_{k-J_\theta+l}^{(1)} \right|^2 \middle| \Omega_e \right\} \\
&= 2E \left\{ \sum_{l_1=J_I+1}^{L-1} \sum_{l_2=J_I+1}^{L-1} \mathbf{e}_{k-J_I}^H \mathbf{H}(l_1) \mathbf{H}(l_1)^H \mathbf{x}_{k-J_I+l_1}^{(1)} (\mathbf{x}_{k-J_I+l_2}^{(1)})^H \mathbf{H}(l_2) \mathbf{e}_{k-J_I} \middle| \Omega_e \right\} + \quad (\text{B.2}) \\
&\quad \mathbf{1}\{J_I > J_\theta\} 2E \left\{ \sum_{l_1=J_\theta+1}^{L-1} \sum_{l_2=J_\theta+1}^{L-1} \mathbf{e}_{k-J_\theta}^H \mathbf{H}(l_1) \mathbf{H}(l_1)^H \mathbf{x}_{k-J_\theta+l_1}^{(1)} (\mathbf{x}_{k-J_\theta+l_2}^{(1)})^H \mathbf{H}(l_2) \mathbf{e}_{k-J_\theta} \middle| \Omega_e \right\}
\end{aligned}$$

After taking expectation over future symbols \mathbf{b}'_1 by using that $E\{\mathbf{x}_k^{(1)} (\mathbf{x}_{k-l}^{(1)})^H\} = \frac{1}{M} \mathbf{I}_M \delta_l$ if $P \geq 2$ and $E\{\mathbf{x}_k^{(1)} (\mathbf{x}_{k-l}^{(1)})^H\} = \frac{1}{M^2} \mathbf{1} \mathbf{1}^H + (\frac{1}{M} - \frac{1}{M^2}) \mathbf{I}_M \delta_l$ if $P = 1$, and ignoring terms for $l_1 \neq l_2$ in (B.2) for $P = 1$, (B.2) is simplified to

$$\begin{aligned}
E_{\mathbf{h}, \mathbf{e}, \mathbf{b}'_1} \{|\gamma|^2\} &= 2\mathbb{P}\{\mathbf{e}_{k-J_I} \neq 0 | \Omega_e\} E_{\mathbf{h}, \mathbf{e}} \left\{ \sum_{l=J_I+1}^{L-1} \frac{1}{M} \mathbf{e}_{k-J_I}^H \mathbf{H}(l) \mathbf{H}(l)^H \mathbf{e}_{k-J_I} \middle| \mathbf{e}_{k-J_I} \neq 0 \right\} + \quad (\text{B.3}) \\
&\quad \mathbf{1}\{J_I > J_\theta\} 2\mathbb{P}\{\mathbf{e}_{k-J_\theta} \neq 0 | \Omega_e\} E_{\mathbf{h}, \mathbf{e}} \left\{ \sum_{l=J_\theta+1}^{L-1} \frac{1}{M} \mathbf{e}_{k-J_\theta}^H \mathbf{H}(l) \mathbf{H}(l)^H \mathbf{e}_{k-J_\theta} \middle| \mathbf{e}_{k-J_\theta} \neq 0 \right\}
\end{aligned}$$

By assuming that all *weight one* error events in (B.3) are equally likely¹, the expression in (B.4) is obtained.

$$\begin{aligned}
E\{|\gamma|^2\} &= 2E_{\mathbf{h}} \left\{ \frac{\mathbb{P}\{\mathbf{e}_{k-J_I} \neq 0 | \Omega_e\}}{MP(MP-1)} \sum_{\mathbf{e}_{k-J_I} = \mathbf{x}_{k-J_I}^{(2)} - \mathbf{x}_{k-J_I}^{(1)}, \mathbf{e}_{k-J_I} \neq 0} \right. \\
&\quad \left. \sum_{l=J_I+1}^{L-1} \frac{1}{M} \mathbf{e}_{k-J_I}^H \mathbf{H}(l) \mathbf{H}(l)^H \mathbf{e}_{k-J_I} \right\} + 2E_{\mathbf{h}} \left\{ \mathbf{1}\{J_I > J_\theta\} \frac{\mathbb{P}\{\mathbf{e}_{k-J_\theta} \neq 0 | \Omega_e\}}{MP(P-1)} \right. \\
&\quad \left. \sum_{\mathbf{e}_{k-J_\theta} = \mathbf{x}_{k-J_\theta}^{(2)} - \mathbf{x}_{k-J_\theta}^{(1)}, \mathbf{e}_{k-J_\theta} \neq 0} \sum_{l=J_\theta+1}^{L-1} \frac{1}{M} \mathbf{e}_{k-J_\theta}^H \mathbf{H}(l) \mathbf{H}(l)^H \mathbf{e}_{k-J_\theta} \right\} \quad (\text{B.4})
\end{aligned}$$

Then, by using that $\mathbb{P}\{\mathbf{e}_{k-J_I} \neq 0 | \Omega_e\} + \mathbb{P}\{\mathbf{e}_{k-J_\theta} \neq 0 | \Omega_e\} = 1$, and the conditional probabilities $\mathbb{P}\{\mathbf{e}_{k-J_I} \neq 0 | \Omega_e\}$ and $\mathbb{P}\{\mathbf{e}_{k-J_\theta} \neq 0 | \Omega_e\}$ are proportional to their cardinalities $|\mathbf{e}_{k-J_I} \neq 0| = MP(MP-1)$ and $|\mathbf{e}_{k-J_\theta} \neq 0| = MP(P-1)$ respectively, the following expression in (B.5) can be obtained from (B.4).

¹ Exact values for PEPs can be used instead, but this neither brings significant improvement nor any additional insight especially for practical values of modulation parameters such as $P \leq 4$. On the other hand, $P > 4$ is not desirable due to the smaller error event distances compared to increasing M at the same spectral efficiency.

$$\begin{aligned}
E\{|\gamma|^2\} &= \frac{2}{M^2P[MP-1+\mathbf{1}\{J_I > J_\theta\}(P-1)]} \left[E_{\mathbf{h}} \left\{ \sum_{\mathbf{x}_k^{(1)}} \sum_{\mathbf{x}_k^{(2)}, \mathbf{x}_k^{(2)} \neq \mathbf{x}_k^{(1)}} \sum_{l=J_I+1}^{L-1} \right. \right. \\
&\quad \left. \left. \mathbf{e}_k^H \mathbf{H}(l)^H \mathbf{H}(l) \mathbf{e}_k \left| I_k^{(1)} \neq I_k^{(2)} \text{ or } \theta_k^{(1)} \neq \theta_k^{(2)} \right. \right\} \\
&\quad \left. + \mathbf{1}\{J_I > J_\theta\} E_{\mathbf{h}} \left\{ \sum_{\mathbf{x}_k^{(1)}} \sum_{\mathbf{x}_k^{(2)}, \mathbf{x}_k^{(2)} \neq \mathbf{x}_k^{(1)}} \sum_{l=J_\theta+1}^{L-1} \mathbf{e}_k^H \mathbf{H}(l)^H \mathbf{H}(l) \mathbf{e}_k \left| I_k^{(1)} = I_k^{(2)} \text{ and } \theta_k^{(1)} \neq \theta_k^{(2)} \right. \right\} \right] \quad (\text{B.5})
\end{aligned}$$

By using $\mathbf{x}_k = \mathbf{c}_k e^{j\theta_k}$, the definition of \mathbf{c}_k in (2.8) and $\mathbf{H}(l)$ in (A.7), and the symmetry of PSK modulation, the expression in (B.5) is simplified to

$$\begin{aligned}
E\{|\gamma|^2\} &= \frac{2}{M^2[MP-1+\mathbf{1}\{J_I > J_\theta\}(P-1)]} \left[\sum_{m_1=1}^M \sum_{m_2=1, m_2 \neq m_1}^M \sum_{p=0}^{P-1} \sum_{l=J_I+1}^{L-1} \sum_{n=1}^M \right. \\
&\quad \left. E_{\mathbf{h}} \left\{ |R_{m_1,n}(l)|^2 + |R_{m_2,n}(l)|^2 - 2 \operatorname{Re} \left\{ e^{j\frac{2\pi}{P}p} R_{m_1,n}(l) R_{m_2,n}(l)^* \right\} \right\} + \right. \\
&\quad \left. \sum_{m_1=1}^M \sum_{p=1}^{P-1} \sum_{l=J_\theta+1}^{L-1} \sum_{n=1}^M (1 + \mathbf{1}\{J_I > J_\theta\} \mathbf{1}\{l > J_I\}) 4 \sin^2 \left(\frac{\pi}{P} p \right) E_{\mathbf{h}} \left\{ |R_{m_1,n}(l)|^2 \right\} \right] \quad (\text{B.6})
\end{aligned}$$

Then, by using (2.7), one obtains the result in (2.27).

The expectations $E_{\mathbf{h}} \left\{ \left| \mathbf{h}^H \mathbf{A}_l^{(m_1, m_2, p, n)} \mathbf{h} \right|^2 \right\}$ and $E_{\mathbf{h}} \left\{ \left| \mathbf{h}^H \mathbf{B}_l^{(m_1, p, n)} \mathbf{h} \right|^2 \right\}$ in (2.27) can be obtained as follows.

$$\begin{aligned}
E_{\mathbf{h}} \left\{ \left| \mathbf{h}^H \mathbf{A}_l^{(m_1, m_2, p, n)} \mathbf{h} \right|^2 \right\} &= E_{\mathbf{h}} \left\{ \left(\operatorname{Re} \left\{ \mathbf{h}^H \mathbf{A}_l^{(m_1, m_2, p, n)} \mathbf{h} \right\} \right)^2 \right\} + E_{\mathbf{h}} \left\{ \left(\operatorname{Im} \left\{ \mathbf{h}^H \mathbf{A}_l^{(m_1, m_2, p, n)} \mathbf{h} \right\} \right)^2 \right\} \\
&= E_{\mathbf{h}} \left\{ \left[\mathbf{h}^H \left(\frac{\mathbf{A}_l^{(m_1, m_2, p, n)} + \left(\mathbf{A}_l^{(m_1, m_2, p, n)} \right)^H}{2} \right) \mathbf{h} \right]^2 \right\} \\
&\quad + E_{\mathbf{h}} \left\{ \left[\mathbf{h}^H \left(\frac{\mathbf{A}_l^{(m_1, m_2, p, n)} - \left(\mathbf{A}_l^{(m_1, m_2, p, n)} \right)^H}{2j} \right) \mathbf{h} \right]^2 \right\} \quad (\text{B.7})
\end{aligned}$$

Then, $E_{\mathbf{h}} \left\{ \left[\mathbf{h}^H \left(\frac{\mathbf{A}_l^{(m_1, m_2, p, n)} + \left(\mathbf{A}_l^{(m_1, m_2, p, n)} \right)^H}{2} \right) \mathbf{h} \right]^2 \right\}$ term in (B.7) used to calculate (2.27) can be evaluated easily by using a Moment Generating Function (MGF) [1] based approach developed below. First, we define a $L_c \times L_c$ matrix \mathbf{A} and a random variable β as

$$\mathbf{A} \triangleq \frac{\mathbf{A}_l^{(m_1, m_2, p, n)} + \left(\mathbf{A}_l^{(m_1, m_2, p, n)}\right)^H}{2}, \quad \beta \triangleq \mathbf{h}^H \mathbf{A} \mathbf{h}. \quad (\text{B.8})$$

For the case of complex Gaussian channel vector \mathbf{h} studied here, the MGF of β can be found as

$$\Phi_\beta(s) = E_\beta \{e^{-s\beta}\} = \frac{\exp(-\boldsymbol{\mu}_h^H \mathbf{T}(s) \boldsymbol{\mu}_h)}{|\mathbf{I} + s\mathbf{A}\mathbf{P}_h|} \quad \text{where} \quad (\text{B.9})$$

$$\mathbf{T}(s) = \mathbf{P}_h^{-1} - \mathbf{P}_h^{-1} (s\mathbf{A} + \mathbf{P}_h^{-1})^{-1} \mathbf{P}_h^{-1} \quad (\text{B.10})$$

Defining $F(s) \triangleq \exp(-\boldsymbol{\mu}_h^H \mathbf{T}(s) \boldsymbol{\mu}_h)$ and $G(s) \triangleq |\mathbf{I} + s\mathbf{A}\mathbf{P}_h|$, one can calculate the second order moment of β by using (B.9) such that

$$E\{\beta^2\} = \left. \frac{\partial^2 \Phi_\beta(s)}{\partial s^2} \right|_{s=0} = \left. \frac{\frac{\partial^2 F(s)}{\partial s^2} G(s) - F(s) \frac{\partial^2 G(s)}{\partial s^2} - 2 \frac{\partial F(s)}{\partial s} \frac{\partial G(s)}{\partial s} + \frac{2F(s) \left(\frac{\partial G(s)}{\partial s}\right)^2}{G(s)^3}}{G(s)^2} \right|_{s=0} \quad (\text{B.11})$$

where

$$\begin{aligned} \frac{\partial F(s)}{\partial s} &= -\left(\boldsymbol{\mu}_h^H \frac{\partial \mathbf{T}(s)}{\partial s} \boldsymbol{\mu}_h\right) F(s), & \frac{\partial^2 F(s)}{\partial s^2} &= -\left(\boldsymbol{\mu}_h^H \frac{\partial^2 \mathbf{T}(s)}{\partial s^2} \boldsymbol{\mu}_h\right) F(s) + \left(\boldsymbol{\mu}_h^H \frac{\partial \mathbf{T}(s)}{\partial s} \boldsymbol{\mu}_h\right)^2 F(s), \\ \frac{\partial \mathbf{T}(s)}{\partial s} &= \mathbf{A}\mathbf{P}_h (s\mathbf{A}\mathbf{P}_h + \mathbf{I})^{-2} \mathbf{P}_h^{-1}, & \frac{\partial^2 \mathbf{T}(s)}{\partial s^2} &= -2(\mathbf{A}\mathbf{P}_h)^2 (s\mathbf{A}\mathbf{P}_h + \mathbf{I})^{-3} \mathbf{P}_h^{-1}. \end{aligned} \quad (\text{B.12})$$

We use the following definitions to calculate (B.11) based on (B.12):

$$f_0 \triangleq F(s) \Big|_{s=0} = 1, \quad f_1 \triangleq \frac{\partial F(s)}{\partial s} \Big|_{s=0} = -\boldsymbol{\mu}_h^H \mathbf{A} \boldsymbol{\mu}_h, \quad f_2 \triangleq \frac{\partial^2 F(s)}{\partial s^2} \Big|_{s=0} = 2\boldsymbol{\mu}_h^H \mathbf{A} \mathbf{P}_h \mathbf{A} \boldsymbol{\mu}_h + \left(\boldsymbol{\mu}_h^H \mathbf{A} \boldsymbol{\mu}_h\right)^2, \quad (\text{B.13})$$

$G(s)$ in (B.11) can also be expressed as a sum of powers of s such that $G(s) = \sum_{k=0}^{L_c} g_k s^k$ where

$$g_0 = 1, \quad g_1 = \sum_{m=1}^{L_c} (\mathbf{A}\mathbf{P}_h)_{m,m}, \quad g_2 = \sum_{(m,n) \in P_2} \left[(\mathbf{A}\mathbf{P}_h)_{m,m} (\mathbf{A}\mathbf{P}_h)_{n,n} - (\mathbf{A}\mathbf{P}_h)_{m,n} (\mathbf{A}\mathbf{P}_h)_{n,m} \right] \quad (\text{B.14})$$

by using the Leibniz formula for determinants [100] and P_2 is the set containing all possible 2 element combinations of $\{1, 2, \dots, L_c\}$. Then, we can calculate (B.11) as

$$E\{\beta^2\} = E\left\{\left(\mathbf{h}^H \mathbf{A} \mathbf{h}\right)^2\right\} = f_2 - 2g_2 - 2f_1 g_1 + 2g_1^2 \quad (\text{B.15})$$

by using (B.13) and (B.14). The expectations $E_{\mathbf{h}} \left\{ \left(\text{Im} \left\{ \mathbf{h}^H \mathbf{A}_l^{(m_1, m_2, p, n)} \mathbf{h} \right\} \right)^2 \right\}$ and $E_{\mathbf{h}} \left\{ \left| \mathbf{h}^H \mathbf{B}_l^{(m_1, p, n)} \mathbf{h} \right|^2 \right\}$ in (2.27) can be calculated in a similar manner.

APPENDIX C

APPROXIMATE BER ANALYSIS FOR U-RSSE-BDF

Assuming that all input sequences are equally likely and weight one error events dominate the others, the bit error probability for Ungerboeck RSSE can be upper bounded as ¹

$$\begin{aligned}
 P_b &\leq E_{\mathbf{h}} \left\{ \sum_{\forall \mathbf{e} \mid \mathbf{e}_k = \mathbf{x}_k^{(2)} - \mathbf{x}_k^{(1)}, \mathbf{e}_k \neq \mathbf{0}} \frac{w_b(\mathbf{e})}{\log_2(MP)} \mathbb{P}\{\mathbf{b}_1\} \mathbb{P}\{\mathbf{e} \mid \mathbf{h}\} \right\} \\
 &\approx E_{\mathbf{h}} \left\{ \sum_{\forall \mathbf{x}_k^{(1)} \forall \mathbf{x}_k^{(2)}, \mathbf{x}_k^{(2)} \neq \mathbf{x}_k^{(1)}} \frac{w_b(\mathbf{e}_k)}{\log_2(MP)} \frac{1}{MP} \mathbb{P}\{\mathbf{x}_k^{(1)} \rightarrow \mathbf{x}_k^{(2)} \mid \mathbf{h}\} \right\} \quad (\text{C.1})
 \end{aligned}$$

where $w_b(\mathbf{e})$ shows the number of bit errors corresponding to the error event sequence \mathbf{e} and \mathbf{b}_1 is the vector sequence for the transmitted symbols $\{\mathbf{x}_k^{(1)}\}_{k=0}^{N-1}$ on path-1. Then, one can express the BER in (C.1) by using the definition of \mathbf{c}_n in (2.8) and noting that $\mathbf{x}_n = \mathbf{c}_n e^{j\theta_n}$ as well as the symmetry in PSK modulation as

$$\begin{aligned}
 P_b &\approx \frac{1}{M} \left[\sum_{I_1=1}^M \sum_{I_2=1, I_2 \neq I_1}^M \sum_{p=0}^{P-1} w_b(I_1, I_2, p) \right. \\
 &\quad E_{\mathbf{h}} \left\{ \mathbb{P}\{I_k^{(1)} \rightarrow I_k^{(2)}, \theta_k^{(1)} \rightarrow \theta_k^{(2)} \mid I_k^{(1)} = I_1, I_k^{(2)} = I_2, \theta_k^{(2)} = \theta_k^{(1)} + \frac{2\pi}{P}p, \mathbf{h}\} \right\} \\
 &\quad \left. + \sum_{I_1=1}^M \sum_{p=1}^{P-1} w_b(I_1, I_1, p) E_{\mathbf{h}} \left\{ \mathbb{P}\{\theta_k^{(1)} \rightarrow \theta_k^{(2)} \mid I_k^{(1)} = I_k^{(2)} = I_1, \theta_k^{(2)} = \theta_k^{(1)} + \frac{2\pi}{P}p, \mathbf{h}\} \right\} \right] \quad (\text{C.2})
 \end{aligned}$$

P_b in (C.2) requires the calculation of expected PEPs. By resorting an approxi-

¹ For severe ISI channels where the error events with larger duration become more effective, the error state diagram [18] can be exploited to incorporate the error events of greater lengths by using $d^2(\mathbf{e})$ in (A.10). However, this elaborates the BER analysis especially for large M and L values.

mation of Q -function as $Q(x) \approx \sum_{i=1}^K \frac{1}{2K} \exp\left(-\frac{x^2}{2\sin^2(\frac{\pi}{2K}i)}\right)$ [101] and ignoring the bias term in (A.9), PEP can be obtained as

$$\mathbb{P}\{\mathbf{x}_k^{(1)} \rightarrow \mathbf{x}_k^{(2)} \mid \mathbf{h}\} \approx Q\left(\sqrt{\frac{d^2(\mathbf{e}_k)}{2N_0}}\right) \approx \sum_{i=1}^K \frac{1}{2K} \exp\left(\frac{-1}{4\sin^2(\frac{\pi}{2K}i)} \frac{E_c}{N_0} d^2(\mathbf{e}_k)\right) \quad (\text{C.3})$$

where the distance metric $d^2(\mathbf{e}_k)$ is provided in terms of channel and code correlations in (C.4) as

$$\begin{aligned} d^2(\mathbf{e}_k) &= \mathbf{e}_k^H \mathbf{H}(0) \mathbf{e}_k = \left(\mathbf{c}_k^{(2)} e^{j\theta_k^{(2)}} - \mathbf{c}_k^{(1)} e^{j\theta_k^{(1)}}\right)^H \mathbf{H}(0) \left(\mathbf{c}_k^{(2)} e^{j\theta_k^{(2)}} - \mathbf{c}_k^{(1)} e^{j\theta_k^{(1)}}\right) \quad (\text{C.4}) \\ &= R_{I_k^{(1)}, I_k^{(1)}}(0) + R_{I_k^{(2)}, I_k^{(2)}}(0) - e^{-j(\theta_k^{(2)} - \theta_k^{(1)})} R_{I_k^{(1)}, I_k^{(2)}}(0) - e^{j(\theta_k^{(2)} - \theta_k^{(1)})} \left(R_{I_k^{(1)}, I_k^{(2)}}(0)\right)^* \\ &= \mathbf{h}^H \left[\mathbf{R}_g^{I_k^{(1)}, I_k^{(1)}}(0) + \mathbf{R}_g^{I_k^{(2)}, I_k^{(2)}}(0) - e^{-j(\theta_k^{(2)} - \theta_k^{(1)})} \mathbf{R}_g^{I_k^{(1)}, I_k^{(2)}}(0) - e^{j(\theta_k^{(2)} - \theta_k^{(1)})} (\mathbf{R}_g^{I_k^{(1)}, I_k^{(2)}}(0))^H \right] \mathbf{h} \end{aligned}$$

by using (2.7). The expectations over \mathbf{h} in (C.2) can be found easily by using the MGF of $d^2(\mathbf{e}_k)$ as in (B.9) which results in (2.29).

APPENDIX D

CUTOFF RATE ANALYSIS OF CODED MCS SCHEME

The pairwise error probability, that corresponds to deciding on \mathbf{X}_j when \mathbf{X}_i is sent after Ungerboeck type processing in (2.10) can be written by using (A.8) as

$$\begin{aligned}
 \mathbb{P}\{\mathbf{X}_i \rightarrow \mathbf{X}_j\} &= \mathbb{P}\left\{ \Lambda_N(\mathbf{X}_i) < \Lambda_N(\mathbf{X}_j) \mid \mathbf{X}_i \text{ is sent} \right\} \\
 &\approx \sum_{q=1}^K \frac{1}{2K} \exp\left(\frac{-1}{4 \sin^2(\frac{\pi}{2K}q)} \frac{E_c}{N_0} \sum_{n=0}^{N-1} \sum_{k=0}^{N-1} (\mathbf{x}_n^i - \mathbf{x}_n^j)^H \mathbf{H}(n-k) (\mathbf{x}_k^i - \mathbf{x}_k^j) \right) \\
 &= \sum_{q=1}^K \frac{1}{2K} \prod_{n=0}^{N-1} \exp\left\{ \frac{-1}{4 \sin^2(\frac{\pi}{2K}q)} \frac{E_c}{N_0} f(\mathbf{D}_n^{ij}) \right\} \tag{D.1}
 \end{aligned}$$

where

$$f(\mathbf{D}_n) = \sum_{l=-(L-1)}^{L-1} \mathbf{d}_n^H \mathbf{H}(l) \mathbf{d}_{n-l}, \quad \mathbf{D}_n = [\mathbf{d}_{n-L+1}, \dots, \mathbf{d}_n, \dots, \mathbf{d}_{n+L-1}]. \tag{D.2}$$

since $\mathbf{H}(l) = (\mathbf{R}(l))^T = \mathbf{0}$ if $|l| \geq L$.

Instead of attempting to find a single set of 2^k coded waveforms for which we compute the error probability, let us consider the ensemble of $((MP)^N)^{2^k}$ distinct ways associated with random coding in which we can select 2^k vertices from the $(MP)^N$ vertices of the hypercube. Therefore, in this work, we find the average performance over an ensemble of communication systems that employ different set of 2^k codebooks selected randomly from the set of $((MP)^N)^{2^k}$ possible choices. After averaging (D.1) over the ensemble of codes, one can get the

following

$$\overline{\mathbb{P}\{\mathbf{X}_i \rightarrow \mathbf{X}_j\}} = E_{\mathbf{D}^{ij}} \left\{ \sum_{q=1}^K \frac{1}{2K} \prod_{n=0}^{N-1} \exp \left[\frac{-1}{4 \sin^2(\frac{\pi}{2K}q)} \frac{E_c}{N_0} f(\mathbf{D}_n^{ij}) \right] \right\} \quad (\text{D.3})$$

$$\begin{aligned} &= \frac{1}{2K} \sum_{q=1}^K \frac{1}{|\mathfrak{D}|^N} \sum_{\forall \mathbf{D} \in \mathfrak{D}^N} \prod_{n=0}^{N-1} \exp \left[\frac{-1}{4 \sin^2(\frac{\pi}{2K}q)} \frac{E_c}{N_0} f(\mathbf{D}_n) \right] \\ &\approx \frac{1}{2K} \sum_{q=1}^K \frac{1}{|\mathfrak{D}|^{N(2L-1)}} \sum_{\{\forall \mathbf{D}_m \in \mathfrak{D}^{(2L-1)}, m=0, \dots, N-1\}} \prod_{n=0}^{N-1} \exp \left[\frac{-1}{4 \sin^2(\frac{\pi}{2K}q)} \frac{E_c}{N_0} f(\mathbf{D}_n) \right] \end{aligned} \quad (\text{D.4})$$

$$= \frac{1}{2K} \sum_{q=1}^K \prod_{n=0}^{N-1} \left(\frac{1}{|\mathfrak{D}|^{(2L-1)}} \sum_{\{\forall \mathbf{D}_n \in \mathfrak{D}^{(2L-1)}\}} \exp \left[\frac{-1}{4 \sin^2(\frac{\pi}{2K}q)} \frac{E_c}{N_0} f(\mathbf{D}_n) \right] \right) \quad (\text{D.5})$$

$$\begin{aligned} &= \frac{1}{2K} \sum_{q=1}^K \left[\frac{1}{|\mathfrak{D}|^{(2L-1)}} \sum_{\forall \mathbf{d}_n \in \mathfrak{D}} \left\{ \sum_{\{\forall \mathbf{d}_{n-m} \in \mathfrak{D}, m \neq 0, m=-L+1, \dots, L-1\}} \right. \right. \\ &\quad \left. \left(\prod_{l=-(L-1), l \neq 0}^{L-1} \exp \left(\frac{-1}{4 \sin^2(\frac{\pi}{2K}q)} \frac{E_c}{N_0} \mathbf{d}_n^H \mathbf{H}(l) \mathbf{d}_{n-l} \right) \right) \right. \\ &\quad \left. \left. \exp \left(\frac{-1}{4 \sin^2(\frac{\pi}{2K}q)} \frac{E_c}{N_0} \mathbf{d}_n^H \mathbf{H}(0) \mathbf{d}_n \right) \right\} \right]^N \end{aligned} \quad (\text{D.6})$$

$$= \frac{1}{2K} \sum_{q=1}^K \left[\sum_{\forall \mathbf{d}_n \in \mathfrak{D}} A(\mathbf{d}_n) \exp \left(\frac{-1}{4 \sin^2(\frac{\pi}{2K}q)} \frac{E_c}{N_0} \mathbf{d}_n^H \mathbf{H}(0) \mathbf{d}_n \right) \right]^N \quad (\text{D.7})$$

where

$$A(\mathbf{d}_n) = \frac{1}{|\mathfrak{D}|^{(2L-1)}} \prod_{l=-(L-1), l \neq 0}^{L-1} \left(\sum_{\{\forall \mathbf{d}_{n-l} \in \mathfrak{D}\}} \exp \left[\frac{-1}{4 \sin^2(\frac{\pi}{2K}q)} \frac{E_c}{N_0} \mathbf{d}_n^H \mathbf{H}(l) \mathbf{d}_{n-l} \right] \right) \quad (\text{D.8})$$

In (D.3), expectation is taken over all possible codeword difference matrices $\mathbf{D} \in \mathfrak{D}^N$. The approximation made in (D.4) is valid as long as N is larger than L , and it is equality when $L = 1$. (D.6) is due to the independence of the inner term $\left(\frac{1}{|\mathfrak{D}|^{(2L-1)}} \sum_{\{\forall \mathbf{D}_n \in \mathfrak{D}^{(2L-1)}\}} (\cdot) \right)$ from n in (D.5).

The average probability of error when codeword \mathbf{X}_i is sent can be found by using

union bound as

$$\begin{aligned} \overline{\mathbb{P}_e\{\mathbf{X}_i\}} &\leq \sum_{j=1, j \neq i}^{2^k} \overline{\mathbb{P}\{\mathbf{X}_i \rightarrow \mathbf{X}_j\}} \\ &\approx \frac{2^k}{2K} \sum_{q=1}^K \left[\sum_{\forall \mathbf{d}_n \in \mathcal{D}} A(\mathbf{d}_n) \exp\left(\frac{-1}{4 \sin^2(\frac{\pi}{2K}q)} \frac{E_c}{N_0} \mathbf{d}_n^H \mathbf{H}(0) \mathbf{d}_n\right) \right]^N \end{aligned} \quad (\text{D.9})$$

Finally, the unconditional packet error probability $\overline{P_e}$ is obtained by averaging over all possible k -bit information sequences such that

$$\overline{P_e} = \sum_i \overline{\mathbb{P}_e\{\mathbf{X}_i\}} \mathbb{P}\{\mathbf{X}_i\} = \overline{\mathbb{P}_e\{\mathbf{X}_i\}} \sum_i \mathbb{P}\{\mathbf{X}_i\} = \overline{\mathbb{P}_e\{\mathbf{X}_i\}} \quad (\text{D.10})$$

We can write this equation in a more convenient form by defining a parameter R_c , which is called the cutoff rate and has units of bits/dimension, and using (D.9) as

$$\overline{P_e} \leq 2^{-N_{\text{total}}(R_c - R)} \quad (\text{D.11})$$

where $N_{\text{total}} = N_c N$, $R = \frac{R_b}{D} = \frac{k}{N_{\text{total}}}$ (bits/dim) and R_c with units of bits/dimension can be found as

$$\begin{aligned} R_c &= -\frac{1}{N_{\text{total}}} \log_2 \left(\frac{\overline{P_e}}{2^k} \right) \\ &= -\frac{1}{N_c} \log_2 \left(\frac{1}{2K} \sum_{q=1}^K \left[\sum_{\forall \mathbf{d}_n \in \mathcal{D}} A(\mathbf{d}_n) \exp\left(\frac{-1}{4 \sin^2(\frac{\pi}{2K}q)} \frac{E_c}{N_0} \mathbf{d}_n^H \mathbf{H}(0) \mathbf{d}_n\right) \right]^N \right)^{\frac{1}{N}} \\ &\approx -\frac{1}{N_c} \log_2 \left[\sum_{\forall \mathbf{d}_n \in \mathcal{D}} A(\mathbf{d}_n) \exp\left(-\frac{E_c}{4N_0} \mathbf{d}_n^H \mathbf{H}(0) \mathbf{d}_n\right) \right] \quad \text{for } K = N \rightarrow \infty \end{aligned} \quad (\text{D.12})$$

To obtain (D.12), we assume relatively large values of K for better Q -function approximation. Then, by letting $K = N$, and as $N \rightarrow \infty$, $\left(\sum_{i=1}^N (a_i)^N\right)^{\frac{1}{N}} \rightarrow \max_i a_i$ and $N^{\frac{1}{N}} \rightarrow 1$, one obtains the result in (D.12).

We assume that the proposed Ungerboeck receiver in Chapter 2 is capable for removing all pre- and post-cursor ISI so that the MFB is achievable. This corresponds to setting $L = 1$, $A(\mathbf{d}_n) = \frac{1}{|\mathcal{D}|}$ in (D.8). Then, (D.12) is simplified to the final expression given in (3.5).

We conclude that when $R < R_c$, the average probability of error $\overline{P_e} \rightarrow 0$ as the code block length $N_{\text{total}} \rightarrow \infty$. Since the average value of the probability of error

can be made arbitrarily small as $N_{\text{total}} \rightarrow \infty$, it follows that there exist codes in the ensemble of $((MP)^N)^{2^k}$ codes that have a probability of error no larger than \overline{P}_e by using an argument similar to channel coding theorem in [102].

CURRICULUM VITAE

PERSONAL INFORMATION

Surname, Name: Güvensen, Gökhan Muzaffer

Nationality: Turkish (TC)

Date and Place of Birth: 05.11.1982, Burdur, TURKEY

Marital Status: Single

Phone: 0312 210 4583

Fax: 0312 210 2304

EDUCATION

Degree	Institution	Year of Graduation
M.S.	Middle East Technical University	February 2009
B.S.	Middle East Technical University	June 2006
High School	Burdur Anatolian High School	2001

PROFESSIONAL EXPERIENCE

Year	Place	Enrollment
10/2006 - 1/2014	Middle East Technical University	Research Assistant

PUBLICATIONS

- Gökhan Muzaffer Güvensen, Yalçın Tanık, Ali Özgür Yılmaz, A Reduced-State Ungerboeck Type MAP Receiver with Bidirectional Decision Feedback for M-ary Quasi Orthogonal Signaling, IEEE Transactions on Com-

munications, Vol. 62, No. 2, pp. 552-566, February 2014.

- Gökhan Muzaffer Güvensen, Ali Özgür Yılmaz, A General Framework for Optimum Iterative Blockwise Equalization of Single Carrier MIMO Systems and Asymptotic Performance Analysis, IEEE Transactions on Communications, Vol. 61, No. 2, pp. 609-619, February 2013.
- Gökhan Muzaffer Güvensen, Ali Özgür Yılmaz, An Upper Bound for Limited Rate Feedback MIMO Capacity, IEEE Transactions on Wireless Communications, Vol. 8, No. 6, pp. 2748-2754, June 2009.

International Conference Publications

- Gökhan Muzaffer Güvensen, Ali Özgür Yılmaz, Diversity analysis of optimal SC-FDE MIMO systems and comparison with OFDM based transmission, IEEE International Symposium on Personal, Indoor and Mobile Radio Communications (IEEE PIMRC), Toronto-Canada, September 2011.
- Gökhan Muzaffer Güvensen, Yalçın Tanık, Ali Özgür Yılmaz, On the Carrier Frequency Offset Estimation for Frequency Hopping Burst Mode Mobile Radio, Military Communications Conference (MILCOM), San Jose, CA, USA, October 2010.
- Gökhan Muzaffer Güvensen, Yalçın Tanık, Ali Özgür Yılmaz, Cut-off Rate based Outage Probability Analysis of Frequency Hopping Mobile Radio under Jamming Conditions, Military Communications Conference (MILCOM), San Jose, CA, USA, October 2010.
- Gökhan Muzaffer Güvensen, Ali Özgür Yılmaz, Iterative Frequency Domain Equalization for Single-Carrier Wideband MIMO Channels, IEEE International Symposium on Personal, Indoor and Mobile Radio Communications (IEEE PIMRC), Tokyo-Japan, September 2009.
- Gökhan Muzaffer Güvensen, Tuğcan Aktaş, Ali Özgür Yılmaz, Probability of Full-Diversity for Simple Coded and Rotated Multidimensional Constellation Systems, IEEE International Symposium on Personal, Indoor and

Mobile Radio Communications (IEEE PIMRC), Tokyo-Japan, September 2009.

- Gökhan Muzaffer Güvensen, Ali Özgür Yılmaz, Iterative Decision Feedback Equalization and Decoding for Rotated Multidimensional Constellations in Block Fading Channels, IEEE Vehicular Technology Conference (IEEE VTC), Spring, Barcelona-Spain, April 2009.

National Conference Publications

- Gökhan Muzaffer Güvensen, Yalçın Tanık, Ali Özgür Yılmaz, M-ary Yaklaşık Dikgen Sinyalleşme ile Çoklu Erişim için Etkin Ungerboeck Tipinde MAP Alıcısı, IEEE Sinyal İşleme ve İletişim Uygulamaları Kurultayı (IEEE SIU), 2013.
- Gökhan Muzaffer Güvensen, Yalçın Tanık, Ali Özgür Yılmaz, M-ary Yaklaşık Dikgen Sinyalleşme ile Yayılı Spektruma Sahip Sistemler için Etkin Telsiz Haberleşme, IEEE Sinyal İşleme ve İletişim Uygulamaları Kurultayı (IEEE SIU), 2012.
- Gökhan Muzaffer Güvensen, Tuğcan Aktaş, Yalçın Tanık, Kara ve Yağmur Kargaşası Altında Çalışan Yüksek Başarımli Bir Radar Tespit Birimi Tasarımı, Savunma Teknolojileri Kongresi (SAVTEK), 2012.
- Gökhan Muzaffer Güvensen, Ali Özgür Yılmaz, MIMO Kanallarda Sınırlı Hızda Geribesleme ve RVQ, IEEE Sinyal İşleme ve İletişim Uygulamaları Kurultayı (IEEE SIU), 2007.